

Radiation Monitoring and Remediation Following
the
Fukushima Daiichi Nuclear Power Plant Accident

Cooperation between
Fukushima Prefecture and the IAEA

INTERIM REPORT
(2013 to 2020)

【Fukushima Prefecture Initiative Projects】

【Detailed version】

(Temporary translation)

March 2021

Fukushima Prefecture

Index

Introduction	1
1. FIP1 Survey, and evaluation of the effect, of radiocaesium dynamics in the aquatic systems based on the continuous monitoring	
1.1. Abstract	5
1.2. Purpose	5
1.3. Content of implementation	6
1.4. Results	8
1.5. Conclusions	15
2. FIP2 Survey of radionuclide movement with wildlife	
2.1. Abstract	17
2.2. Purpose	17
2.3. Content of implementation	18
2.4. Results	19
2.5. Conclusions	26
3. FIP3 Sustainable countermeasures to radioactive materials in freshwater system	
3.1. Abstract	27
3.2. Purpose	27
3.3. Content of implementation	27
3.4. Results	31
3.5. Conclusions	35
4. FIP4 Development of environmental mapping technology using GPS walking surveys (Ended in FY2015)	
4.1. Abstract	37
4.2. Purpose	37
4.3. Content of implementation	39
4.4. Results	41
4.5. Conclusions	48
5. FIP5 Study of proper treatment of waste containing radioactive material	
5.1. Abstract	49
5.2. Purpose	49
5.3. Content of implementation	51
5.4. Results	55
5.5. Conclusions	69
Report summary	70

Introduction

The Great East Japan Earthquake occurred on 11 March 2011. It was followed by the accident of Tokyo Electric Power Company's Fukushima Daiichi Nuclear Power Plant¹, and radioactive materials have been released into the environment which contaminated the land. Due to the contamination of the land and other relevant reasons, more than 160,000 prefectural residents were forced to evacuate. About 38,000 residents have not been able to return home, as of 2020 July, about 9 years after the disaster (Fukushima Prefecture's website "Fukushima Revitalization Station"; <https://www.pref.fukushima.lg.jp/uploaded/attachment/403521.pdf>).

In order for Fukushima Prefecture to recover from the severe and unprecedented nuclear disaster and create an environment where the residents can live with peace of mind in the future, it was necessary to respond at the aftermath by collecting knowledge and world-wide experience, so the prefecture decided to cooperate with the International Atomic Energy Agency (hereinafter referred to as the "IAEA"), which owns high-level nuclear-related knowledge. In December 2012, a memorandum for cooperation was signed between the prefecture and the IAEA.

Based on the memorandum, an agreement relating to the fields of "radiation monitoring" and "decontamination" was signed between the parties on the same day (projects based on this agreement is referred to as "FCPs; Fukushima Cooperative Project").

Subsequently in April and October 2013, agreements were signed for five projects (hereinafter referred to as "FIPs; Fukushima Initiative Project") as described below in a new framework in which these projects would be supported by the IAEA for three years, and the FIPs started (hereinafter referred to as "previous Project"). In April and May 2016, they signed agreements for extending the FIP cooperation period (originally set at "until December 2017") expanding the range of their cooperation².

【Themes of the FIPs before the extension of cooperation period (From April 2013 to December 2017)】

- 1 Survey of radionuclide movement in river systems
- 2 Survey of radionuclide movement with wildlife
- 3 Countermeasures for radioactive materials in rivers and lakes
- 4 Development of environmental mapping technology using GPS walking surveys
- 5 Study of the proper treatment of waste containing radioactive materials at municipal solid waste incinerators

The achievements of the FIPs conducted between April 2013 and December 2017 were compiled in the report on "Cooperation between Fukushima Prefecture and the IAEA – SUMMARY REPORT (2013 to 2017) [Fukushima Prefecture Initiative Projects]" in March 2018 (hereinafter referred to as "previous report"). The previous report is available in a book form and also in the following website:

<https://www.pref.fukushima.lg.jp/sec/298/iaeasummary2017.html>

- 1 *The owner of the Fukushima Daiichi Nuclear Power Plant was renamed from Tokyo Electric Power Company to Tokyo Electric Power Company Holdings, Incorporated in April 1, 2016.*
- 2 *In accordance with the change of the cooperation range, the names of some FIPs were changed.*

However, because remediation of the environment in the Prefecture was halfway through and the accomplishment of the proposed projects required further support from the IAEA, the prefecture obtained in December 2017 the IAEA's agreement and signature for a continued support until December 2022 (hereinafter referred to as "this Project"). Subsequently, according to the contents of the projects, some project themes were renamed. This report is an interim report on activities from Fiscal Year (hereinafter referred to as "FY") 2013, focusing on activities from FY2018 to FY2019, excluding FIP4. FIP4 was completed in FY2015 and has not been extended, so the previous report is reprinted with some wordings revised and updated since FY2015.

FIP1: Survey of radionuclide movement in river systems

Survey, and evaluation of the effect, of radiocaesium dynamics in the aquatic systems based on the continuous monitoring <Renamed>

The purpose of this project is to determine the movements of radionuclides in the river waters in Fukushima Prefecture to foster the sense of safety and security of its residents. From the achievements attained by Fiscal Year 2017 (as described in the previous report), it was confirmed that the cesium concentrations decreased to about 1/10 during the five years after the accident and that their decrease rates were different depending on whether decontamination had been performed. It was decided to further continue this project because it was necessary to obtain the IAEA's advice and proposals regarding the identification of radionuclide movements as well as radiocesium movement prediction and impact assessment using numerical models derived from monitoring results. An impact assessment review was also included in this project, so the project theme was renamed.

FIP2: Survey of radionuclide movement with wildlife (theme name unchanged)

The project is intended to determine the movements of radionuclides among wild animals such as wild boars, with a view to lifting their shipment restrictions and relieving the concerns of the residents in the prefecture. Outcomes obtained by Fiscal Year (FY) 2017 revealed that the Cs-137 concentrations in the muscles of wild boars tended to be higher than those in the muscles of Asian black bears and that the Cs-137 concentrations in the muscles of both animals fluctuated seasonally and increased particularly during winter. It was also found that the Cs-137 concentrations in the muscles of wild boars were positively linked to those contained in their gastric contents. With regard to birds, the Cs-137 concentrations in the muscles of copper pheasants were higher than those in the muscles of Japanese pheasants, mallards, and spot-billed ducks. The continuation of the project was decided because of the necessity of the IAEA's further advice and proposals in the measurements of radionuclide concentrations in wild animals' muscle tissues, gastric contents and food, in the analyses of their feeding habits, investigations

on behavioral patterns and population structures, and in the estimation of factors contributing to the high radiocesium concentrations in the muscles of some wild animals and the long-term fluctuations of radiocesium concentrations in the wild animals.

FIP3: Countermeasures for radioactive materials in rivers and lakes

Sustainable countermeasures to radioactive materials in freshwater system

<Renamed>

The purpose of this project is to check the effectiveness of measures that have been taken for rivers and lakes to identify effective radioactive material countermeasures. As achievements attained by FY 2017, radiocesium countermeasures applicable to the freshwater systems in Fukushima Prefecture were organized and it was found that topsoil removal according to cesium concentration distribution is effective in riverside areas and a decontamination effect was found to be maintained even after flooding.

These findings were made known to the municipalities. On the other hand, the presence of persistent anxieties regarding the water environment in seriously contaminated regions was recognized. It was decided to continue the project further because the IAEA's advice and proposals were still necessary to continuously determine the movements of radioactive materials in the future and clarify causes in case of re-contamination and establish effective countermeasures. In addition, the project theme was renamed because it was decided to take medium- to long-term measures.

FIP4: Development of environmental mapping technology using GPS walking surveys

The purpose of this project is to improve the efficiency of radiation monitoring by developing a system capable of quickly and precisely measuring radioactivity even in locations where radioactivity is immeasurable using a vehicle. This system was established by the end of March 2015 and was utilized since FY 2016 while walking surveys were carried out and survey equipment was lent in response to requests from the municipalities. Because the purpose of the project was achieved, it ended in FY 2015.

FIP5: Study of the proper treatment of waste containing radioactive materials at municipal solid waste incinerators

Study of proper treatment of waste containing radioactive material <Renamed>

This project is intended to promote the treatment of incinerated ash generated in general waste incineration facilities and check the migration of cesium from incinerated ash to fly ash depending upon incineration conditions. By FY 2017 it was found that the clarification of cesium migrations between incinerated ash and fly ash is difficult and that the mixture of zeolite or the like into incinerated ash decreases cesium leaching rate. These findings were made known to the municipalities. It was decided to further continue the project because it was necessary to obtain the IAEA's advice and proposals in analyzing the forms of radiocesium present in

incinerated ash and identify an effective method of making radiocesium hardly soluble and of its removal technique. The project theme was renamed to cover general waste containing radioactive materials.

1. FIP1 Survey, and evaluation of the effect, of radiocesium dynamics in the aquatic systems based on the continuous monitoring.

1.1. Abstract

More than nine years after the Fukushima Daiichi Nuclear Power Plant accident, the concentration of radiocesium in river water has fallen considerably. However, continuous monitoring of the effects of various social conditions and sudden events on the dynamics of radiocesium in rivers is still considered necessary. This project is thus an extension of the previous project that monitored the concentration of radiocesium in several rivers in Fukushima Prefecture. In addition, the efficacy of decontamination activities on radiocesium concentrations in river water were investigated. Model simulations were also performed to assess changes in the suspended and dissolved forms of radiocesium under both base- and high-flow conditions. The estimated results showed good agreement with measured values, although some improvements are considered necessary.

1.2. Purpose

As a result of the Fukushima Daiichi Nuclear Power Plant accident in March 2011, large amounts of radioactive materials were released as fallout into the environment. Previous studies showed that these materials were deposited on the surrounding areas and that they contaminated the soil. To ensure the safe use of rivers and river waters, which is widely used for drinking, agriculture and industry, it is important to clarify the actual situation of the dynamics of radioactive materials (especially radiocesium) in rivers. In addition, predictions of future dynamics of these materials in rivers also need to be performed. Radiocesium in river water occurs as suspended (adsorbed by fine particles) and dissolved (dissolved in water) forms. Since the role of each form of radiocesium in the environment is likely to be different, it is important to understand the radiocesium dynamics of these forms separately.

In the previous project (“Survey of radionuclide movement in river systems” in the previous report), we conducted long-term monitoring and clarification of the dynamics of radiocesium concentrations in rivers in Fukushima Prefecture. We also used models to predict changes in radionuclide concentrations following advice from the International Atomic Energy Agency. That project was comprised of two parts; the first was “Wide-area Multipoint Survey”, in which we conducted long-term monitoring of suspended cesium-137 concentrations in the Abukuma River Basin and rivers in the Hamadori area. The second was a “Survey of the Hirose River Basin”, in which we predicted the dynamics of radiocesium in the Hirose River, which is a primary tributary of the Abukuma River, using a numerical model. The results showed that the concentration of suspended radiocesium in river water tended to decrease over time, that dams and decontamination activities in the basin both affect the transport dynamics of radiocesium along the length of the rivers, and that land use in the basin affects the rate of decrease in the concentration of suspended radiocesium in river water. Some of the findings of the report were published as an academic paper¹⁾. In addition, changes in the radiocesium concentration under baseflow conditions in the

Hirose River were reproduced by using the TODAM model^{2), 3)}.

More than nine years after the accident, the concentration of radiocesium in the rivers in Fukushima Prefecture has decreased sufficiently, and levels are now well below the level recommended for drinking waters (10 Bq L^{-1}). However, changes in social conditions (e.g., completion of surface decontamination activities, return of residents, and resumption of farming following the lifting of evacuation orders) or the occurrence of sudden events (e.g., fires in the mountains and forests, large-scale high flows due to typhoons, heavy rains, etc.) may change the dynamics of radiocesium in rivers. Thus, it is important to continue monitoring and disseminating information based on the results of monitoring.

In this project, to better understand the trends in radiocesium concentrations over time, we will monitor radiocesium concentrations in river water, mainly in the Abukuma River system and rivers in the Hamadori area, as a continuation of the "Wide-area Multipoint Survey". In addition, the effects of decontamination on the transport of suspended radiocesium in river water and rates of transport will be analyzed in detail. Furthermore, a small number of the suspended solids (SS) samples collected to date in the Wide-area Multipoint Survey showed much higher radiocesium concentrations compared with other samples. It is therefore important to elucidate the causes of this particular increase in radiocesium concentration in SS samples to understand the transport dynamics of radiocesium in rivers, as radiocesium concentrations typically decrease over time. In this project, we hypothesize that the presence of radioactive cesium microparticles (CsMPs) in the samples are the cause of this phenomenon.

In this project, the Kuchibuto River Basin, which was previously monitored as part of the "Wide-area Multipoint Survey", is newly designated as a target basin in the "Single Basin Survey", and preparations for the application of the TODAM model to this basin have been undertaken. In the Hirose River Basin, we will continue monitoring to improve the accuracy of the calculations and to reproduce the changes in radiocesium concentrations under high-flow conditions using the TODAM model. To elucidate the dynamics of radiocesium through the river in more detail, we will estimate the source of suspended radiocesium based on the characteristics of the organic matter (total carbon and stable carbon isotope composition) in SS.

1.3. Content of implementation

Figure 1 shows the monitoring points used in this project; (a) the Kuchibuto River Basin, (b) the monitoring points used in the Wide-area Multipoint Survey, and (c) the Hirose River Basin for the model simulation.

(1) Wide-area Multipoint Survey

In the Wide area Multipoint Survey, monitoring has been continued by maintaining the devices used in the 2013-17 project (including an SS sampler, turbidity meter, and water level meter). Suspended solids were collected by samplers at 1- to 2-month intervals, dried in a vacuum freeze-dryer, and cesium-137 concentrations were measured using a germanium semiconductor detector. Turbidity and water level data were obtained at 10-minute intervals, and the concentration of suspended sediment (mg L^{-1}) and flow rate ($\text{m}^3 \text{ s}^{-1}$) were calculated using the conversion equations

employed in the previous study. The suspended cesium-137 flux was estimated by multiplying the concentration of SS, the river flow rate, and the cesium-137 concentrations in the SS.

In addition, the concentration of suspended and dissolved forms radiocesium in river water was quantified by collecting 40 to 80 L of river water approximately twice a year and then collecting radiocesium using a multi-stage filtration system (Fig. 2(a)). To clarify the actual effect of CsMPs on suspended cesium-137 concentrations in river water, we used SS samples collected by the SS sampler that showed much higher radiocesium concentrations compared with other samples. Using a germanium semiconductor detector, an imaging plate (IP), and other techniques, highly concentrated radioactive particles in SS samples were identified.

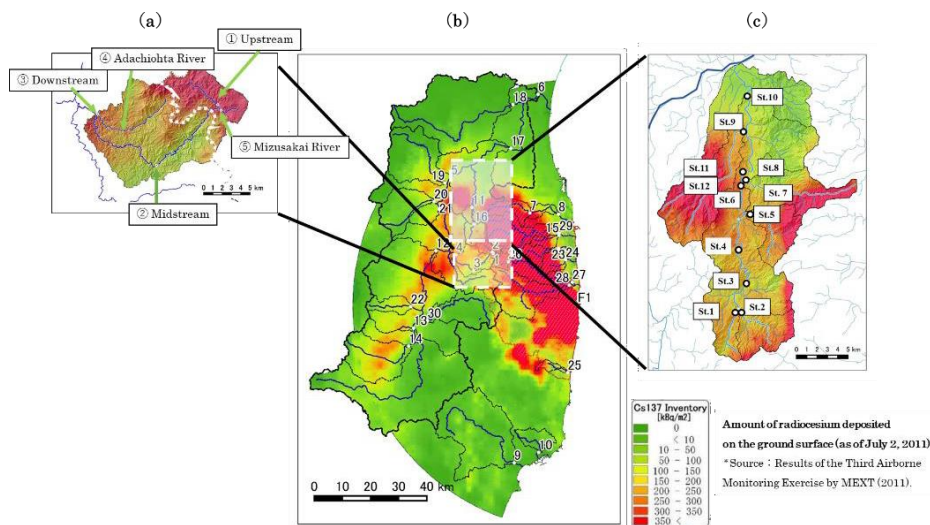


Figure 1. Monitoring points used in this study; (a) Kuchibuto River Basin, (b) Wide-area Multipoint Survey, (c) Hirose River Basin.

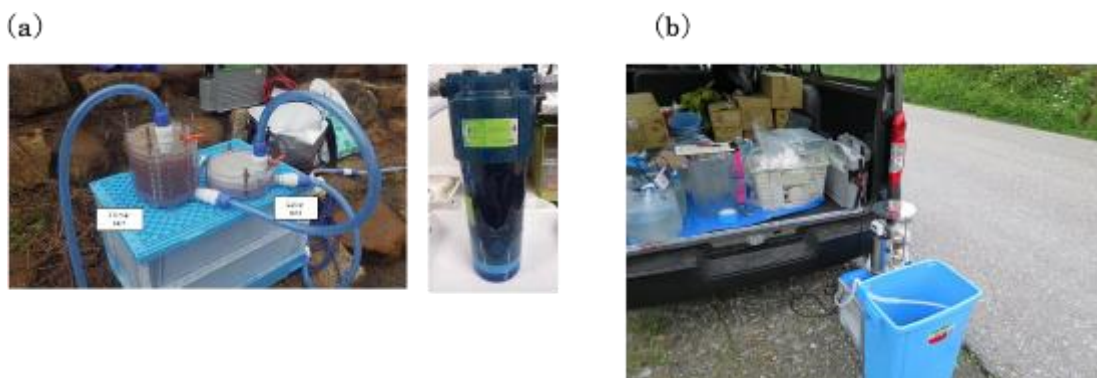


Figure 2. Radiocesium collecting devices; (a) multi-stage filtration system, (b) radiocesium monitoring device.

(2) Single basin survey

In this study, we maintained the monitoring network established in the Hirose River basin during the previous project. In addition, an additional monitoring point was established along the main river channel of the Hirose River in 2019 (St. 4). As for the Kuchibuto River Basin, we have started monitoring at five monitoring points, mainly those that were already included in the Wide-area Multipoint Survey.

Approximately 100 L of river water was collected at each monitoring point at base-flow levels (every 2 to 3 months) and the high-flow levels (7 samples/1 high-flow event, for 24 hours). Water quality (pH, Electrical conductivity (EC), Oxidation–Reduction Potential (ORP)) and SS concentrations were measured at the time of collection. Suspended and dissolved forms radiocesium were collected from river water samples in a cartridge filter for cesium monitoring using a radiocesium monitoring device (Fig. 2(b)). Each form of radiocesium was then measured with a germanium semiconductor detector. In addition, a survey of the riverbed morphology (cross-section) and soil sampling (riverbed and river bed soil) were carried out. Based on these data, we estimated radiocesium concentrations and their changes in the river under base-flow and high-flow conditions using the TODAM model.

To estimate the loading source of suspended radiocesium in river water, each subsample (500 mL to 1 L) was collected and filtrated using glass fiber filter paper (pore size 0.7 μm), which had been heated at 450°C for 4 hours to remove organic matter.

The filters were then dried (105°C, >48 hours), weighed and ground. The total carbon concentration and stable carbon isotope composition of the SS were then measured by elemental analyzer coupled to a stable isotope ratio mass spectrometer.

1.4. Results

(1) Wide-area Multipoint Survey

Figures 3(a) and 3(b) show the results of the changes in suspended and dissolved cesium-137 concentrations over time (as of December 2018) obtained from the Wide-area Multipoint Survey. The data include results from the University of Tsukuba until the end of FY2014 and in the previous report. Although the change was not as rapid as that observed immediately after the accident, the concentration of suspended cesium-137 at each monitoring point showed a tendency to decrease over time after the start of this project. As of December 2018, the concentration was generally less than 1/10 of that observed immediately after the accident (Fig. 3(a)). The concentration of dissolved cesium-137 exhibited an identical decreasing tendency as that of the suspended form of cesium-137 (Fig. 3(b)), although there was a period of missing data, indicating that the concentration of radiocesium in the rivers of Fukushima Prefecture gradually decreased over time and that this tendency continues at present.

In addition, the effective environmental half-lives of suspended and dissolved cesium-137 were estimated to be approximately 2.8 and 3.6 years, respectively (Fig. 4), based on data obtained from 2012 to 2018.

Comparing Chernobyl and Fukushima, the values of effective environmental half-lives of cesium-137 were similar just after the accident (0.24 year in Abukuma River vs 0.31 year in Pripyat River)¹⁾. In the second year and beyond, the decreasing rate of the concentration of suspended cesium-137 has lowered to about 1/10 of the initial rate in Fukushima. However, like just after the accident, the values of effective environmental half-lives are similar still (values of Fukushima are within the same range of values of European rivers; 1 to 4 years⁴⁾).

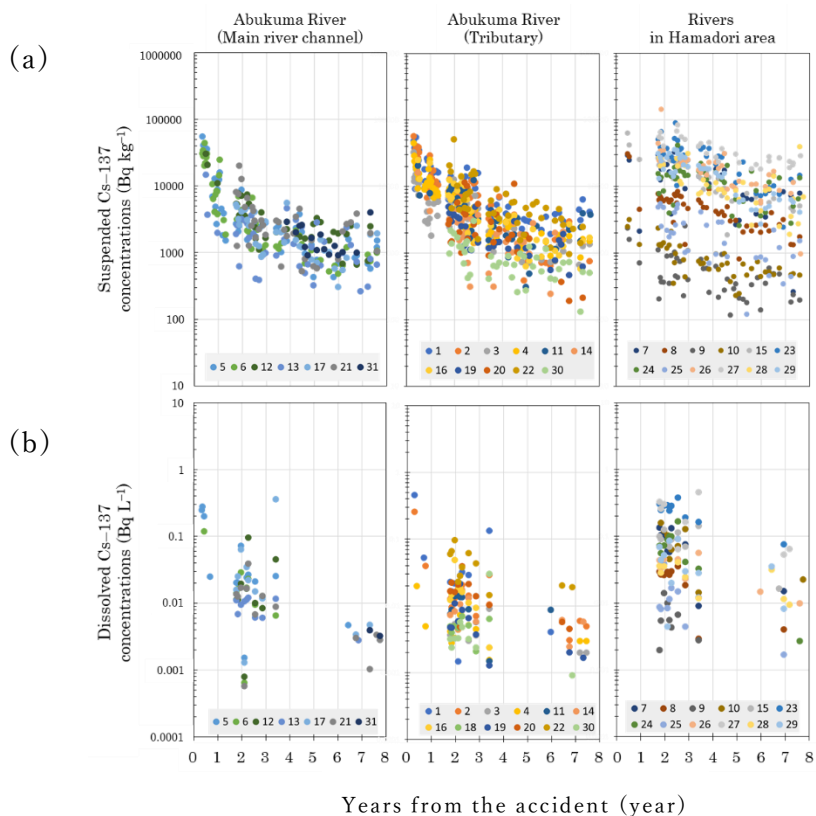


Figure 3. Cesium-137 concentrations in river water.
 (a) Suspended Cs-137, (b) Dissolved Cs-137.

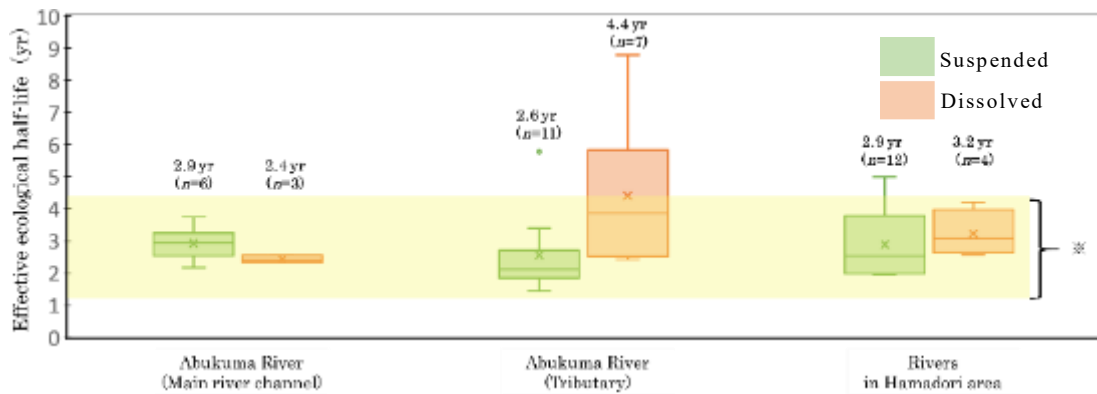


Figure 4. Effective environmental half-life of cesium-137 concentrations in river water in each region (data from 2012-2018). The asterisk indicates the range in the effective environmental half-life reported for European rivers after the Chernobyl Nuclear Power Plant Accident).

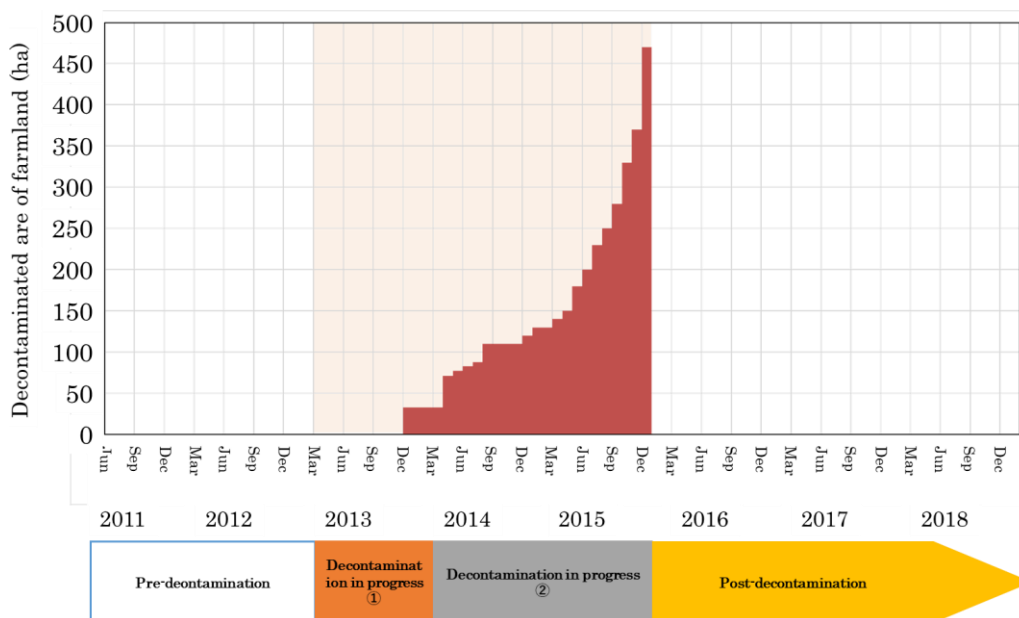


Figure 5. Progress in farmland decontamination

Next, the data for the Kuchibuto River basin were analyzed to examine the effect of the decontamination on the suspended of radiocesium in river water. These data mainly focused on changes in the concentrations of the suspended radiocesium as decontamination activities progressed. The basin was fully designated as a special decontamination area; work in the basin was planned in August 2012, began in March 2013, and was completed in December 2015 (Ministry of the Environment Decontamination Information Site, <http://josen.env.go.jp/area/details/kawamata.html>). Figure 5 shows the changes in the area of decontaminated farmland over time. Decontamination started in March 2013 but did not make much progress until March 2014. However, intensive farmland decontamination was carried out from April 2014 and decontamination was completed in December 2015. Thus, the interval before February 2013 was defined as “Pre-decontamination”, that during which very slow

progress was made, from March 2013 to March 2014, was defined as “Decontamination in progress ①”, and the interval during which rapid progress was made, from April 2014 to December 2015, was defined as “Decontamination in progress ②”. Finally, after January 2016 when decontamination was completed, the interval was defined as “Post decontamination”.

The changes in suspended cesium-137 concentrations at three monitoring points (upstream, midstream, and downstream; Fig. 1(a)) are shown in Fig. 6. The effective environmental half-lives for each period are shown in Table 1. Importantly, the results show an increase in the rate of the decrease in suspended cesium-137 concentration in the upstream and midstream sites of the special decontamination area during “Decontamination in progress ②”. Also, the rate of decrease decreased consistently in the downstream sites and slowed down in the second half of the “Decontamination in progress ②” period (after about 4 years since the accident). In addition, the amount of sediment in runoff as a function of precipitation and catchment area showed a tendency to increase after the start of farmland decontamination, and a significant increase was observed during the “decontamination in progress ②” period. In the “post-decontamination” period, the amount of sediment in runoff decreased, but it was still higher than in the “pre-decontamination” period (Fig. 7).

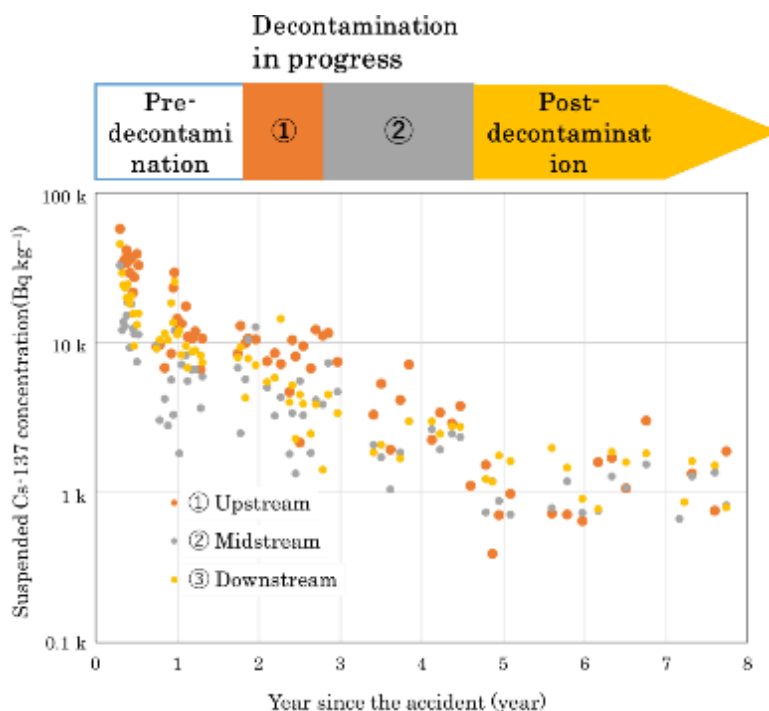


Figure 6. Change in suspended Cs-137 concentration over the course of decontamination.

Table 1. Effective environmental half-life for each period (years)

Monitoring point	Pre-	In progress ①	In progress ②	Post-decontamination
① Upstream	0.77	<i>n.s.</i>	0.98	<i>n.s.</i>
② Midstream	1.2	<i>n.s.</i>	1.6	<i>n.s.</i>
③ Downstream	0.86	0.59	4.2	4.8

n.s. indicates that suspended cesium-137 concentration did not change significantly during each period.

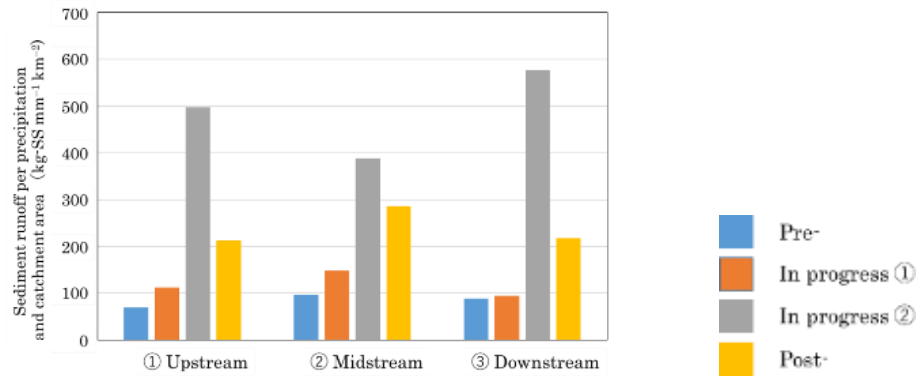


Figure 7. Relationship between decontamination progress and the amount of sediment runoff.

Figure 8 shows the changes in suspended cesium-137 concentration over time at a monitoring point in the Hamadori area included in the Wide-area Multi-point Survey. Since the start of monitoring, the concentration of suspended cesium-137 at the same monitoring point has been gradually decreasing. However, the sample collected at the monitoring point in October 2018 showed extremely high cesium-137 concentrations, a significant deviation from this trend. Thereafter, the concentration returned to normal levels and trended downward over time. Therefore, a hypothesis for the detection of this specific cesium-137 concentration is that a component with a high cesium-137 concentration might be present in the sample only. Previous studies have reported the presence in the environment of radioactive cesium enriched particles (CsMPs) derived from nuclear power plant

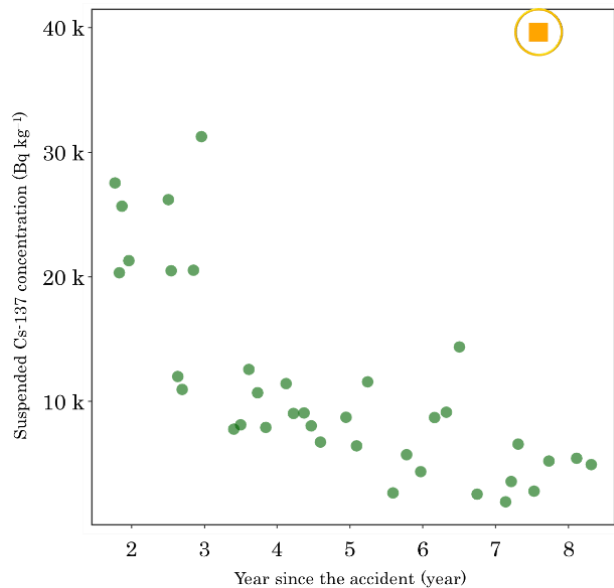


Figure 8. Temporal changes suspended Cs-137 concentrations

accidents 5), 6), 7). Therefore, in this project, we hypothesized that the increase of cesium-137 concentration in the SS sample was caused by the inclusion of CsMPs in the sample, and conducted some experiments to investigate the presence of CsMPs in the sample. In addition, if the presence of CsMPs was found, we tried to characterize them by imaging and elemental analyses. Two CsMPs particles were found in the sample using IP (image processing) and germanium semiconductor detectors. The radioactivity of cesium-137 in those two particles was estimated to be about 13 % of the total radioactivity. In the future, we establish the method to determine the presence of CsMPs in SS samples with very high concentration of cesium-137.

(2) Single basin survey

Figure 9 shows the calculated and measured concentrations of suspended and dissolved cesium-137 concentrations along the Hirose River using the TODAM model under base flow conditions. The solid line represents the values estimated by the TODAM model, and the boxplot represents the actual measurement values obtained at six monitoring points along the main river channel of the Hirose River. The measured values include the results obtained during the previous project undertaken from 2013 to 2017. In the previous report, we were able to reproduce the data obtained at five monitoring points along the main stream of the Hirose River using the TODAM model. At monitoring point St. 4 established in FY2019, the results obtained by the model simulation were in relatively good agreement with the measured values.

A simulation of the change in the concentration of cesium-137 in river water at the time of high-water flows from August 16 to 19, 2016 (total precipitation 67 mm; Japan Meteorological Agency, Yanagawa, Fukushima Prefecture) is shown in Figure 10. The results also showed a good agreement between measured and calculated values at the four monitoring points (St. 3, 7, 9, and 10) under high-water flow conditions. However, some deviations were observed and it will be important to resolve these discrepancies by refining the model and to conduct trials for different scales of water discharge in the future.

In this project we have started the monitoring in the Kuchibuto River basin (Fig. 1(a)) for the simulation of the suspended and dissolved cesium-137 concentrations in river waters by TODAM model. In the Kuchibuto River basin, the water level and turbidity have been monitored at the 4 monitoring point (①Upstream, ②Midstream, ③Downstream, and ⑤Mizusakai River. Fig1(a)). In this survey, we have started monitoring of the concentrations of suspended and dissolved cesium-137 in river water at both base- and high-water flows at a total of five monitoring points, including those points and a new point in a tributary river ④ AdachiOhta River. We will continue this monitoring in this basin and plan to conduct simulations by TODAM model in the future.

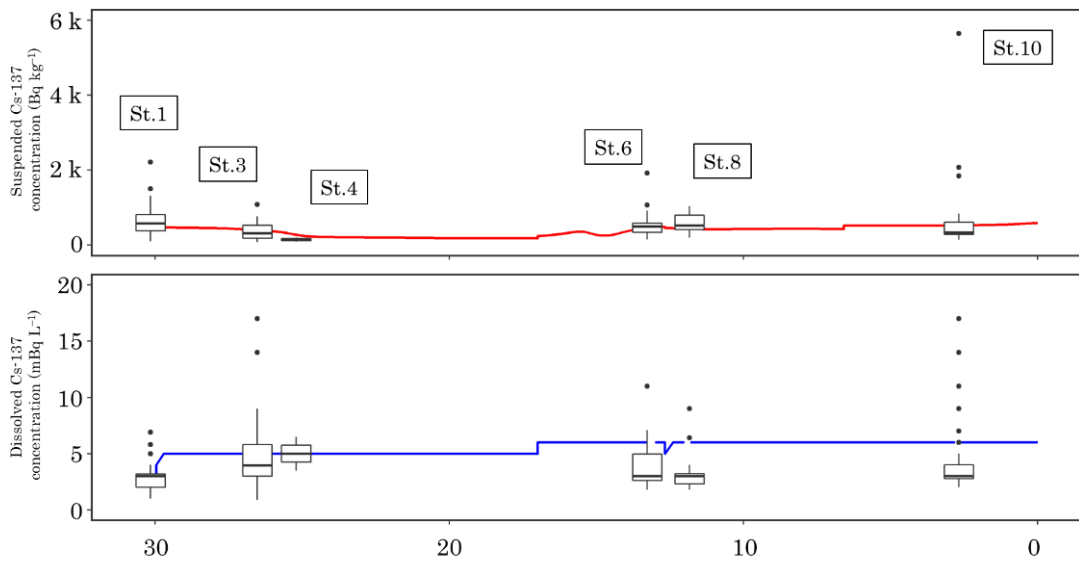


Figure 9. Simulation results of changes of cesium-137 concentration at base-flow levels water estimated using the TODAM model

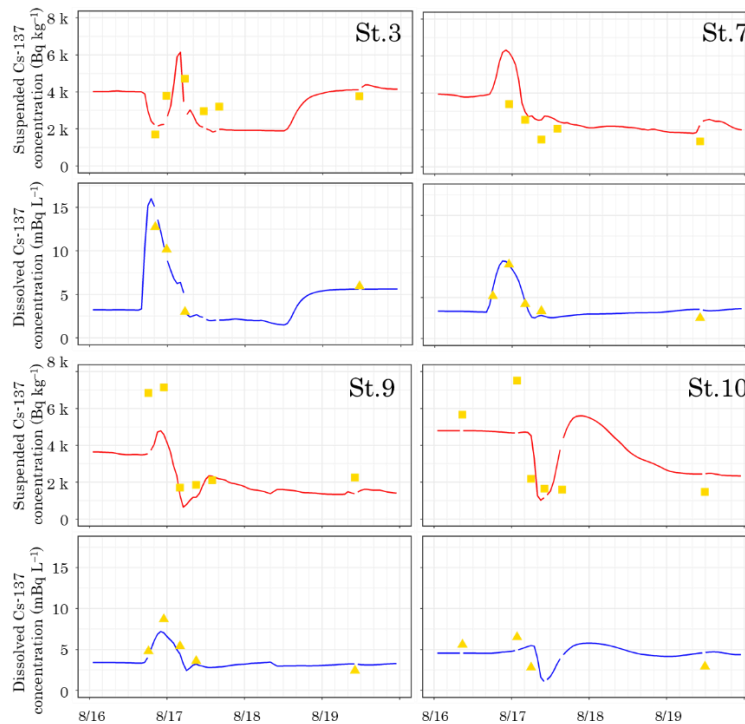


Figure 10. Simulation results of changes in cesium-137 concentrations during flood events estimated using the TODAM model. [Upper rows: Suspended cesium-137 concentration, lower rows: Dissolved cesium-137 concentration] (high-water flow events from 16 August 2016 to 19 August 2016)

The concentration of SS in river water increases substantially during high water flows compared to that in base water. In the Hirose River Basin, significantly higher SS concentrations were also observed under high-flow conditions than under base-flow conditions (Fig. 11). This large amount of SS is transported by the river and carries with it large amounts of radioactive cesium to the ocean. In this project, to clarify the source of the SS loads (a supply source), we focused on SS that is added to the river under high-flow conditions. For this purpose, we estimated the load source of the SS based on the qualitative information of the organic matter (carbon, nitrogen, etc.) in the SS.

The stable isotope ratios ($^{13}\text{C}/^{12}\text{C}$ and $^{15}\text{N}/^{14}\text{N}$), which represent the qualitative information of the organic matter, were also analyzed. In future, the relative contribution of each load source will be estimated by mixing the values of the potential load sources (riverbank soil, riverbed sediments, organic matter from upstream forests, etc.) and the changes in the relative contributions of each load source with the increase in the SS concentration will be verified.

1.5. Conclusions

In this project, continuous monitoring of the radiocesium concentrations in river water in Fukushima Prefecture is reported. The findings of the present study indicate that the decreasing trend observed in radiocesium concentrations reported previously has been maintained. In addition, the decontamination activities carried out in the basin have had a noticeable effect on the concentrations of suspended cesium-137 in the river runoff in the region. The simulation results were refined under base-flow condition. In addition, the simulation was carried out under high-flow condition. Finally, preparations for new surveys and monitoring have been started in another basin.

References

- 1) Taniguchi, K., Onda, Y., Smith, H. G., Blake, W. H., Yoshimura, K., Yamashiki, Y., Kuramoto, T., Saito, K. 2019. Transport and redistribution of radiocaesium in Fukushima fallout through rivers. 2019. *Environ. Sci. Technol.* 53, 12339–12347.
- 2) Onishi, Y., and Perkins, W.A. 1994. *TODAM One-dimensional Sediment and Contaminant Transport Model with Multiply Connected Networks. Theory and Numerical Methods*, vol. 1, Pacific Northwest National Laboratory, Richland, Washington.
- 3) Perkins, W., and Onishi, Y. 1994. *TODAM One-dimensional Sediment and Contaminant Transport Model with Multiply Connected Networks User's Guide*, vol. 2,

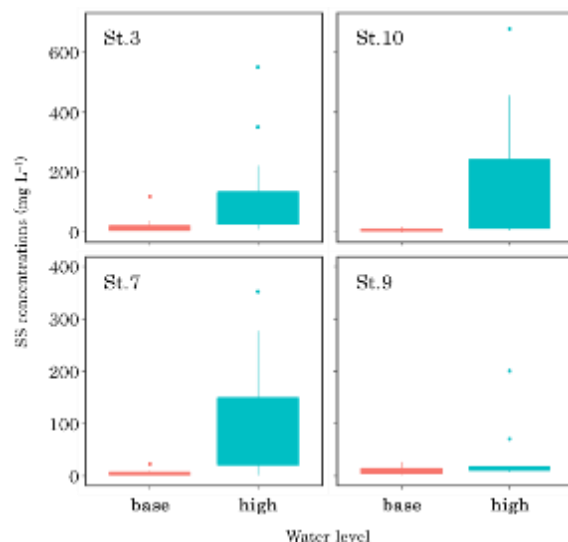


Figure 11. Concentrations of SS in river water under base- and high-flow conditions.

Pacific Northwest National Laboratory, Richland, Washington.

- 4) Smith, J.T., Voitsekhovitch, O. V., Konoplev, A. V., Kudelsky, A. V. 2005. Radioactivity in aquatic systems, in: Smith, J.T., Beresford, N.A. (Eds.), Chernobyl - Catastrophe and Consequences. Praxis Publishing, 139–190.
- 5) Hikaru Miura, Yuichi Kurihara, Aya Sakaguchi, Kazuya Tanaka, Noriko Yamaguchi, Shogo Higaki, Yoshio Takahashi. Discovery of radiocesium-bearing microparticles in river water and their influence on the solid-water distribution coefficient (K_d) of radiocesium in the Kuchibuto River in Fukushima. 2018. *Geochem. J.* 52. (2). 145–154.
- 6) Yukihiro Satou, Keisuke Sueki, Kimikazu Sasa, Hideki Yoshikawa, Shigeo Nakama, Haruka Minowa, Yoshinari Abe, Izumi Nakai, Takahiro Ono, Kouji Adachi, Yasuhito Igarashi. Analysis of two forms of radioactive particles emitted during the early stages of the Fukushima Dai-ichi Nuclear Power Station accident. 2018. *Geochem. J.* 52. (2). 137–143.
- 7) Yasuhito Igarashi, Toshihiro Kogure, Yuichi Kurihara, Hikaru Miura, Taiga Okumura, Yukihiro Satou, Yoshio Takahashi, Noriko Yamaguchi. 2019. A review of Cs-bearing microparticles in the environment emitted by the Fukushima Dai-ichi Nuclear Power Plant accident. *J. Environ. Radioact.* 205–206.101–118.

2. FIP2 Survey of Radionuclide Movements in Wildlife

2.1. Abstract

Fukushima Prefecture is conducting surveys and studies on the migrations of radionuclides to wild animals that constitute a part of the ecosystem to understand the movements of radionuclides in the ecosystem.

The present survey has investigated fluctuations in the concentration of radiocesium contained in the bodies of wild animals over time. Because of a possibility that wild animals with high radiocesium concentrations in their body have been moving into areas where wild animals with relatively low radiocesium concentrations, therefore, the movements and dispersion of animal populations were investigated.

2.2. Purpose

The accident at the Fukushima Daiichi Nuclear Power Plant caused a widespread environmental contamination by radioactive materials. Radionuclides have been detected in many wild animals inhabiting the natural environment there because they ingested radioactive materials from the environment through food.

In order to ensure the safety and security of environment that citizens of Fukushima prefecture are living, the Prefectural government, since immediately after the accident in 2011, has been monitoring radionuclide concentrations in the muscles of game animals whose meat is generally consumed by people. As a result of monitoring, mainly cesium -134 and 137, which are gamma-ray emitting nuclides, have been detected from the muscles of wild animals. This led to the launching of surveys and studies on radiocesium movements in the ecosystem. The migration of cesium-137 from the environment to the wild animals seems to be strongly affected by their ecology such as food habits and behavioral patterns. From 2013 to 2017, radiocesium concentrations in the bodies of wild animals were measured and their fluctuations with time and differences by animal species were investigated. In addition, wild animals' food habits and behavioral patterns deemed to be closely related to radionuclide movements into their bodies were also investigated. There is a positive relationship between the cesium-137 concentrations in the muscle and the stomach contents¹⁾. The relationship between radiocesium and the existing form fraction²⁾ was clarified by the survey from 2013 to 2017. Presently, a food habit survey by the DNA analysis of stomach contents has started, and radiocesium migration to the bodies of wild animals according to food habits have been investigated in detail. A behavioral survey regarding the home ranges of wild boars and Asian black bears using GPS collar has been also carried out, however, the number of surveying has been inadequate. To show their behavioral characteristics, the behavioral survey is being continued concurrently with the food habit survey.

In addition, the survey starting from 2018, analyses using linear models were performed to clarify the long-term fluctuations of cesium-137 concentrations in the muscles of wild animals with seasonal fluctuations taken into account. DNA analyses were carried out in order to show the structure of wild animal populations, which of the populations are increasing and which are

moving into other areas as a result of the long-term abandonment of humans in the evacuation zones (zones where the evacuees still cannot return) and in the residence-restricted zones.

2.3. Content of implementation

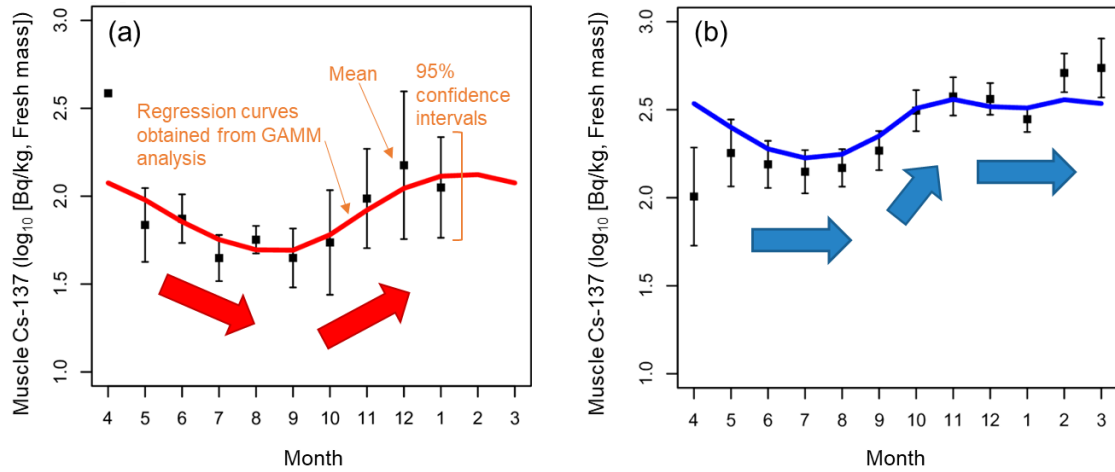
Just as in the 2013 to 2017 period, the present survey has mainly targeted wild boars, whose radiocesium concentrations have been higher than those of other wild animals, and Asian black bears inhabiting the same forestry ecosystem as wild boars.

(1) Measurement of radionuclide concentrations in the muscles of wild animals

Regarding radionuclide concentrations in the muscles of wild animals inhabiting the prefecture, the Nature Conservation Division is monitoring game species such as wild boars, Asian black bears, copper pheasants, Japanese pheasants, spot-billed ducks and mallards captured for the culling by management program or for hunting, thereby identifying the cesium-134 and 137 concentrations in their muscles. Using the measurement results, the variations of cesium-137 in the muscles of wild boars and other animals and the fluctuations over time after the accident were also investigated.

(2) Long-term fluctuations of cesium-137 concentrations in the muscles of wild boars and Asian black bears

The survey conducted from 2013 to 2017 clarified seasonal fluctuations in cesium-137 concentration in the muscles of wild animals (Figure 1) ³⁾. Based on the seasonal fluctuation patterns, the data were divided into the low-concentration period of April to August and the high-concentration period of December to March for wild boars and the low-concentration period of July to September and the high-concentration period of November to January for Asian black bears. The long-term fluctuations of cesium-137 concentrations in the muscle after the accident was analyzed with a linear model that used the \log_{10} conversion of the cesium-137 concentrations in their muscles as objective variable and the dates when they were captured and the \log_{10} conversion of cesium-137 deposition density on soils at the locations where they were captured as explanatory variables. The linear model was applied in each of the low-concentration periods, high-concentration periods and the entire period.



(Nemoto et al.,2018,PLoS ONE, Partially modified)

Figure 1. Seasonal fluctuations of Cs-137 concentrations in the muscles of (a) wild boars and (b) Asian black bears

(3) Population Structure of wild boars

We surveyed the population structure of wild boars in Fukushima prefecture using by MIG-seq analysis. DNA extracted from the muscle tissue of wild boars captured widely in Fukushima prefecture and those captured in part areas in Kumamoto Prefecture that treated as an out-group population. Single-nucleotide polymorphisms (SNPs) were obtained from genome-wide regions by MIG-seq method²⁾ for clarifying genetic structures of wild boars. We conducted STRUCTURE³⁾ and cluster analysis using the derived SNPs information. Incidentally, this survey was conducted in collaboration with the Fukushima Prefectural Center for Environment Creation and the National Institute for Environmental Studies.

2.4. Results

(1) Measurement of radionuclide concentrations in the muscles of wild animals

Figure 2 shows the cesium-137 concentrations in the muscles of wild boars and Asian black bears captured in Fukushima Prefecture in May 2011 to March 2020.

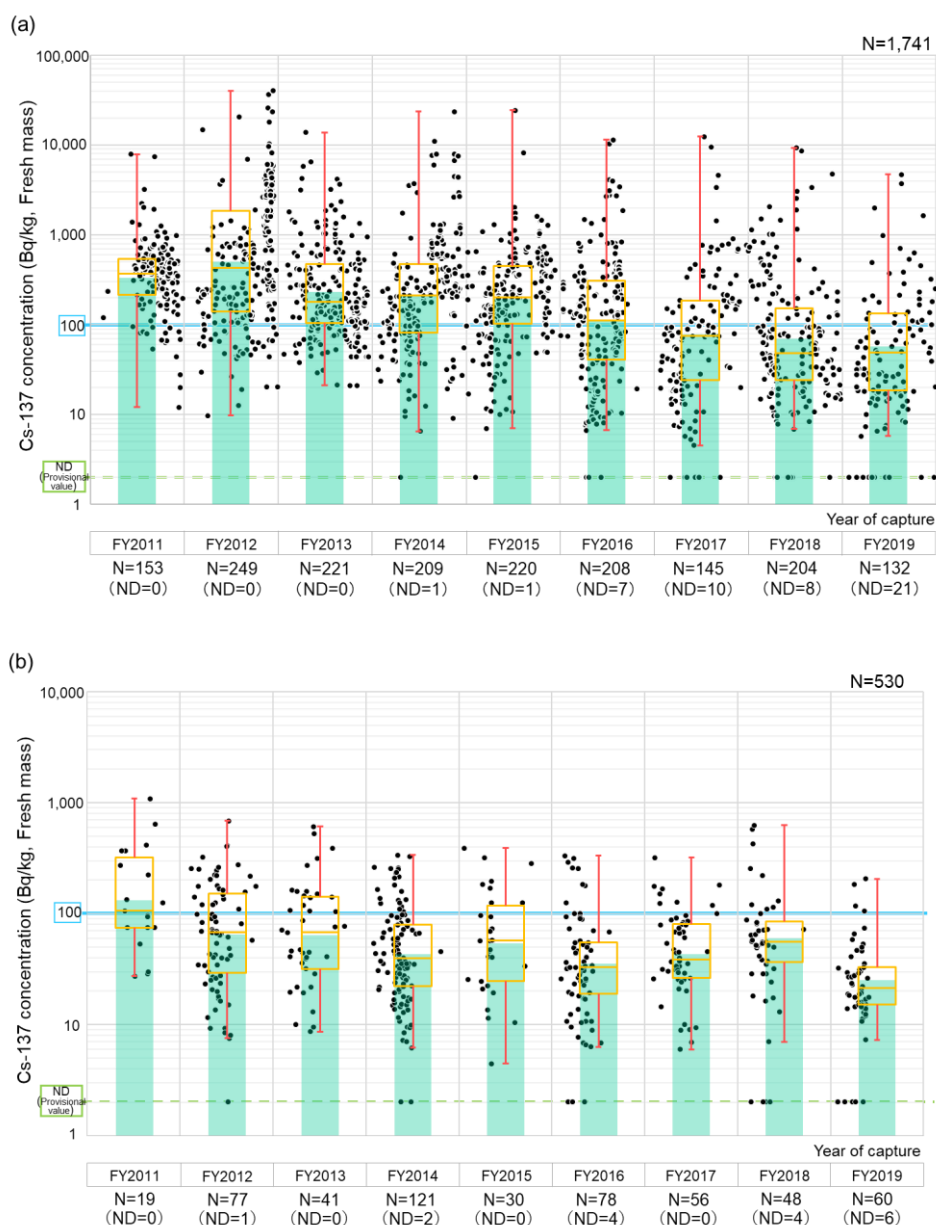


Figure 2. Results of measuring the Cs-137 concentrations in the muscles of (a) wild boars and (b) Asian black bears

* Black dot indicates the measured value of wild animal. The geometric average of Cs-137 concentrations in each fiscal year is indicated by a bar graph, the 1st quartile (25%) and the 3rd quartile (75%) are indicated by the upper and lower ends of each box respectively, and maximum and minimum values are indicated by bars (those less than lower detection limit excluded).

The cesium-137 concentrations in the muscles of wild boars showed large variation among individuals. Some of them showed concentrations lower than the detection limit although those showing concentrations close to 10,000 Bq/kg were observed even in recent years. Asian black bears showed cesium-137 concentrations exceeding 100 Bq/kg^{*1}, which is the limit for general foodstuffs in Japan, were also found in FY 2019 (*¹Sum of cesium-134 and -137).

Figure 3 shows the color-coded results of monitoring cesium-137 concentrations in the muscles of wild boars and Asian black bears by the regions of Fukushima prefecture.

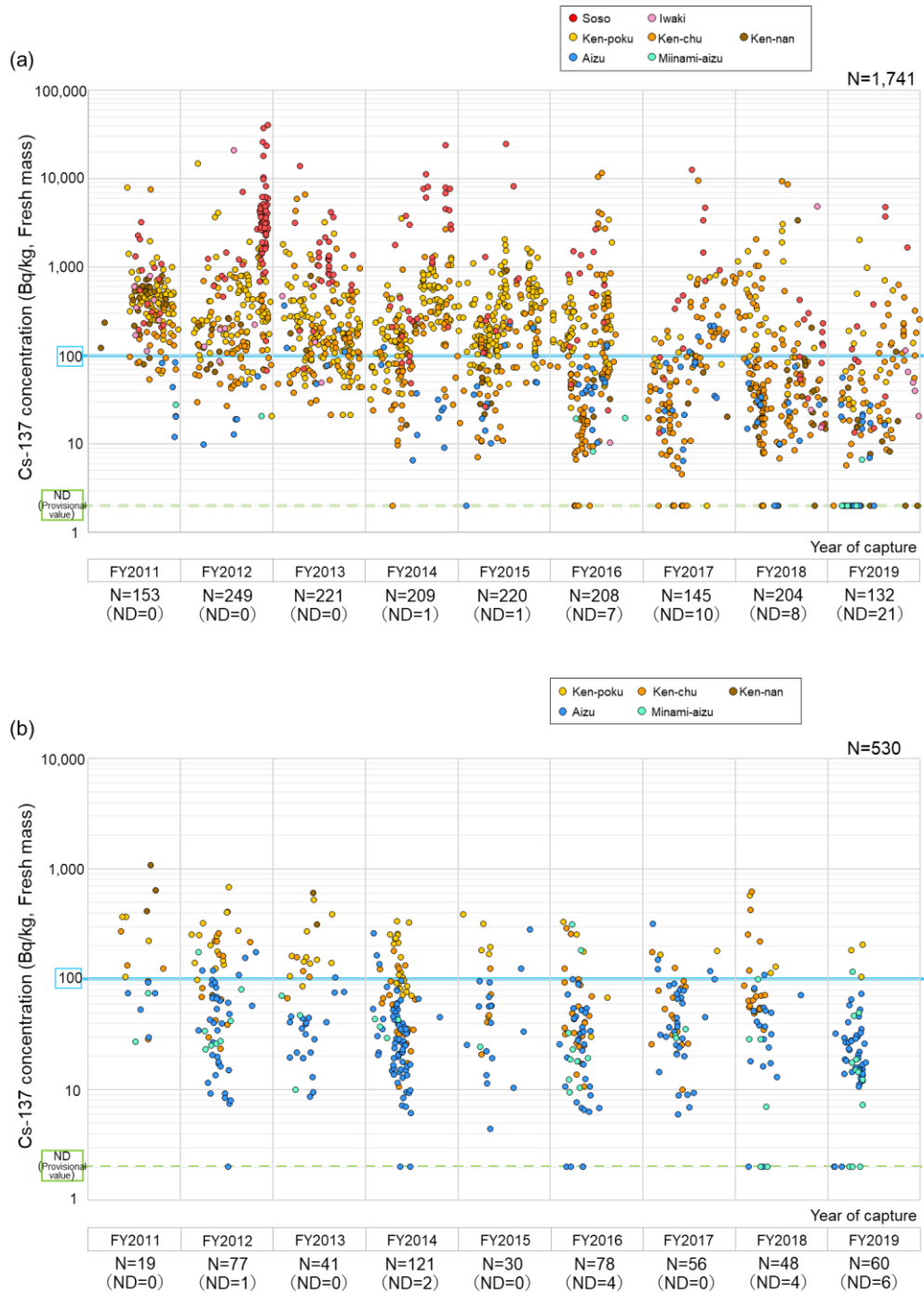
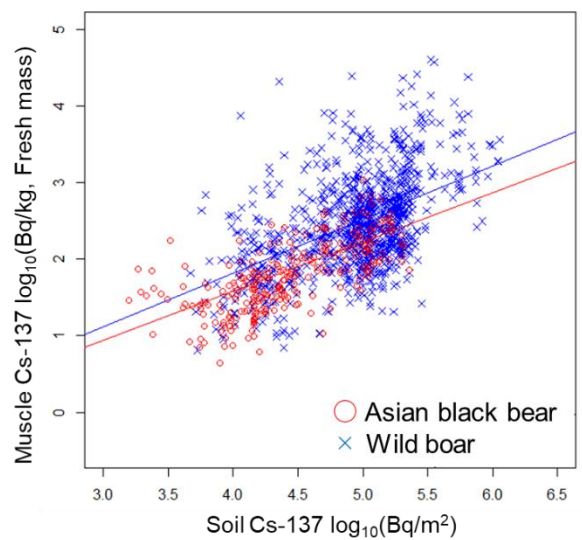


Figure 3. Cs-137 concentrations in the muscles of (a) wild boars and (b) Asian black bears (in regions where they were captured)
 * Each dot indicates the measured value for each wild animal.

The survey conducted from 2013 until 2017 revealed that the cesium-137 concentrations in the muscles of wild boars and Asian black bears were positively affected by the cesium-137 deposition density on the soils of locations where they were captured (Figure 4).¹⁾ In Soso District, Ken-poku District and Ken-chu District, where the cesium-137 deposition density on soils was relatively high, many wild boars and Asian black bears with high cesium-137 concentrations were captured. In Aizu District and Minami-Aizu District, where the cesium-137 deposition density on soils was relatively low, many wild boars and Asian black bears with low cesium-137 concentrations were captured. In Ken-chu District, those whose cesium-137 concentrations in their muscles were lower than the detection limit were captured, however, even in FY 2018, those whose cesium-137 concentrations in their muscles were close to 10,000 Bq/kg were also captured, thus suggesting the wide range of cesium-137 concentrations in their muscles.



(Nemoto et al., 2018, PLoS ONE, Partially modified)

Figure 4. Relationship between the Cs-137 concentrations in the muscles of wild boars and Asian black bears and the Cs-137 deposition density on soils of locations where they were captured

(2) Long-term fluctuations of cesium-137 concentrations in the muscles of wild boars and Asian black bears

Figure 5 shows the results of analyzing the long-term fluctuations of cesium-137 concentrations in the muscles of wild boars and Asian black bears.

With regard to cesium-137 concentrations in the muscles of wild boars, a decreasing trend was observed during the entire period, low-concentration period (April to August) and high-concentration period (December to March). However, the decreasing rate was small, and the cesium-137 concentrations estimated from a regression line showed a wide range in the high-concentration period. The wide cesium-137 concentration range during the high-concentration period and inadequate data are likely to have resulted in the imprecise estimation of a long-term fluctuation.

As for cesium-137 concentrations in the muscles of Asian black bears, a decreasing trend was observed during the entire period and the low-concentration period (July to September), but the range of estimated values widened over time during the high-concentration period (November to January).

These results suggest the necessity of the abundance of data and reconsidering the models in order to precisely estimate the long-term fluctuations of cesium-137 concentrations in both animals particularly during the high-concentration periods.

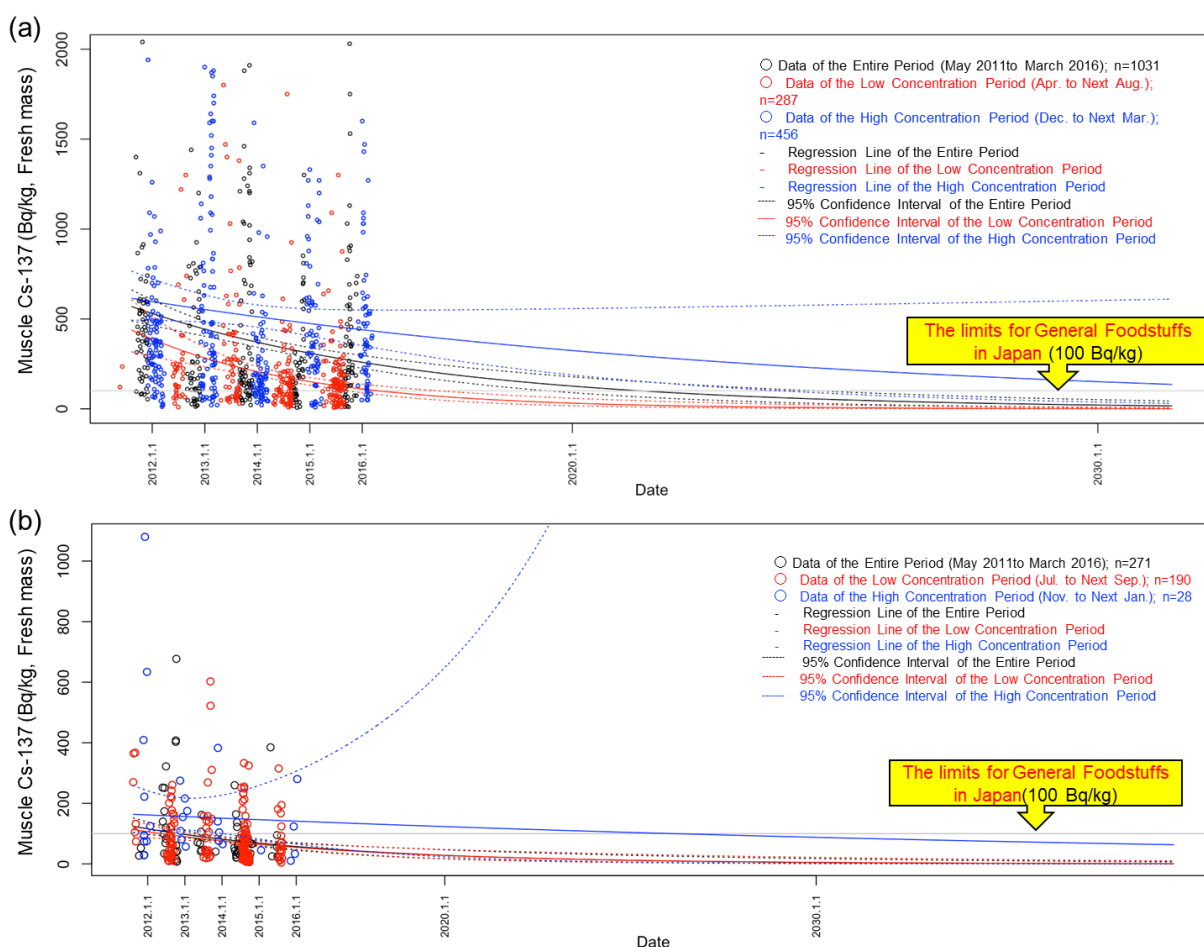


Figure 5. Long-term fluctuations of Cs-137 concentrations in the muscles of (a) wild boars and (b) Asian black bears

(3) Population structure of wild boars

Genomic DNA of wild boars was extracted from 179 specimens in Fukushima prefecture and 9 specimens in Kumamoto prefecture*, and subjecting them to a MIG-seq analysis. As a result, in a total of 688 Single-nucleotide polymorphisms (SNPs) were extracted. For confirming the geographical trends of population structure, the wild boars captured in Fukushima prefecture were classified into seven groups based on their captured locations and those captured in Kumamoto Prefecture into one group (eight groups in total) (Figure 6). A STRUCTURE³) analysis and cluster analysis using the SNPs information was then carried out. According to ΔK value under STRUCTURE analysis data, the results for wild boars suggested that they were divided into two genetic lineages (Figure 7). Moreover, the results of cluster analysis revealed two clusters that can be divided into an eastern group inhabiting northern Soso District, southern Soso District, Iwaki District and Ken-nan District of Fukushima Prefecture, and a western group inhabiting Ken-poku District, Ken-chu District and Aizu District of Fukushima Prefecture and

Kumamoto Prefecture (Figure 8). (*The meat specimens obtained in Kumamoto Prefecture are provided by Munemasa Kousan, a stock company.)

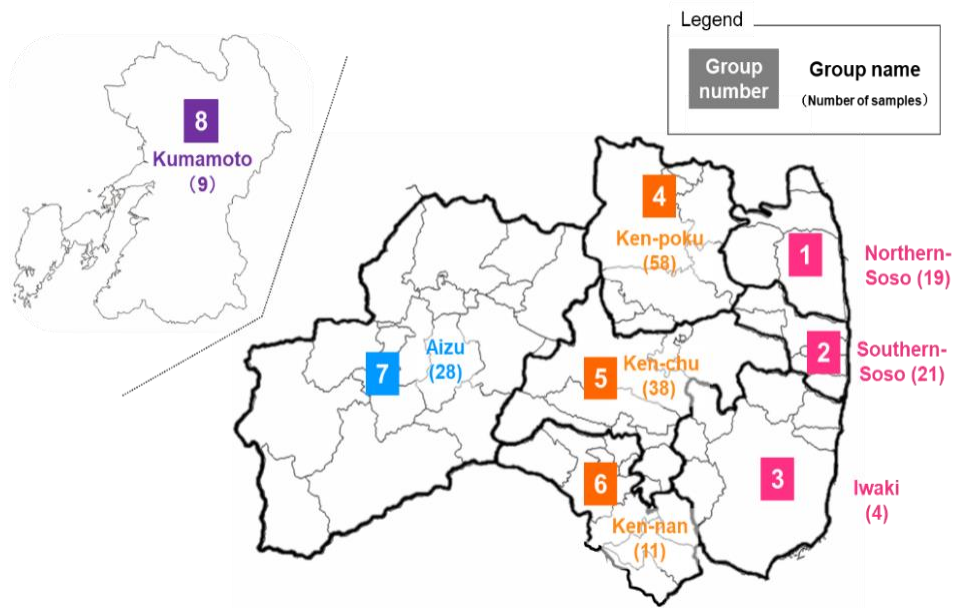


Figure 6. Grouping of specimens after their MIG-seq analyses and the number of analyses

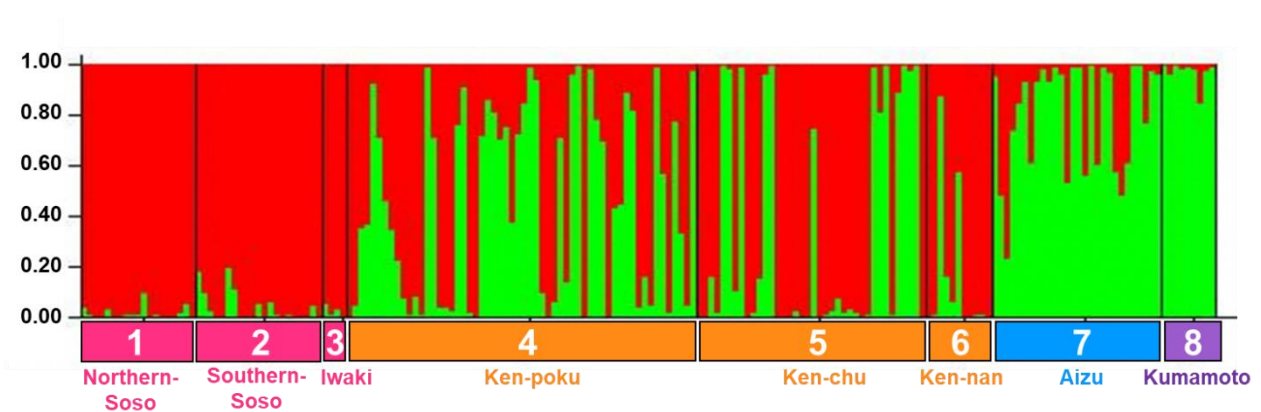


Figure .7. Results of STRUCTURE analysis based on wild boars DNA data. 2 colors (red and green) represent genetic lineages suggested by the results of STRUCTURE analysis. Ratio of the colors are of the lineages in each sample shown by vertical column (0.00–1.00)

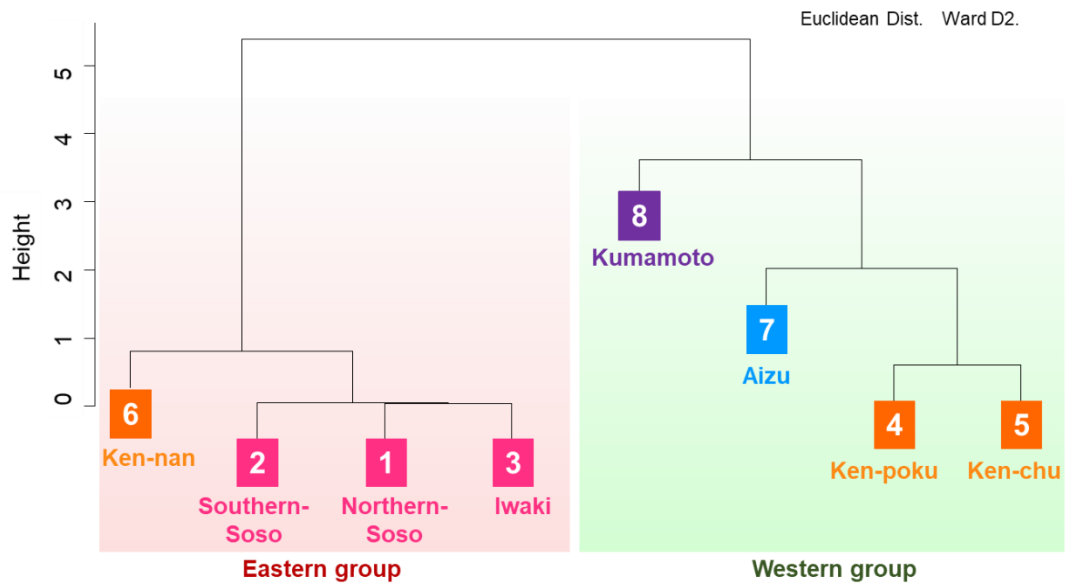


Figure 8. Results of cluster analysis based on wild boars' DNA data

Figure 9 shows the results of the detection rates of two genetic lineages in each city, town and village. These results suggested that two genetic lineages divided by the east and west area along with Abukuma river as the boundary that restricted the movement to east and west.

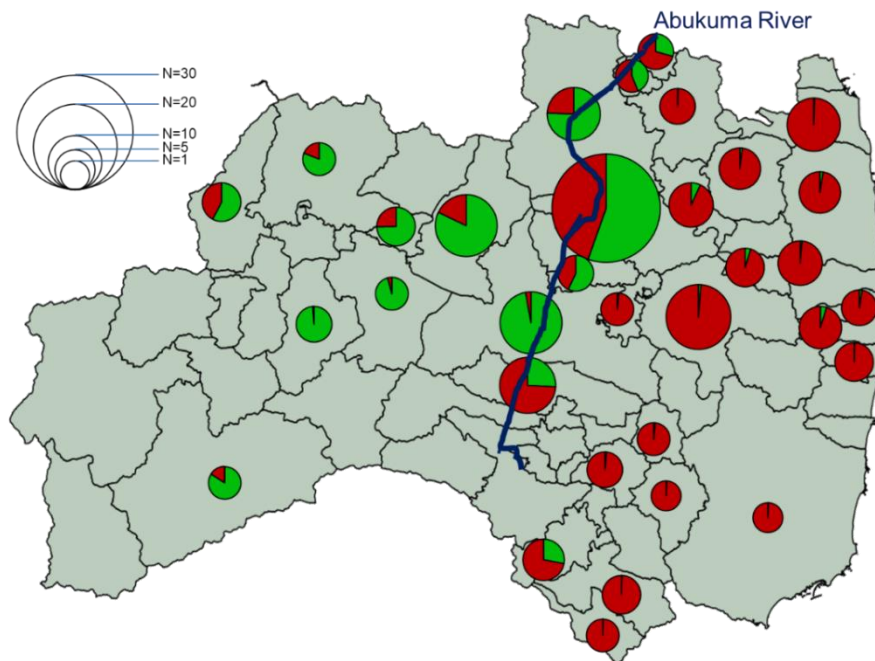


Figure 9. Geographical distribution of wild boars of two genetic lineages Ratio of genetic lineages shown by the STRUCTURE analysis (See Figure 7) in each municipality. Size of the circle represents the amount of samples.

2.5. Conclusions

High cesium-137 concentrations of muscle were observed in wild boars and Asian black bears captured in areas where the cesium-137 deposition density were high, but the concentrations significantly varied among individuals in the areas. Even in recent years, those showing concentrations exceeding the limit for general foodstuffs in Japan were captured sometimes.

Regarding long-term fluctuations of cesium-137 concentrations in the muscles of wild boars and Asian black bears, it decreased over time during the entire period and low-concentration periods. But during the high-concentration periods, the range of estimated values increased over time.

Wild boars in Fukushima Prefecture were suggested that they were divided into two lineages and these populations divided by east and west area along with Abukuma River and around as the boundary that restricted the movement to east and west.

Cesium-137 concentrations in muscles of wild boars and Asian black bears were on a decreasing trend, but they varied among individuals and fluctuated seasonally. Therefore, in order to precisely estimate their long-term fluctuations, further data expansion is necessary. Moreover, the movement and dispersion of the wild animals seem to be a factor contributing to the variation of cesium-137 concentrations observed even among those captured in the same region.

In the future, the monitoring of radiocesium concentrations in the bodies of wild boars and others will be continued, the factors contributing to the high radiocesium concentrations in some wild animals will be investigated, and survey methods to the conservation and management of wild animals will be studied.

References

- 1) Nemoto, Y., Oomachi, H., Saito, R., Kumada, R., Sasaki, M., Takatsuki, S. Effects of ¹³⁷Cs contamination after the TEPCO Fukushima Dai-ichi Nuclear Power Station accident on food and habitat of wild boar in Fukushima Prefecture. *J. Environ. Radioact.* (in press)
- 2) Saito, R., Nemoto, Y., Tsukada, H. Relationship between radiocaesium in muscle and physicochemical fractions of radiocaesium in the stomach of wild boar. 2020. *Sci. Rep.* 10, 6796.
- 3) Nemoto, Y., Saito, R., Oomachi, H. Seasonal variation of Cesium-137 concentration in Asian black bear (*Ursus thibetanus*) and wild boar (*Sus scrofa*) in Fukushima Prefecture, Japan. *PLoS ONE.* 2018. 13, e0200797.
- 4) Suyama, Y., Matsuki, Y. MIG-seq: an effective PCR-based method for genome-wide single-nucleotide polymorphism genotyping using the next-generation sequencing platform. 2015. *Sci. Rep.* 5, 16963.
- 5) Evanno, G., Regnaut, S., Goudet, J. Detecting the number of clusters of individuals using the software STRUCTURE: a simulation study. 2005. *Mol. Eco.* 14, 2611–2620.

3. FIP3 Sustainable countermeasures to radioactive materials in freshwater system

3.1. Abstract

In order to clarify the sustainability of the decontamination effect and natural radiation attenuation effect resulting from the large-scale flooding in riverside areas, field surveys were conducted targeting the decontaminated riverside areas and parks. As a result, it was found that decontamination is still in effect for five years after the test were conducted in the target riverside areas, even under the vegetation growth. It was also found that air dose rates tend to decrease at riverside parks after large flooding. It was confirmed that the effect was large near a river, and generally no re-contamination was found.

3.2. Purpose

Radioactive materials (mainly radiocesium) spreading in the environment due to the accident at the Fukushima Daiichi Nuclear Power Plant had contaminated the water environment. As a response, monitoring surveys on water, deposited materials and aquatic products were conducted to clarify the behavior of radioactive materials, and decontamination and some other measures were taken by administrative agencies and research institutions. In this project that lasted until December 2017, applicable radioactive material countermeasures were organized based on the existing knowledge accumulated domestically and abroad. A decontamination test was also performed at a river where limited decontamination measures were taken, thereby clarifying the effectiveness of sustainability of decontamination. In addition, contamination situations were surveyed targeting public riverside areas in Fukushima Prefecture. Above survey results were shown in previous report. However, flood can cause the erosion and deposition of sediments containing radioactive materials and change the contamination situation at the river. This could raise the concern of re-contamination of these public areas. For this reason, in 2018 and onward, the sustainability of decontamination effect on riverside areas where the decontamination test had been performed was continuously checked, and the contamination situations and changes in air dose rate at riverside parks due to large flooding caused by typhoon No. 19 (Hagibis) in 2019 were investigated.

3.3. Content of implementations

(1) Verification of the sustainability of decontamination effect on riverside areas under the vegetation

(a) Purpose

As a measure against external exposure at riverside areas, a decontamination test was performed in 2014 by removing deposited materials based on radiocesium distribution to check the reduction effect of the radiation dose. In most cases, however, rivers have a non-decontaminated forest area in their upstream catchments, from which earth and sand contaminated by radiocesium are supplied to the rivers when floods occur. Although the particulate radiocesium concentrations in the river water are decreasing over time, the

deposition of sediment contaminated by radiocesium raises the concern of river area re-contamination. Particularly in the case of a riverside area with a vegetation growth, fine-grained sediments with a relatively high radiocesium concentration may deposit because plants easily capture the fine sediments, which can lead to re-contamination. Therefore, in areas where decontamination tests were carried out, re-contamination due to vegetation growth was checked by a continuous monitoring of air dose rates and sediment deposition while keeping the vegetation growth unchanged.

(b) Method

The test site was set at the downstream end of the Kami-Oguni River, which is a tertiary branch of the Abukuma River, and is located 55 km northwest from the Fukushima Daiichi Nuclear Power Plant (Figure 1). The deposition amount of radiocesium (Cs-134 and Cs-137) is 300 to 600 kBq/m²¹⁾. Most of the river basin is covered by a forest, with farmlands and residential areas existing along the river (Figure 1 (b)). The decontaminated zone's total length is 170 meters, width is 15 meters on average, and the width of river channel at the base flow level is two to six meters (Figure 1 (c), 1 (d)). The river's left bank area had been used for an elementary school and access routes to the school. The right bank area had been used for an orchard, and the flood channel had been used for the elementary school's outdoor education. The elementary school and its access routes were decontaminated before the test. In the decontamination test conducted in 2014 for the riverside area, the depth distribution of radiocesium concentrations in sediments was measured first. According to the distribution, the depths of sediment removal (scraping) were set at 15 to 35 cm, and then decontamination was conducted. As a result, the average air dose rate at the decontaminated zone decreased from 0.66 μSv/h to 0.34 μSv/h. The details of the test are described in Nishikiori and Suzuki (2017)²⁾. During the period after the decontamination test until the end of 2016, all the flood channel vegetation was cut down and then observations were made. On the other hand, since 2017, observations were made without cutting down the vegetation. In 2018, an embankment construction was carried out as disaster-relief work at the upstream side of the right bank.

The air dose rates 1 meter above the ground surface of the test zone were measured during a base flow period. Newly-deposited sediments that accumulated during an observation interval and previously-deposited materials that had accumulated earlier were distinguished based on the ring method (erosion pins), and then samples of deposited materials were taken from seven points in the riverside area. Radiocesium concentrations in the deposited materials were measured after removing gravels and pebbles. The ratio of mud (silt and clay) in the entire sample mass was also calculated. Vegetation was cut down partially in the test zone, and plant biomass on the flood channel was measured. Because plant biomass before the decontamination test had not been measured, plant biomass on the flood channel without any artificial disturbance was measured in 2019 to compare the plant biomass before and after the decontamination test in 2014.

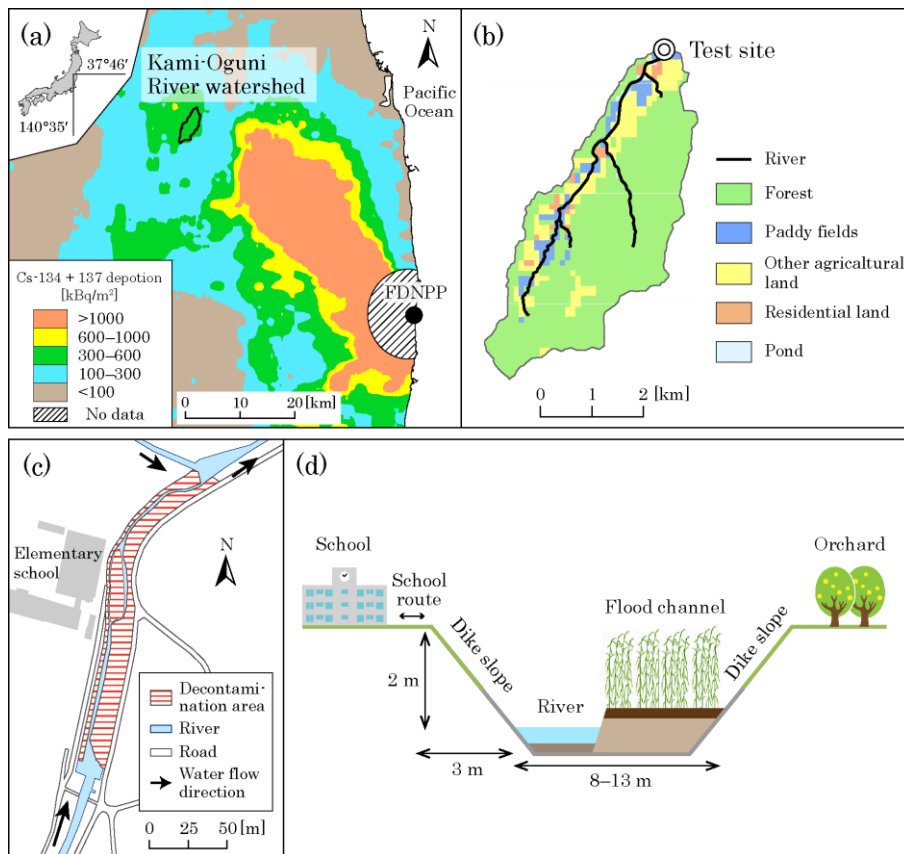


Figure 1. Outline of the Kami-Oguni River Survey Area

Note: The amounts of radiocesium deposition were derived based on the results of the 3rd aircraft monitoring (converted on July 2, 2011)¹⁾.

(2) Changes in contamination situation in riverside area due to large flooding

(a) Purpose

In a riverside area, the deposition of sediment can lead to the accumulation of radioactive materials. Surveys conducted by December 2017 also indicated that radiocesium had accumulated at river vicinities, with air dose rate increasing. In a riverside area, the erosion and the new deposition of sediments caused by large flooding due to typhoons can change the depth distribution of radiocesium concentrations (Konoplev et al., 2017³⁾; Nakanishi et al., 2019⁴⁾). Such a phenomenon reportedly lowers the air dose rate in a riverside area and is called natural attenuation.

The impact of Typhoon No. 19 (Hagibis) in October 2019 caused river dike breaches and overflows in Fukushima Prefecture, resulting in submergence of the riverside areas and causing significant damage. To clarify the presence or absence of re-contamination due to previously reported flood-caused erosion and deposition or a decrease in air dose rate due to natural attenuation, changes in air dose rate and contamination situations in the riverside area and parks after the passage of typhoon No. 19 were surveyed.

(b) Method

Surveys were carried out at two riverside parks (Figure 4) located in Hamadori area in

Fukushima Prefecture and the decontamination test site at the Kami-Oguni River (Figure 1). Park A is located along the Niida River's mainstream and Park B is located along the Mizunashi River, which is the primary branch river of the Niida River. The amount of radiocesium deposition (Cs-134 and Cs-137) at the watershed exceeded 1000 kBq/m² in the upstream area but was below 100 kBq/m² at the lowest point downstream¹⁾. The amount of radiocesium deposition was 490 kBq/m² at Park A and 210 kBq/m² at Park B⁵⁾. The areas of Park A and Park B are 2.7 ha and 1.6 ha, respectively.

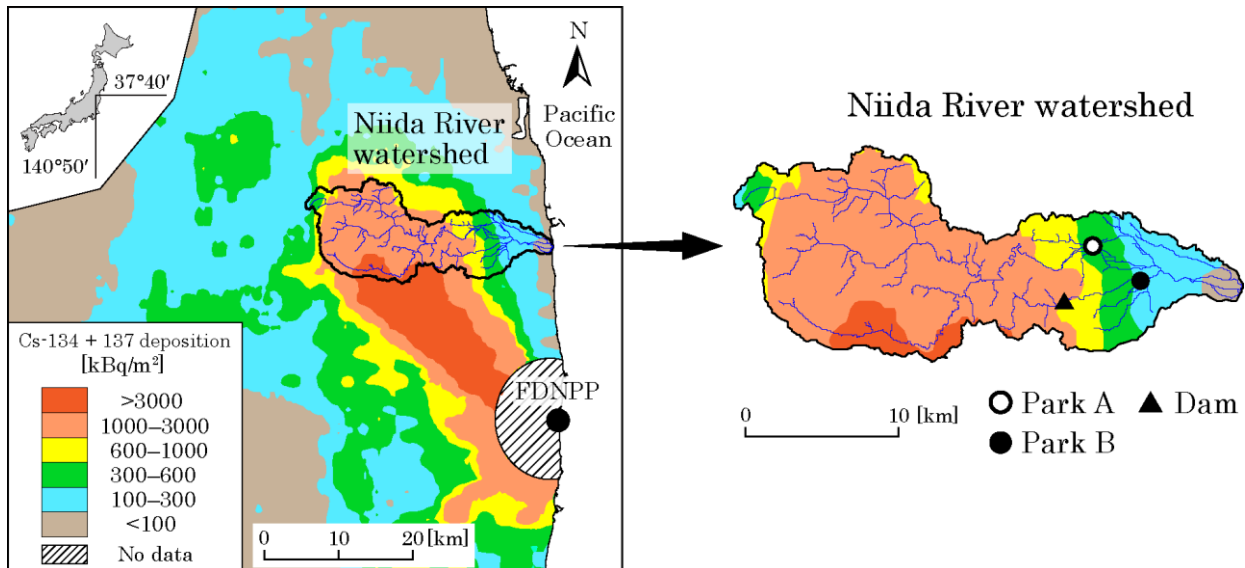


Figure 2. Survey areas in riverside parks

Note: The amounts of radiocesium deposition were derived based on the results of the 3rd aircraft monitoring (converted on July 2, 2011).¹⁾

Typhoon No. 19 Hagibis passed through Fukushima Prefecture on October 12 to 13, 2019. At the meteorological observatory (in Hara-machi) nearest to Parks A and B, a precipitation of 274.5 mm was observed as a result of a series of rainfalls⁶⁾. Dike breaches and flooding damage occurred at the major river, namely Abukuma River, and other rivers in the prefecture. River dike breaches and overtopping occurred also at the survey area.

Using a portable gamma-ray-measuring device (gamma plotter H, Japan Radiation Engineering Co., Ltd.), the air dose rates one meter above the ground surfaces were measured in the survey area. Measurements were carried out on January 31, 2018 (before the typhoon) and October 17, 2019 (after the typhoon). After the passage of the typhoon, a field observation was performed to check the sediment erosion and deposition situations in the riverside areas and parks.

3.4. Results

(1) Verification of the sustainability of decontamination effect on riverside areas under the vegetation

Figure 2 shows changes in air dose rate until the end of 2018. In the test zone, the air dose rate continued to decrease from 2017 when the cutting down of vegetation was stopped. In the decontaminated zone, a decontamination test revealed that the air dose rate generally halved and then decreased slightly faster than the pace of physical decay.

Also regarding the non-decontamination zone, the air dose rate decreased at a pace faster than physical decay, and the environmental half-life obtained by applying an exponential function was 5.9 years, which was shorter than 8.1 years for the decontaminated zone. The largest air dose rate decrease was observed after the passage of a typhoon in September 2015. It is likely that the decrease was caused by large flooding of the area. The measuring of air dose rates after the decontamination test confirmed no re-contamination.

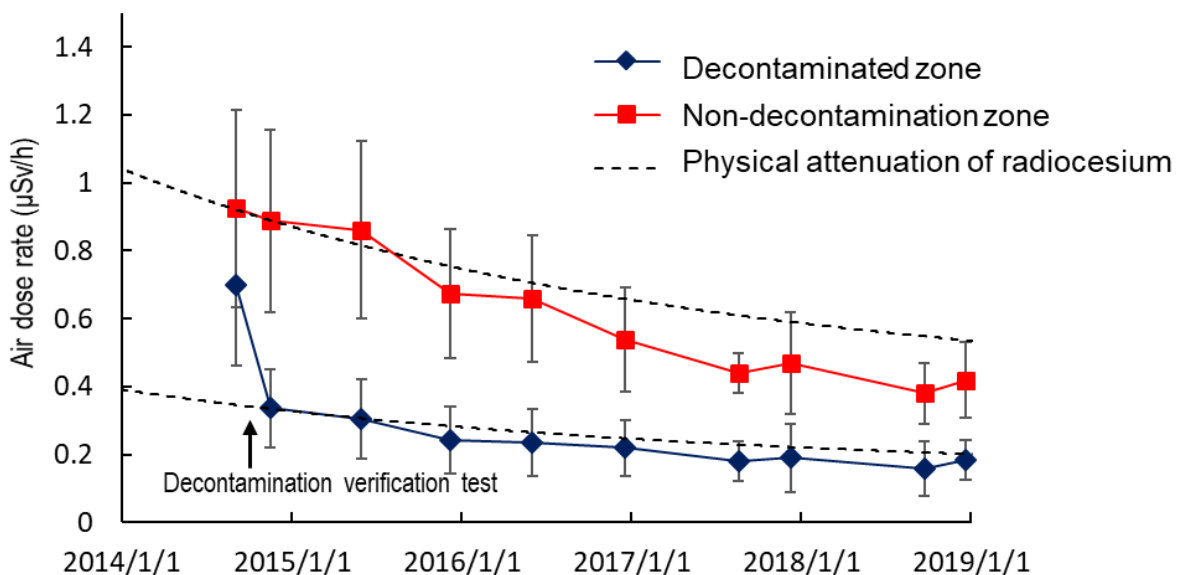


Figure 3. Changes in air dose rate at the Kami-Oguni River

Note: The physical decay of radiocesium 134 and 137 was calculated with the initial deposition ratio being 1:1. Initial values were fitted to the values measured on November 16, 2014 after the completion of the decontamination test.

From the end of 2016 until August 2017, the radiocesium concentrations in newly-deposited materials that accumulated on the flood channel with vegetation were higher than those without vegetation sampled until the end of 2016 and were higher than those in previously-deposited materials sampled in August 2017 (Figure 4). These sediments contained relatively high ratios of clay and silt, and it is understood that the vegetation trapped the fine-grained sediment. However, compared with deposited materials in the riverside area before the decontamination test, radiocesium concentration and mud ratio were smaller in these sediments. It is likely that, because the amount of their deposition was not high, the measurement in August 2017 did not

show an increase in air dose rate.

On the other hand, after typhoon No. 21 (Lan) in 2017, a 20 cm thick sediment deposited in the riverside area (Figure 3). However, their radiocesium concentration was lower than that of surface soil after the decontamination test, and their mud ratio was low. Biomass quantity in the riverside area in the summer of 2017 was 40 % of the pre-decontamination-test reference value measured in 2019. After one-year vegetation recovery, a normal rainfall can cause the deposition of fine-grained sediment whose cesium concentrations are high, but the trapping effect of the fine-grained sediments is deemed to have been small in large-scale flooding caused by typhoons. In 2018, large-scale rainfalls that involved the deposition of sediments were few and the radiocesium concentrations and mud ratios in deposited materials were also low.

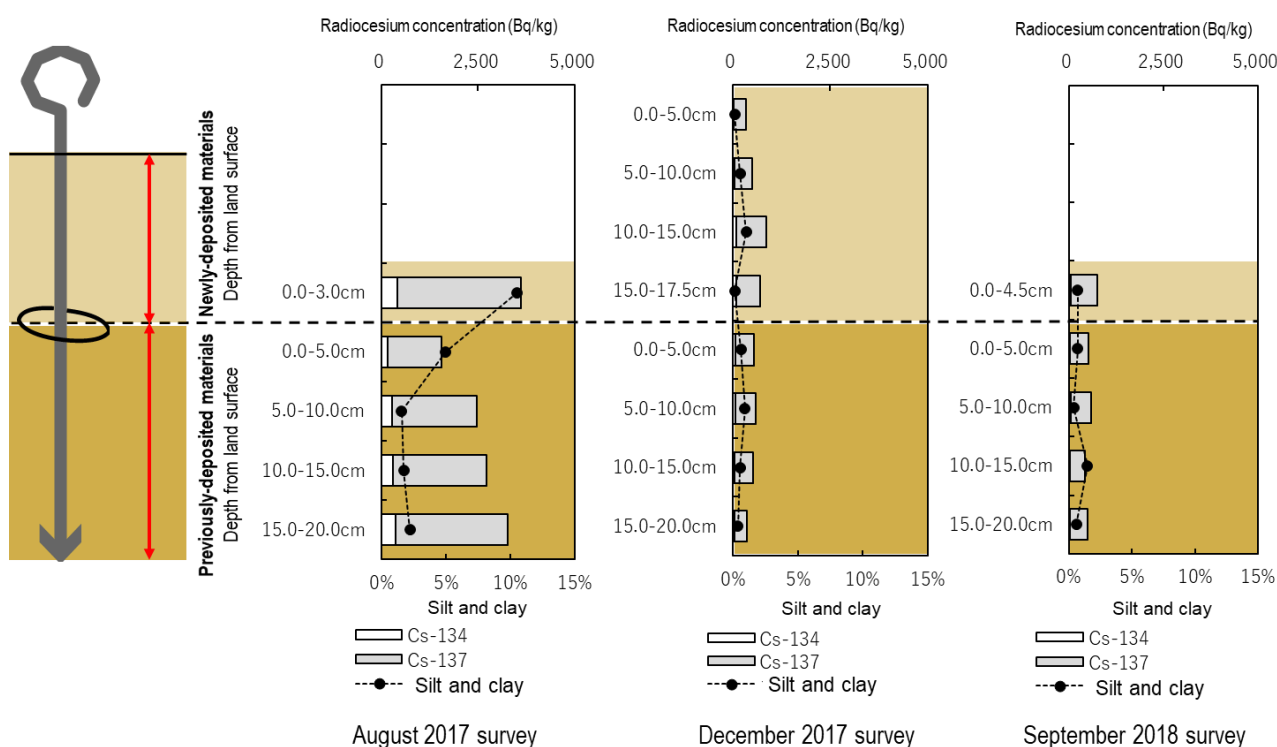


Figure 4. An example of depth distribution of radiocesium concentrations in deposited materials in a riverside area (center of the survey area)

(2) Changes in contamination situation in riverside area due to large flooding

The results of air dose rate measurement in Park A are shown in Figure 5. The average air dose rates before the typhoon Hagibis (January 31, 2018) and after the typhoon (October 17, 2019) were 0.30 $\mu\text{Sv/h}$ and 0.20 $\mu\text{Sv/h}$, respectively. The air dose rate decreased by 13% during the interval between two measurements because of physical decay. With this taken into account, the typhoon and rainfall effect decreased the air dose rate by 23% compared with that before the typhoon. In comparison, the air dose rate after the passage of Typhoon No. 15 (Etau) in September 2015 decreased to 14% of that before its passage. It was obvious that the effect of typhoon Hagibis was stronger than typhoon Etau. This difference in effect resulted from differences in

the scales of erosion and deposition. As shown in the aerial photographs (Figure 5), Typhoon Hagibis also eroded a significant amount of sediments along the Niida River. Portions that had shown the highest radiation level during the pre-typhoon measurement flowed away, and the bank protections of the parks were exposed (Figure 6 (a)).

In this area, highly-concentrated radiocesium was present at first, but the passage of Typhoon Etau in 2015 also resulted in less contaminated sediment depositing on the surface and shielded the highly-contaminated portions, thus lowering the air dose rate as shown in the previous report. However, as Figure 6 (b) shows, sediment remained deposited and vegetation was growing on the bank protections. A decrease in air dose rate after the passage of Typhoon Hagibis was caused by the removal of radiation sources by the typhoon, so the typhoon's effect seems to have been larger than the shielding effect that occurred after Typhoon Etau. On the other hand, because the deposition of a large amount of sand was observed at the Niida River flowing in the park and the branch river north of the park (Figure 6 (c) and (d)), a decrease in air dose rate inside the park seems to have resulted from a shielding effect.

As for Park B, the average air dose rates before and after the passage of Typhoon Hagibis were 0.21 $\mu\text{Sv/h}$ and 0.16 $\mu\text{Sv/h}$, respectively. After the correction of physical decay, the average after the passage of the typhoon decreased by 12% of that before its passage because of the effect of typhoon Hagibis (Figure 7). In comparison with the effect of Typhoon Etau in 2015 decreasing the air dose rate by 5% of that before its passage, Typhoon Hagibis in 2019 significantly decreased the air dose rate in Park B in the same way as in Park A. The passage of Typhoon Etau caused almost no erosion or deposition in Park B, but the passage of Typhoon Hagibis flooded the entire park, changed the river channels at the park's upstream, and deposited a large amount of sand, gravel and pebble particularly at the upstream area in the park. Decrease in the air dose rate was also larger in the upstream side of the park. This would imply that the shielding effect by deposited sediments decreased the air dose rate.

In the Kami-Oguni River survey area, air dose rate decreased not only in the river channel but also on the river bank. Although most of sediments in the river channel had been removed by the excavation work immediately before the survey, a large amount of sediments such as sand, pebble and gravel were re-deposited.

This survey revealed that Typhoon No. 19 Hagibis in 2019 did not cause re-contamination in all survey sites generally; rather, it was confirmed that natural attenuation has caused the decreased air dose rate.

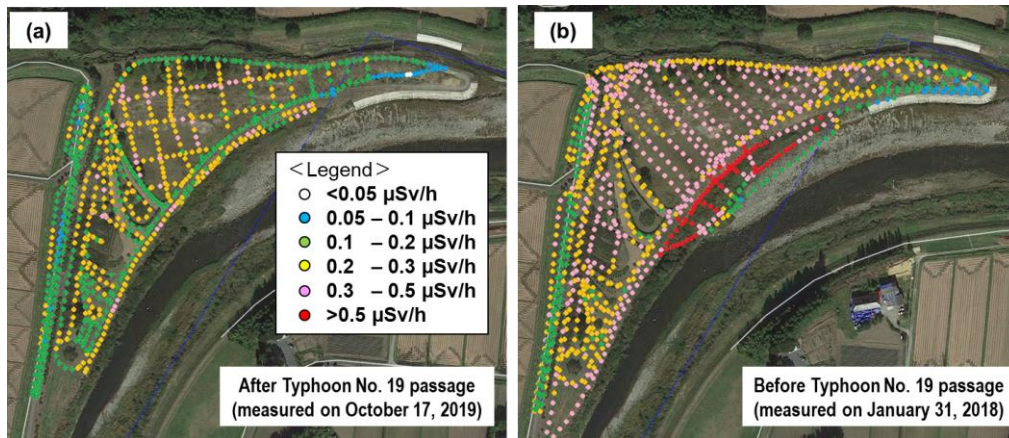


Figure 5. Air dose rate distribution in Park A [(a) after the passage of Typhoon No. 19, (b) before its passage]

Note: Background photograph (a) is a satellite image taken by the Cabinet Intelligence and Research Office⁷⁾ on October 17, 2019. Background photograph (b) was obtained from Google Earth Pro⁸⁾ (date of the photo: October 21, 2018).

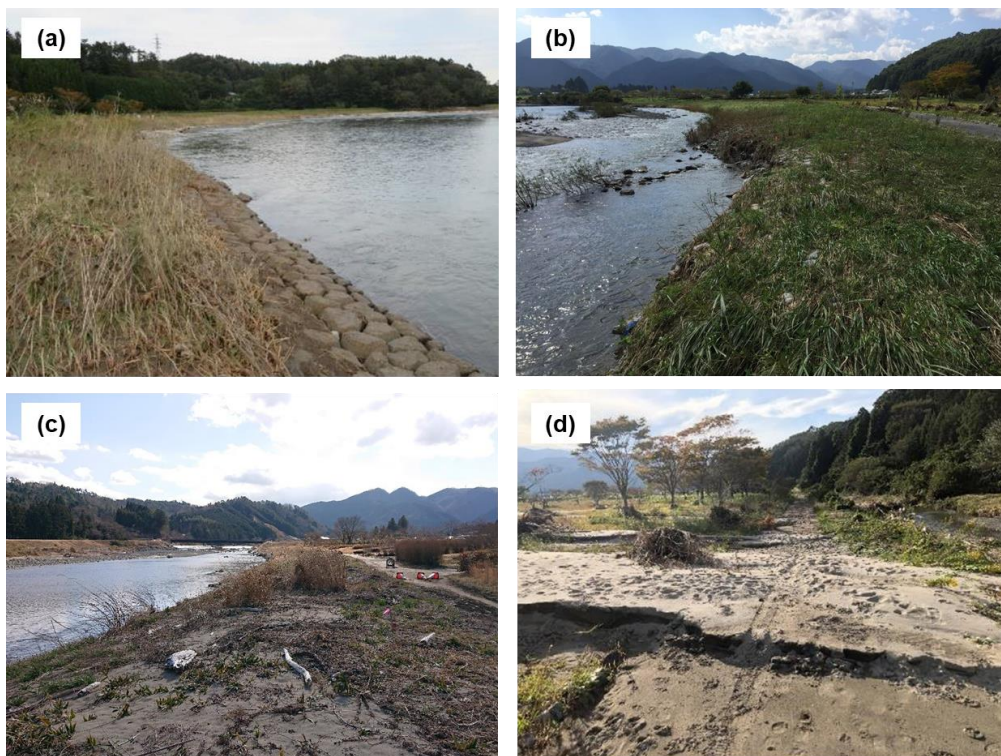


Figure 6. Photos showing the situations of riverside areas (a) River revetment exposed due to river bank erosion caused by the passage of Typhoon No. 19, (b) The same river revetment before being eroded (a photo taken from the opposite side on September 28, 2015), (c) Sediments deposited along the Niida River, (d) Sediment deposited along the branch river north of the park

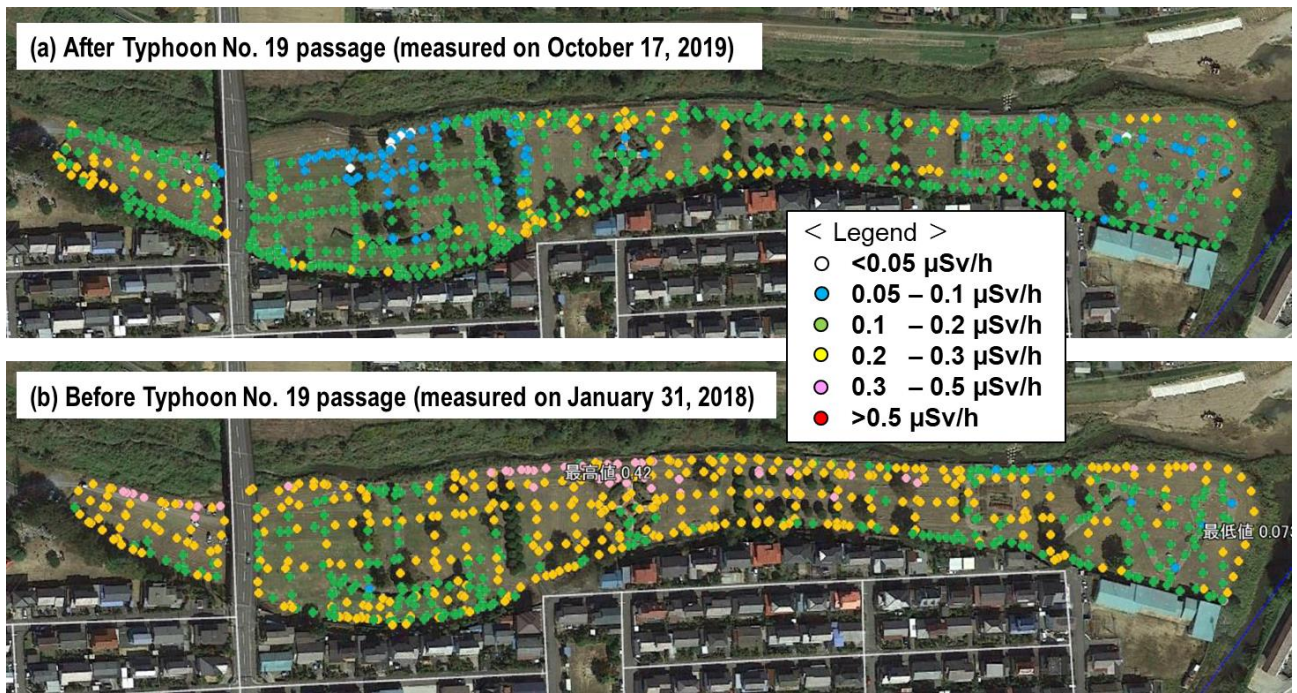


Figure 7. Air dose rate distribution in Park B

(a) After the passage of Typhoon No. 19, (b) Before its passage

Note: The background photographs were obtained from Google Earth Pro⁸⁾ (date of the photos: October 21, 2018).

3.5. Conclusions

In this project, we continued to confirm the persistence of the decontamination test in 2014. In the decontaminated riverside site, air dose rate decreased with time even on the vegetated flood channel after 2017 following typhoons. An increase in radiocesium accumulation on the flood channel was not observed. These results show the persistence of the decontamination test. In addition, we surveyed the change in the air dose rate in the riverside parks after typhoon No. 19, Hagibis, which caused significant damage in Fukushima Prefecture in 2019. After the passage of typhoon Hagibis, air dose rate in the riverside parks generally decreased. Recontamination by the deposition of the sediments with high radiocesium concentration was not observed, rather natural attenuation during the flooding occurred.

In the future, we continue to monitor the riversides and the riverside parks to confirm the persistence of the impact of the decontamination test as well as to understand the recontamination and the change in the air dose rate after the large flooding by typhoons.

References

- 1) Ministry of Education, Culture, Sports, Science and Technology. 2011. The Results of Measuring Radiocesium Deposition by the 3rd Aircraft Monitoring https://radioactivity.nsr.go.jp/ja/contents/5000/4858/24/1305819_0708.pdf
- 2) Nishikiori, T., Suzuki, S. 2017. Radiocesium decontamination of a riverside in Fukushima, Japan. *Journal of Environmental Radioactivity* 177, 58-64.
- 3) Konoplev A., Golosov V., Wakiyama Y., Takase T., Yoschenko V., Yoshihara T., Parenjuk O., Cresswell A., Ivanov M., Carradine M., Nanba K., Onda Y. 2017. Natural attenuation of Fukushima-derived radiocesium in soils due to its vertical and lateral migration. *Journal of Environmental Radioactivity*. doi:10.1016/j.jenvrad.2017.06.019.
- 4) Nakanishi T., Sato S., Matsumoto T. 2019. Temporal changes in radiocesium deposition on the Fukushima Floodplain. *Radiation Protection Dosimetry*, 1–4. doi:10.1093/rpd/ncz086
- 5) Nuclear Regulatory Authority. 2017. Radiation Distribution Map Website. <http://ramap.jmc.or.jp/map/>
- 6) Japan Meteorological Agency. 2020. Data and documents <http://www.jma.go.jp/jma/menu/menureport.html>
- 7) Cabinet Intelligence and Research Office. 2019. Processed Images of Areas Damaged by Typhoon No. 19 in 2019 <https://www.cas.go.jp/jp/houdou/191017csice.html>
- 8) Google Earth Pro aerial photograph

4.FIP4 Development of environmental mapping technology using GPS walking surveys

(Note: Reprint of the previous report with some wordings revised and update added since the theme ended in FY2015)

4.1. Abstract

Fukushima Prefecture developed environmental mapping technology with GPS walking surveys as a tool for surveying the regional distribution of air dose rates.

This report covers the results of parameter verification necessary for the development of this technology and the history of development.

4.2. Purpose

To understand the air dose rate (hereinafter simply referred to as the dose rate) in Fukushima Prefecture after the accident at the Fukushima Daiichi Nuclear Power Plant, we have conducted fixed-point measurements with monitoring posts and dose rate measurements in car-borne surveys using the GPS-linked dose rate measurement device KURAMA (Kyoto University Radiation Mapping System)-II, and have provided information to prefecture residents on the prefecture homepage (Figure 1 and 2).

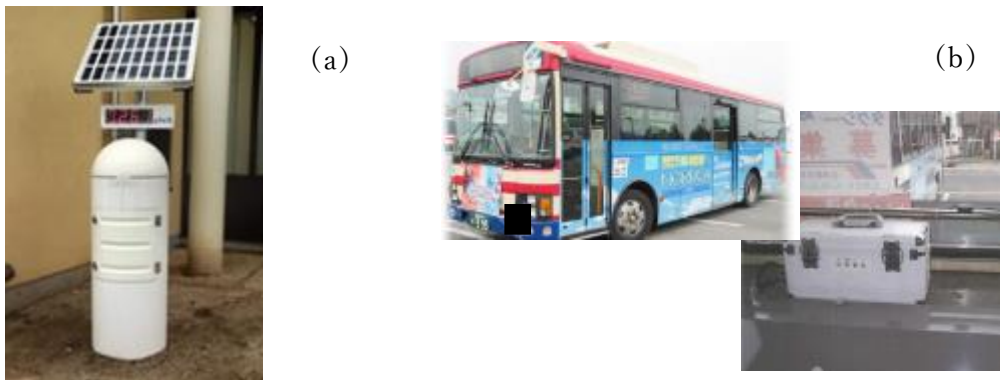


Figure 1. Example of current monitoring

(a): Example of a fixed-point measurement(using a real-time dose-rate measurement system)

(b): Example of a car-borne survey (KURAMA-II installed on the back of a local bus)



Figure 2. Fukushima Prefecture radiation measurement map
 (<http://fukushima-radioactivity.jp/pc/>)
 (a): Example of a fixed-point measurement
 (b): Example of a traveling survey

As of March 2016, measurements are being made at 3500 fixed points with monitoring posts in Fukushima Prefecture. Car-borne surveys using local buses are also being conducted with the purpose of interpolating the fixed-point measurements.

It is, however, difficult to conduct fixed-point measurements or car-borne surveys in some places, including parks, forests, and alleys near residential areas, and dose rates sometimes differ between fixed measuring points at the same facility or site (Figure 3). For these reasons, in addition to fixed-point measurements and car-borne surveys, we require measurement technology with which to understand a more detailed distribution of dose rates, and we need to present the measurement results in a format that is easy to understand.

Therefore, to employ interpolation to obtain dose rates for parks, forests, and alleys near residential areas where fixed-point measurements and car-borne surveys are difficult, we developed environmental mapping technology using GPS walking surveys together with unmanned aerial vehicles (UAVs) developed by the IAEA.

The prefecture and IAEA have shared the development of environmental mapping technology with GPS walking surveys (FIP4) and environmental mapping technology with unmanned aerial vehicles (FCP3), and by combining these technologies and visualizing measurement results, we were able to create dose distribution maps that are more detailed and effective.

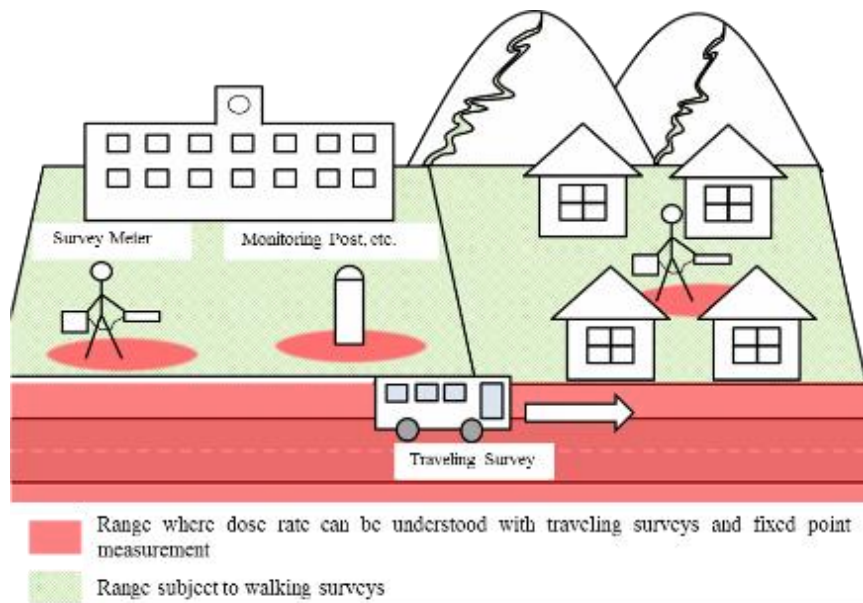


Figure 3. Measurement ranges of conventional measurement methods

4.3. Content of implementation

(1) Development of equipment

We used the KURAMA-II, which was developed by Kyoto University, for walking surveys, and assembled five pieces of equipment in a way suited to walking surveys (Figure 4). The orange backpack contains a CsI (T1) scintillation detector, which is a low-dose-rate detector, and a high-precision GPS unit. The back packer measures the dose rate by walking on a transverse course while merging dose rate data from the low-dose CsI detector and position information from the high-precision GPS device.



Figure 4. Walking survey equipment

(a): Appearance of the devices

(b): Low-dose-rate CsI detector (Hamamatsu Photonics K.K. C12137-01) and high-precision GPS unit (SOKKIA GIR1600)

The measurement screen is shown in Figure 5. The measurement interval may be selected as 3 seconds, 5 seconds, and so on. At the start of the measurement, information such as the current position and dose rate are recorded to a notebook computer, and the position information, dose rate, trends, and mapping results are displayed on the computer screen.

Measurers can look at the screen to check the measurement position and dose rate while conducting detailed measurements.

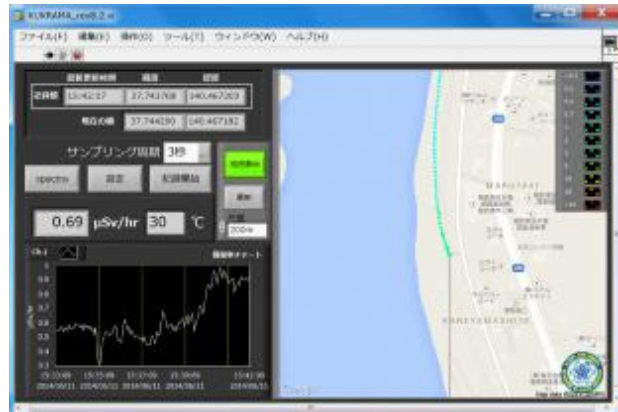
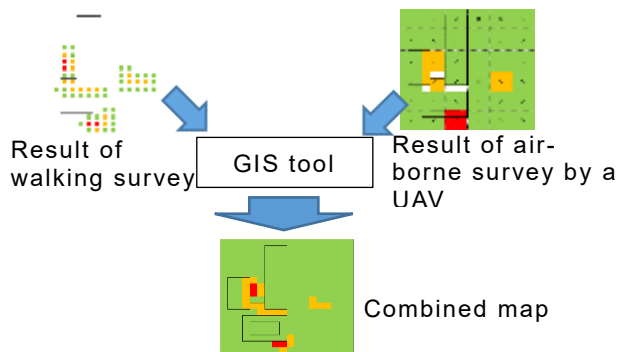


Figure 5. Display screen on a personal computer

(2) Development of mapping technology using Geographic Information System (GIS)

We conducted a specification study and developed a GIS tool for capturing, combining, and mapping the dose rate and position information gained from walking surveys and UAVs. An overview of the tool is shown in Figure 6.



1	年月日	時間	緯度	経度	標高	速度	方位	線量率	補正線量率	検出器温度
2	2013/12/12	13:50:19	37.478630	140.857104	27.2	0.7	202.37	1.9		10.37
3	2013/12/12	13:50:22	37.478629	140.85710	27.1	0.4	213.87	1.05		10.37
4	2013/12/12	13:50:25	37.478631	140.857101	28.9	0.5	341.95	1.02		10.37
5	2013/12/12	13:50:28	37.478628	140.857106	27.2	4.4	143.05	1.93		10.37
6	2013/12/12	13:50:21	37.478625	140.857194	27.3	8	182.24	2.09		10.37
7	2013/12/12	13:50:24	37.478624	140.85721	29.1	3.2	52.5	2.1		10.37
8	2013/12/12	13:50:27	37.478625	140.857241	29.2	8.8	111.9	2.43		10.37
9	2013/12/12	13:50:40	37.478628	140.857289	29.3	0.2	125.81	2.55		10.38
10	2013/12/12	13:50:43	37.478705	140.857253	29.2	8.4	169.00	2.67		10.38
11	2013/12/12	13:50:46	37.478750	140.857284	29.3	8.7	165.82	2.75		10.38
12	2013/12/12	13:50:49	37.478735	140.857319	29.2	0.4	112.31	2.3		10.38
13	2013/12/12	13:50:52	37.478717	140.857340	29.2	7.5	132.10	2.7		10.38
14	2013/12/12	13:50:55	37.4787	140.857314	29.1	8.4	133.22	2.68		10.38
15	2013/12/12	13:50:58	37.478694	140.857384	29.2	7	135.09	2.32		10.38
16	2013/12/12	13:51:01	37.478692	140.857384	29.2	0.2	222.58	2.13		10.38

Figure 6. Overview of the GIS tool

Figure 7. Data including the dose rate

It is possible to produce a contour map using the GIS tool. Data in comma-separated-value format recorded in walking surveys are converted to Microsoft Excel file format (Figure 7), and point data with dose rate information are created from the latitudinal and longitudinal information contained in the data (Figure 8). With the GIS tool, it is possible to estimate the dose rate at unmeasured positions and to produce contour maps from the point data created using any interpolation algorithm, such as Inverse Distance Weighting (IDW) algorithm (Figure 9).

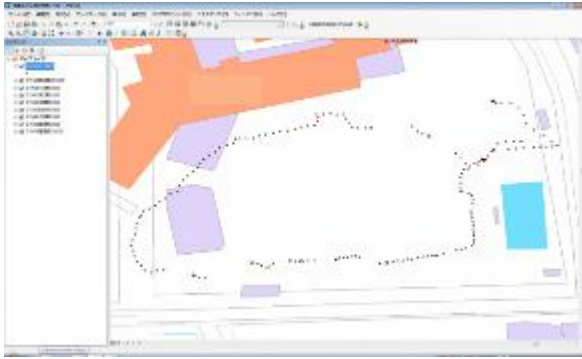


Figure 8. Map data and dose rate plotting

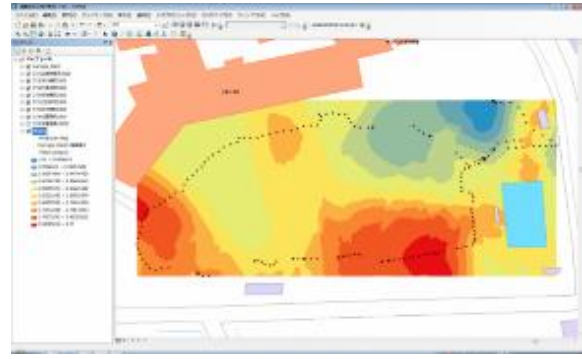


Figure 9. Interpolated dose map

(3) Walking survey implementation

We collected parameters necessary for walking surveys, and carried out the survey in several areas.

(4) Manual preparation

We created a manual surveying the walking survey method. Photos and sentences are combined in this manual for easy understanding.

4.4. Results

(1) Gathering parameters necessary for walking surveys

We conducted a field test of walking surveys, and gathered data for evaluation and analysis (Figure 10). Data were gathered to check the direction characteristics and appropriate measurement density, as well as to determine correction factors.



Figure 10. View of a walking survey

A Checking direction characteristics

Shielding from the measurers themselves affects the contribution from the radiation source depending on the walking direction in walking surveys (Figure 11). Walking surveys were therefore conducted by changing the walking speed and by walking back and forth so as to straddle the radiation source and check the effect of direction characteristics.

As a result, while shifts occurred in places where peaks appeared, they fell within a range of about 2 meters, and measurements showed that the maximum value of the dose rate was nearly the same during forward and reverse passes (Figure 12). We also confirmed that reducing the walking speed caused the peaks of the dose rate distribution to grow sharply (Figures 13 and 14). Judging from the above result, the impact of direction characteristics on a measured value of a walk survey was considered small at a constant walking speed.

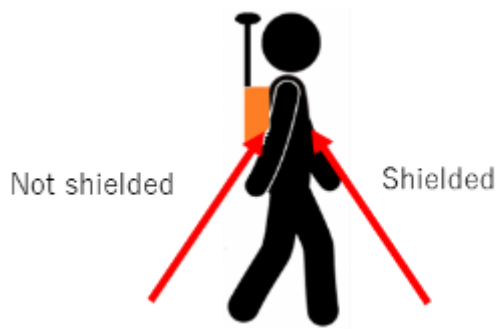


Figure 11. Measurement of direction characteristics



Figure 13. Change in walking speed

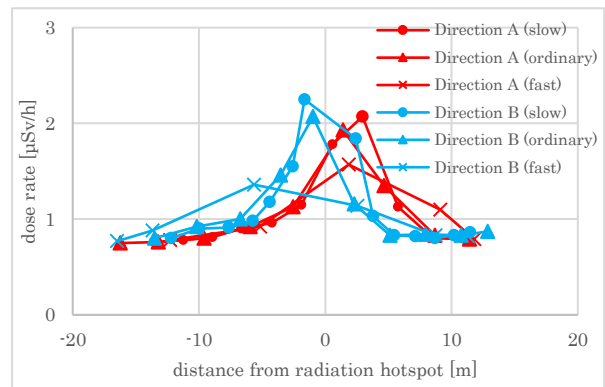


Figure 12. Measurements after changing speed and direction

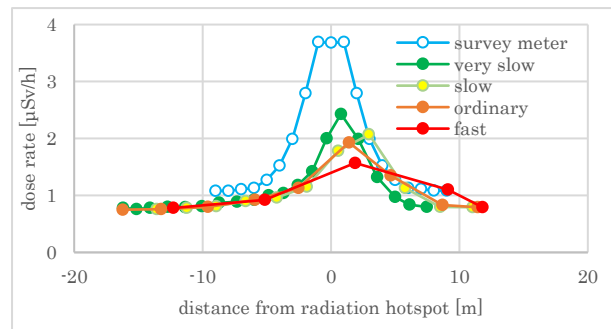


Figure 14. Change in measurements due to walking speed

B Determination of correction factors in a comparison test with survey meters

We assumed measurements made with a NaI (TI) scintillation survey meter (TCS-172B) at a height of 1m to be the most reliable, and the survey meter was calibrated with traceability. We compared measurements made using a survey meter with those obtained in a walking survey (Figure 15). A comparison was made at several points with differing dose rates. At each point, we faced north, south, east, and west and made measurements five times in each direction to mitigate direction characteristics. We then took the average value for all directions as the measurement for that point. We next plotted the measurements of walking surveys against the survey meter to determine the correction factor.

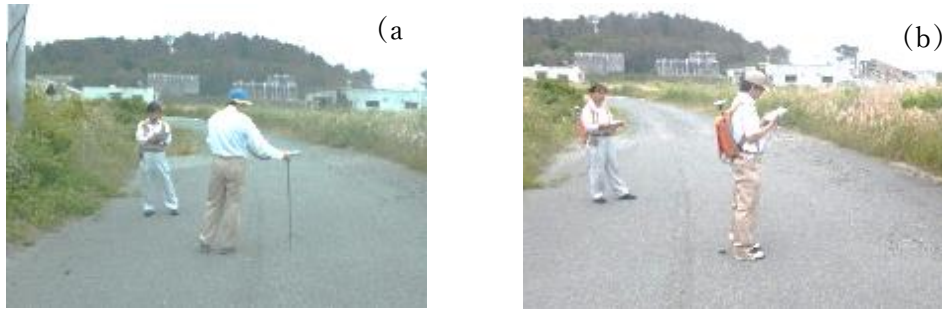


Figure 15. Images of measuring
(a): Measurement with a survey meter
(b): Measurement with a walking survey
Both measurements were made facing four directions.

The results of the comparison are shown in Figure 16(a). There was good linearity between the measurements of walking surveys and the survey meter below a survey meter measurement of $1 \mu\text{Sv/h}$, whereas the linearity deteriorated above approximately $1 \mu\text{Sv/h}$. This phenomenon is due to count loss caused by excessive radiation incidence on the low-dose CsI detector.

In light of the above results, we changed the detector to a high-dose-rate CsI detector (Figure 17) and compared the results obtained using the survey meter with measurement results of walking surveys again. The results are shown in Figure 16(b). We confirmed that as a result of changing the detector, the linearity of walking survey measurements against survey meter measurements is obtained even in the high dose range.

We also confirmed that the high-dose CsI detector can make better measurements than the low-dose rate CsI detector in the high dose range in field tests. This is also confirmed in Figure 18, which shows the walking survey results having changed detectors at the same geographic point. The maximum indicated value is higher for the high-dose-rate CsI detector than for the low-dose-rate CsI detector, and the high-dose-rate area represented by red markers appears, indicating that measurements are made without counting loss of radiation.

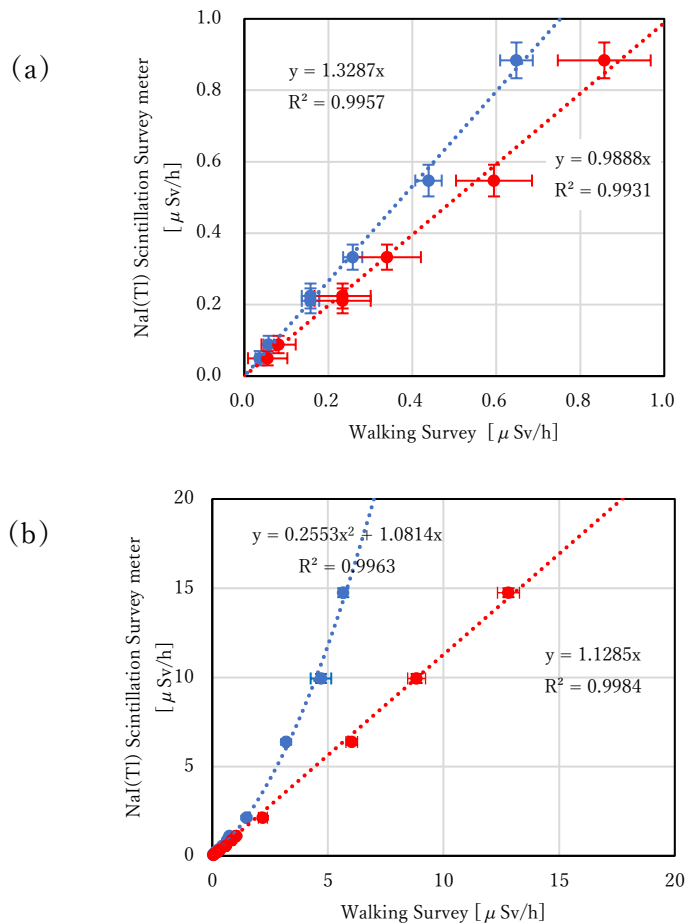


Figure 16. Comparison of measurements of the survey meter and walking survey

(a): Chart plotting data below 1 $\mu\text{Sv/h}$

(b): Chart plotting all data

- Comparison of the measurements of the low-dose-rate CsI detector (Cs-137, 662keV measuring range: 0.001 to 10 $\mu\text{Sv/h}$) and NaI survey meter.
- Comparison of the measurements of the high-dose-rate CsI detector (Cs-137, 662keV measuring range: 0.01 to 100 $\mu\text{Sv/h}$) and NaI survey meter.

Note that the approximate curve is not affected by the self-dose from the measurement detector, with the intercept being zero.



Figure 17. High-dose CsI detector (Hamamatsu Photonics C12137)

According to the above comparisons, we set the correction factors of walking surveys to 1.3 when using the low-dose-rate CsI detector at points with a dose rate less than $1 \mu\text{Sv/h}$ and 1.1 when using the high-dose-rate CsI detector.

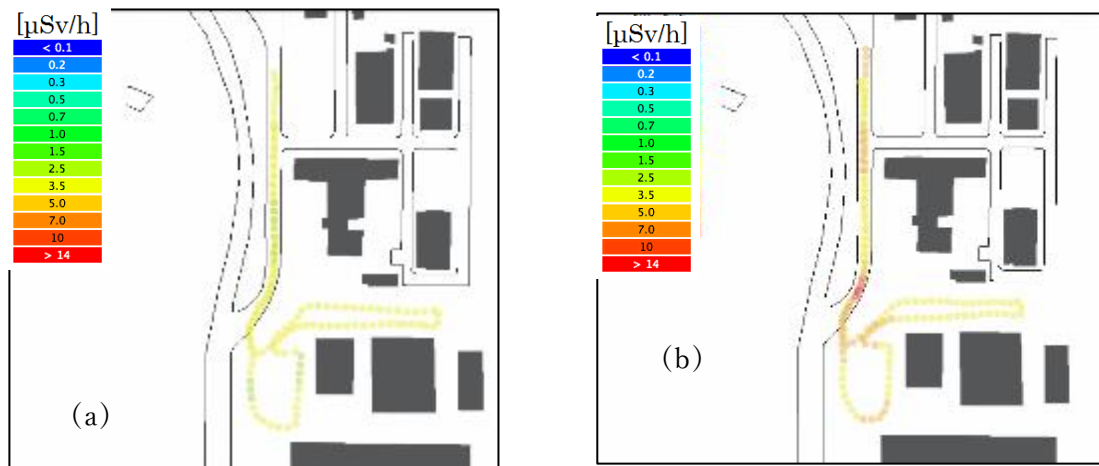


Figure 18. Walking surveys having changed the detector
 (a): Walking survey with the low-dose-rate CsI detector.
 The indicated value range is 2.77 to 5.99 $\mu\text{Sv/h}$.
 (b): Walking survey with the high-dose-rate CsI detector.
 The indicated value range is 5.00 to 29.5 $\mu\text{Sv/h}$.

C Confirming variations in measurements

We conducted fixed point measurements to confirm variations in measurements for a measurement time of 3 seconds in the low dose rate range. Fixed-point measurements were made with both the low-dose-rate CsI detector and the high-dose-rate CsI detector.

Results showed that the variation in measurement results was larger for the high-dose-rate CsI detector at points with a low dose rate (Figure 19). The variation coefficient obtained from dividing the standard deviation of measurements by the average value was 19.7% for the low-dose-rate CsI detector but 42.7% for the high-dose-rate detector. Error in measurements made with the low-dose-rate detector was small because of the high counting rate achieved with the large crystal while error in measurements made with the high-dose-rate detector was large because of the small counting rate achieved with the small crystal.

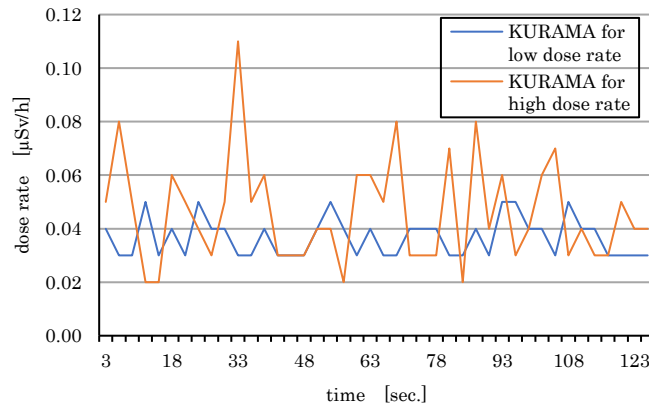


Figure 19. Measured value dispersion check

On this basis, we decided to use the low-dose-rate CsI detector, which has a small variation at low dose rates, at geographic points with a dose rate less than 1 $\mu\text{Sv/h}$, and to use the high-dose-rate CsI detector at geographic points with a dose rate greater than 1 $\mu\text{Sv/h}$.

(2) Conducting walking surveys

With the purpose of studying the operation of walking surveys and acquiring basic data, we conducted walking surveys at places with differing conditions. Examples of such walking surveys are described below.

A Walking survey in western Fukushima City

We conducted a walking survey on a trial basis in western Fukushima City. At the center of this geographic area is a surface paved with asphalt, with ditches along the edges. There were no obstructions on the outside of the asphalt surface, leaving the surface wide open and surrounded by grass.

Results of a walking survey conducted at this geographic point are shown in Figure 20. The paved surface at the center of the range of the walking survey had a low dose rate compared with that of the surroundings. It is considered that this low dose rate is due to the easy decontamination of the paved surface and the strong effect of weathering. In addition, the radiation dose in the vicinity of the ditch was higher than that of the surroundings. This is probably because there was an inflow of radioactive material from the surrounding area.

We conducted a high-density walking survey and tested interpolation with a GIS tool (Figure 21). Interpolation was conducted with IDW. The interpolated radiation dose rate in the paved area was low, and the dose rate in the vicinity of the ditch was high.

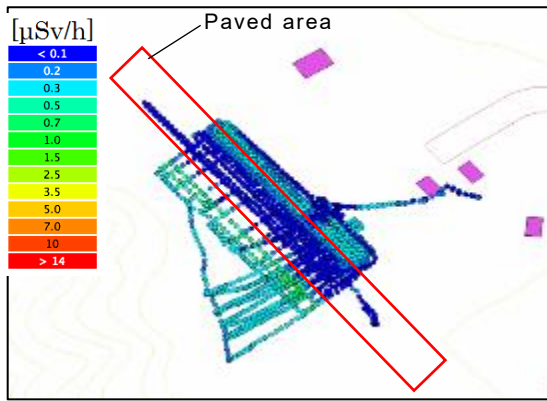


Figure 20. Results of a walking survey in western Fukushima City

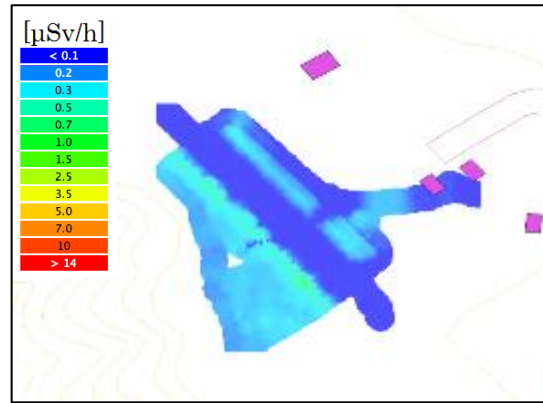


Figure 21. Results of interpolation with IDW

B Walking survey in the periphery of a temporary storage area

We conducted a walking survey in a temporary storage area and its periphery in the Nakadori region of Fukushima Prefecture (Figure 22). The area inside the red frame in the figure is the temporary storage area. The dose rate near the temporary storage area was equal to or less than the dose rate in the periphery, and no effect of external decontaminated waste on the outside area was seen in this temporary storage area.

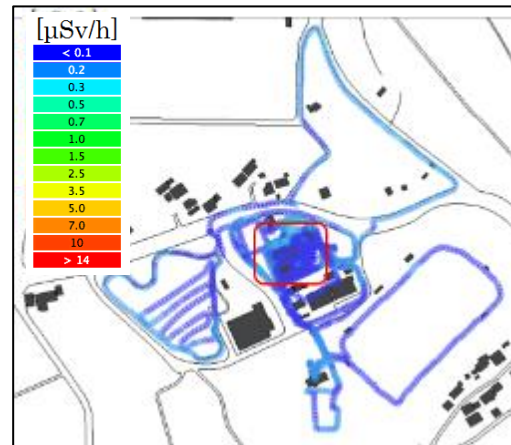


Figure 22. Dose map (with the temporary storage area indicated by the red frame.)

C Walking survey in the Hamadori region (outside the evacuation zone)

We conducted a walking survey around rivers in the Hamadori region of Fukushima Prefecture (outside the evacuation zone) (Figures 23 and 24). There is a paved surface on the left side of the figure, with the rest of the study area being gravel or grassland. The dose rate was low on the paved surface and nearly uniform in other areas.

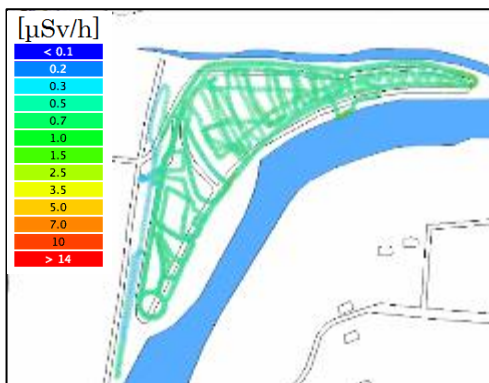


Figure 23. Dose map

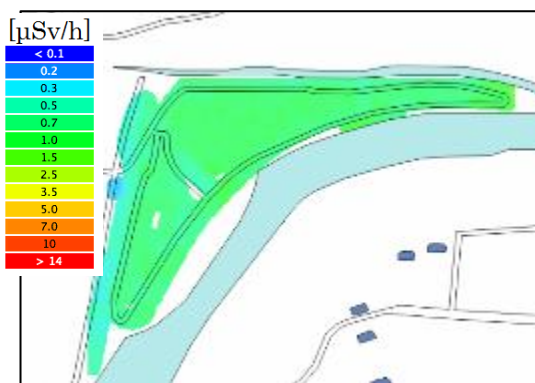


Figure 24. IDW interpolation result

D Walking survey in a difficult-to-return evacuation zone

We conducted a walking survey in a difficult-to-return evacuation zone in Fukushima Prefecture (Figures 25 and 26). The area where the walking survey was conducted was nearly uniform grassland. The dose rate was nearly uniform in the area, with no large deviation observed.

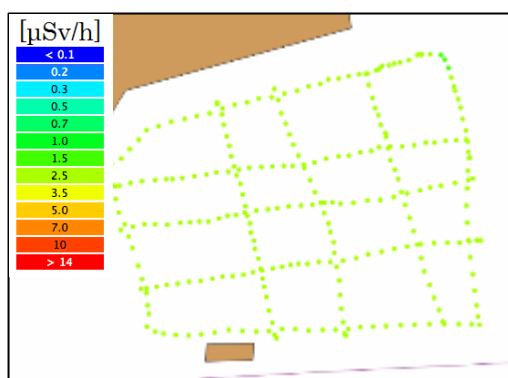


Figure 25. Dose map

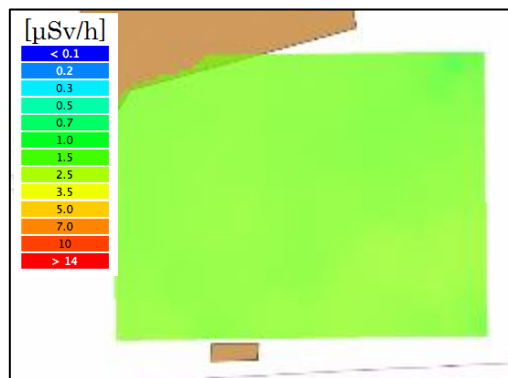


Figure 26. Results of interpolation by IDW

4.5. Conclusions

Results were obtained in developing walking surveys by 2015.

In terms of developed equipment, the walking survey system adopted KURAMA, which was designed by Kyoto University and has a structure suitable for a walking survey. Additionally, to analyze the obtained data or to work with other monitoring methods, such as a UAV survey, we prepared a GIS data processing system. Furthermore, by collecting data for the determination of direction characteristics and calibration constants, it has become possible to measure the dose rate in a walking survey.

We conducted walking surveys at several points and confirmed that it is possible to measure the air dose rate and to create a contour map with a GIS processing system.

We published a manual for walking surveys and made the manual available to the general public.

In fiscal 2016, we conducted walking surveys or lent the necessary equipment at the request of municipalities. In recent years, walking surveys have been utilized in the public projects for monitoring of the air dose rates (e.g., Satoyama Restratement Model Project).

5. FIP5 Examination of Proper Treatment of Waste Containing Radioactive Materials

5.1. Abstract

Using incineration ash (bottom ash and fly ash) containing radiocesium generated in Fukushima Prefecture, laboratory tests were conducted to investigate radiocesium elution and the suppression of radiocesium elution by acid clay and zeolite. Based on the results, experiments regarding the suppression of radiocesium elution from fly ash using two different addition methods were carried out at actual municipal waste incineration facilities.

Moreover, each status of the landfill disposal sites was investigated regarding incineration ash and radiocesium elution. While a study on landfill disposal sites was included in this project from FY 2018, Fukushima Prefecture had launched the same study on its own before that, so this report also includes the contents of the study conducted by FY 2017.

5.2. Purposes

The incineration of municipal waste containing radiocesium scattered due to the accident at Tokyo Electric Power Company Holdings' Fukushima Daiichi Nuclear Power Plant Station resulted in the migration of radiocesium to incineration ash and its concentration. Some incineration ash generated in this way cannot be subjected to landfill disposal even when its radioactive concentration is below 8,000 Bq/kg, a standard value provided by law, and so, some are forced to be stored.

Although the concentrations of radioactive materials significantly decreased after nine years from the accident, incineration ash containing radioactive materials is daily generated from the incineration of municipal waste, and its proper disposal is an urgent task.

Thus, as described in the final report for the previous project, the distribution of radiocesium between bottom ash and fly ash, the proper treatment of bag-filter waste cloths and the suppression of radiocesium elution from fly ash were studied until FY 2017.

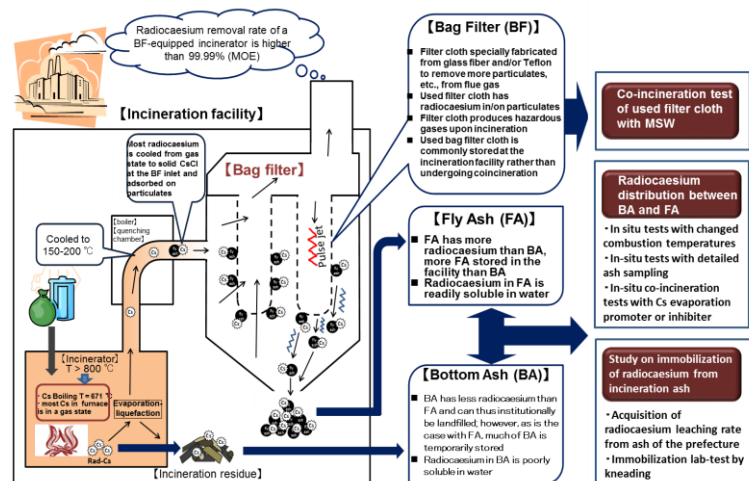


Figure 1. The contents of the past studies

(1) Distribution of radiocesium between bottom ash and fly ash

It is generally known that radiocesium volatilizes upon its combustion and tends to migrate to fly ash rather than to bottom ash. The factors that influence the migration of radiocesium were classified into five, i.e. combustion temperature, air ratio, waste quality, chemical addition and

ash particle diameter. Among these factors, the correlation between “combustion temperature and chemical addition,” which are relatively easy to control and “radiocesium migration behavior” were investigated through verification tests at actual facilities. As a result, it was found that it is difficult to change the combustion temperature in an operating incinerator because maintenance and management standards stipulating an allowable combustion temperature range have been established by laws relating to Waste Management and Public Cleaning Act. As for a chemical addition method, the addition of hydrated lime to incinerated waste somewhat promoted radiocesium migration to fly ash at some facilities, but the reproducibility of such a phenomenon was scarce.

(2) Tests on the proper treatment of bag-filter waste cloths

At each of the facilities B (filter cloth: glass fiber) and E (filter cloth: Teflon), a normal operation without the co-combustion of waste filter cloths and municipal waste and another operation with the co-combustion of radiocesium-containing waste filter cloths and municipal waste by changing the input ratio and input time interval of the radiocesium-containing waste filter cloths were carried out. The results revealed that the co-combustion of bag-filter waste cloths with municipal waste at the facilities is safe and appropriate as long as the co-combustion ratio is managed properly.

(3) A study on the suppression of radiocesium elution from fly ash

Radiocesium elution tests were conducted for fly ash and bottom ash (64 samples in total) at 15 facilities in Fukushima Prefecture to obtain cesium elution data. At facility K, zeolite or bentonite, both of which are expected to be effective in cesium elution suppression, was added to and kneaded with incineration ash and then a radiocesium elution test was performed. The results showed the excellent effects of zeolite and bentonite in the suppression of radiocesium elution from the fly ash, and the effect of zeolite was particularly remarkable.

For this interim report, as a development from (3) above, verification tests were performed at incineration facilities when in operation to investigate the effectiveness of techniques for removing radiocesium or suppressing the elution of radiocesium from incineration ash based on the understanding of radiocesium elution property, for the purpose of safely and properly disposing of incineration ash (bottom ash and fly ash).

In order to assess the future safety of landfill disposal sites where radiocesium-containing incineration ash is subjected to landfill disposal, landfill disposal sites having started burying radiocesium-containing incineration ash were investigated in terms of their status of incineration ash landfill and a correlation between a disposal site structure and radiocesium elution

5.3. Content of implementation

(1) Tests on radiocesium elution suppression

A Tactical agitation tests using a germanium semiconductor detector

Using a germanium semiconductor detector, radiocesium concentrations in bottom ash, humidified bottom ash (treated bottom ash), fly ash, and fly ash provided with a heavy metal elution prevention treatment (treated fly ash) sampled from municipal waste incineration facilities in Fukushima Prefecture were measured. Next, an elution test to investigate the elution property of radiocesium was performed using 2.5 L of ultrapure water for about 250 g of incineration ash, in accordance with JIS K 0058-1. A radiocesium elution rate (%) was determined by the following:

$$\frac{[\text{radiocesium concentration (Bq/kg) in the eluate}] \times [\text{the weight of ultrapure water used in the elution test (kg)}]}{[\text{radiocesium concentration in incineration ash (Bq/kg)}] \times [\text{the weight of incineration ash used in as-is agitation test (kg)}]} \times 100.$$

B A test on radiocesium elution suppression (long-term as-is agitation test)

In order to find a method of suppressing radiocesium elution from incineration ash having been exposed to rain water during its storage or after a landfill (elution-suppressing method), an acid clay was added to an incineration ash by 5% in weight, they were mixed with water until the water content reached 30% and then were subjected to a radiocesium measurement using a germanium semiconductor detector and a long-term as-is agitation test. The durations of agitation were set at 6 hours, 24 hours, 7 days, 14 days, and 30 days. Radiocesium elution rates were determined and the radiocesium elution-suppressing effect of an acid clay was investigated by mixing or not mixing it into the incineration ash.

C A test on radiocesium elution suppression (MP-AES / ion chromatography test)

In order to investigate the effect of mixing acid clay into incineration ash on the metal elution from the ash, an elution test was carried out using incineration ash mixed with acid clay and one not mixed with it. Concentrations of elements in the eluates were measured using an MP-AEA spectroscopic analyzer and an ion chromatography device.

(2) Tests on radiocesium elution suppression in incineration ash at municipal waste incineration facilities

Regarding zeolite, which was found to be effective in the suppression of radiocesium elution as described in 5.2.(3), zeolite addition tests were performed at two systems of an actual municipal waste incineration facility to verify the feasibility of a radiocesium elution countermeasure using zeolite at an incineration facility.

A A test during normal operation

This test was performed for three days in total during a normal operation period. Bottom ash, fly ash and treated fly ash were sampled at 11:00 and 14:00 each day, and tests were performed to determine radiocesium concentrations and elution properties.

(a) Germanium semiconductor detector test, a JIS K 0058-1 elution test and the Environment Agency's Notice No. 13 elution test

Using the methods shown in Table 1, tests were conducted to investigate the radiocesium concentration of each sample and the elution properties of radiocesium and heavy metals.

(b) Repetitive elution tests (JIS K 0058-1)

In order to investigate the quantities of repetitive elution of radiocesium and heavy metals, the JIS K 0058-1 elution test shown in Table 1 was repeated four times (each sample used for an elution test was subjected to another elution test by putting it into a new solvent) using bottom ash and treated fly ash

sampled during the same time zone when the radiocesium concentration in fly ash was the highest during a normal operation period. An eluate obtained from each test was examined for radiocesium concentration, heavy metal concentrations, pH and EC.

Table 1. Test Conditions and Others

Sample	Test Methods	Used Equipment	Minimum Determination Limit
Radiocesium Concentration	Contain	Germanium Semiconductor Detector (ORTEC GEM20P4-70)	Fill U8 container up to a height of 5 cm and measure for 3,600 seconds
	Elution		Fill a 2L Marinelli container up to a height of 12 cm and measure for 20,000 seconds
pH	JIS K 0058-1	GST-5741C, DKK-TOA CORPORATION	-
EC		CM-30R, DKK-TOA CORPORATION	-
Hg	JIS K 0058-1 or Environment Agency's Notice No. 13 (Notice No. 13)	RA-3A, Nippon Instruments Corporation	0.0005mg/L
Cd		Agilent Technologies 7500ce ICP-MS or 7800 ICP-MS	0.009mg/L
Pb			0.03mg/L
As			0.01mg/L
Se			0.02mg/L
Cr			0.1mg/L
Cl-		ThermoFisher Scientific ICS-1100	0.1mg/L

(c) Zeolite addition test in laboratory

To study zeolite addition ratios in zeolite addition tests at actual facilities, zeolite was added by 5 to 20% (in 5% increments) to the fly ash and treated fly ash that were sampled during a normal operation test period and that showed the highest radiocesium concentrations, and then water was mixed with the fly ash and treated fly ash until their water content reached 30%. The test shown in table 1 was performed on each mixed sample to check the presence or absence of a radiocesium elution suppression effect and an effect on heavy metals and others.

B Tests on zeolite addition to an exhaust gas treatment agent at actual facilities

At the municipal waste facilities mentioned in A, exhaust gas treatment using an exhaust gas treatment agent mixed with zeolite was performed for five consecutive days. During the treatment period, the treated fly ash was sampled at 14:00 each day. The samples were tested to determine radiocesium concentrations and elution property.

(a) Exhaust gas composition analysis tests

To investigate the effect of the blow injection of chemical mixture on exhaust gas, a test was performed only for one day during the chemical mixture addition test period, using methods described in the Waste Management Division's Notification No. 95, Exhibit 3, II and the Ministry of the Environment's 2011 Notification, No. 111.

(b) Germanium semiconductor detector test, JIS K 0058-1 elution test and the Environment Agency' s Notice No. 13 elution test

To investigate radiocesium concentrations and the elution properties of radiocesium and heavy metals in treated fly ash sampled during the chemical mixture addition test period, tests were performed using the methods shown in Table 1.

(c) Repetitive elution tests (JIS K 0058-1)

The average of radiocesium concentrations in the treated fly ash sampled during the chemical mixture addition test period was calculated. A sample that indicated a radiocesium concentration closest to the average value was subjected to four JIS K 0058-1 repetitive elution tests (a sample having been subjected to an elution test was immersed into a new solvent and this operation was repeated four times) shown in Table 1. An eluate obtained from each test was examined for radiocesium concentration, heavy metal concentrations, pH and EC. Tests using artificial seawater as a solvent were also carried out.

C Tests on zeolite addition to the mixture of fly ash and chelate agent by kneading at actual facilities

At the municipal waste incineration facilities mentioned in A, heavy metal elution suppression treatment in which zeolite was added to a chelate agent kneader for suppressing heavy metal elution from incineration ash was performed for five consecutive days. During the heavy metal elution suppression treatment period, the treated fly ash was sampled at 14:00 each day and tested to determine radiocesium concentrations and elution property.

(a) Germanium semiconductor detector test, JIS K 0058-1 elution test and the Environment Agency' s Notice No. 13 elution test

Tests were conducted using the method shown in Table 1 to examine the radiocesium concentrations and the elution properties of radiocesium and heavy metals in the treated fly ash sampled during the mixing addition test period.

(b) Repetitive elution tests (JIS K 0058-1)

The average of radiocesium concentrations in the treated fly ash sampled during the mixing addition test period was calculated. A sample that showed a radiocesium concentration closest to the average value was subjected to four JIS K 0058-1 repetitive elution tests (a sample having been subjected to an elution test was immersed into a new solvent, and this operation was repeated four times). An eluate obtained from each test was examined for radiocesium concentration, heavy metal concentrations, pH and EC. Tests using artificial seawater as a solvent were also carried out.

(3) Situations of landfill and radiocesium elution

A FY 2015

The investigations regarding the landfill situation of incineration ash (bottom ash and fly ash) were conducted at seven landfill disposal sites in Fukushima Prefecture. From January until March 2016, leachate (seeping water), discharged water, water-treated sludge and nearby underground water were sampled once a month at the sites. Then their radiocesium concentrations were measured to investigate a correlation between landfill situation and radiocesium elution. In addition, radiocesium concentrations in leachate and discharged water were compared to check the radiocesium treatment situations at leachate treatment facilities. The situations of incineration ash landfill at the seven landfill disposal sites are shown in Table 2. Their incineration ash landfill situations fell under the following four types: “landfill in the same way as before the accident,” “landfill of only fly ash without contact with rainwater,” “landfill of only bottom ash,” and “no landfill of incineration ash.” Landfill disposal sites D and E prevent contact between fly ash and rainwater by burying fly ash in the sandbags.

Table 2. Situations of the landfill of incineration

	Disposal Site A	Disposal Site B	Disposal Site C	Disposal Site D	Disposal Site E	Disposal Site F	Disposal Site G
Bottom Ash	○	○	×	○	○	○	○
Fly Ash	○	○	×	△	△	×	×

○: Landfill is done in the same way as before the accident.

△: Landfill is conducted so as not to contact rainwater.

×: Not landfilled.

B FY 2016

In November and February, leachate (seeping water), discharged water, water-treated sludge, and nearby underground water were sampled from six landfill disposal sites in total (Table 3, namely four landfill disposal sites C, E, F and G among seven landfill disposal sites surveyed in FY 2015, landfill disposal site H where incineration ash was buried in the same method used before the accident, and landfill disposal site I where only bottom ash was buried), and their radiocesium was analyzed.

Table 3. The list of landfill disposal sites

	Disposal Site C	Disposal Site E	Disposal Site F	Disposal Site G	Disposal Site H	Disposal Site I
Bottom Ash	×	○	○	○	○	○
Fly Ash	×	△	×	×	○	×

○: Landfill is done in the same way as before the accident.

△: Landfill is conducted as not to contact rainwater.

×: Not landfilled.

(4) Correlation between the annual elution situation of radiocesium and other elements

In FYs 2017 and 2018, leachate (seeping water), discharged water, water-treated sludge, and nearby underground water were sampled from four landfill disposal sites A, B, D and H, whereby their radiocesium concentrations were measured. Water-treated sludge was sampled only in FY 2017. Among the four landfill disposal sites, three landfill disposal sites A, B and H were burying fly ash in the same methods they used before the nuclear power station accident,

and landfill disposal site D was burying fly ash after putting it in large sandbags. However, during a certain period immediately after the accident, site D buried part of fly ash without putting it in large sandbags (Table 4). In FY 2017, elements and others shown in Table 5 in addition to radiocesium were measured for their concentrations.

Table 4. Situations of incineration ash landfill at four disposal sites

	Disposal Site A	Disposal Site B	Disposal Site D	Disposal Site H
Bottom Ash	○	○	○	○
Fly Ash	○	○	△	○

○: Landfilling is done in the same way as before the accident.

△: Landfilling is conducted so as not to contact rainwater.

Table 5. Analyzed elements and others

Elements to be analyzed
Sodium, magnesium, sulfur, potassium, calcium, rubidium, barium, antimony, nickel, cobalt, molybdenum, selenium, cesium, strontium, chloride ion, nitrous acid, nitric acid

5.4. Results

(1) Radiocesium elution suppression test

A Germanium semiconductor detector and as-is agitation tests

Table 6 summarizes test results regarding solid phase radiocesium concentrations, liquid phase radiocesium concentrations (as-is agitation test), radiocesium elution rates and others.

The results of radiocesium concentrations in solid phase sample showed a tendency in which radiocesium concentrations were higher in fly ash and treated fly ash than in the bottom ash and treated bottom ash.

Regarding solid phase samples in the same facility, radiocesium concentrations were lower in treated fly ash than in fly ash. This is probably because of the effect of water added during chelate agent treatment to suppress heavy metal elution from fly ash. Similarly to the test results of the solid phase samples, the test results of radiocesium concentrations in liquid phase samples suggested that radiocesium concentrations tend to be higher in fly ash and treated fly ash than in bottom ash and treated bottom ash. The comparison of radiocesium concentrations in bottom ash and treated bottom ash indicated a tendency in which the radiocesium concentrations in treated bottom ash were lower in general, whereas the comparison of those in fly ash and treated fly ash did not show a similar tendency. The results of calculating radiocesium elution rates indicated a tendency in which those of fly ash and treated fly ash were generally higher than those of bottom ash and treated bottom ash.

Table 6. Results of germanium semiconductor detector and as-is agitation tests

Facility	Sample	Solid Phase Sample		Liquid Phase Sample			
		Cs134+137 (Bq/kg)	Moisture content (%)	Cs134+137 (Bq/kg)	Elution rate (%)	pH	EC (mS/m)
Facility 1	Bottom Ash	1,400	0.3	7.2	5.1	12.5	820
	Fly Ash	13,000	2.0	450	34.6	8.6	2,470
	Treated Fly Ash	5,000	23.8	470	94.0	12.0	5,480
Facility 2	Bottom Ash	210	0.5	2.1	10.0	12.6	1,436
	Fly Ash	1,300	3.9	43	33.1	12.2	3,900
Facility 3	Treated Bottom Ash	49	32.0	0.1	2.0	11.5	244
	Treated Fly Ash	310	23.6	29	93.5	12.2	3,900
Facility 4	Treated Bottom Ash	550	26.2	1.1	2.0	12.1	385
	Treated Fly Ash	3,700	23.0	310	83.8	12.2	3,730
Facility 5	Treated Bottom Ash	260	29.0	0.2	0.8	11.6	235
	Fly Ash	1,900	2.1	120	63.2	12.4	4,110
	Treated Fly Ash	1,800	13.8	140	77.8	11.7	3,050
Facility 6	Treated Bottom Ash	150	26.2	0.5	3.3	12.2	460
	Fly Ash	1,500	0.9	81	54.0	12.2	4,230
	Treated Fly Ash	1,000	19.3	85	85.0	12.1	3,800
Facility 7	Bottom Ash	1,300	0.2	8.6	6.6	12.7	1,201
	Fly Ash	12,000	1.3	680	56.7	12.3	3,690
	Treated Fly Ash	6,100	17.5	390	63.9	11.7	2,650
Facility 8	Treated Bottom Ash	51	28.6	ND	ND	11.4	188
	Fly Ash	620	1.4	48	77.4	12.3	6,140
	Treated Fly Ash	350	19.2	33	94.3	12.2	3,610

B A test on radiocesium elution suppression (long-term as-is agitation test)

Figure 2 summarizes the results (radiocesium elution rates) of radiocesium elution suppression tests by mixing an acid clay into treated fly ash by 5% in weight at facilities 1, 3, 4, 5, 6 and 7.

These results have confirmed that the mixture of an acid clay into any treated fly ash by 5% in weight suppresses radiocesium elution rate to 30% or lower, in other words, an acid clay is effective in the suppression of radiocesium elution. This is probably because a clay mineral, which is the major component of a clay, captures radiocesium into its structure and suppresses its elution. The maximum duration of these tests were 30 days, during which no radiocesium elution rate exceeded 30%.

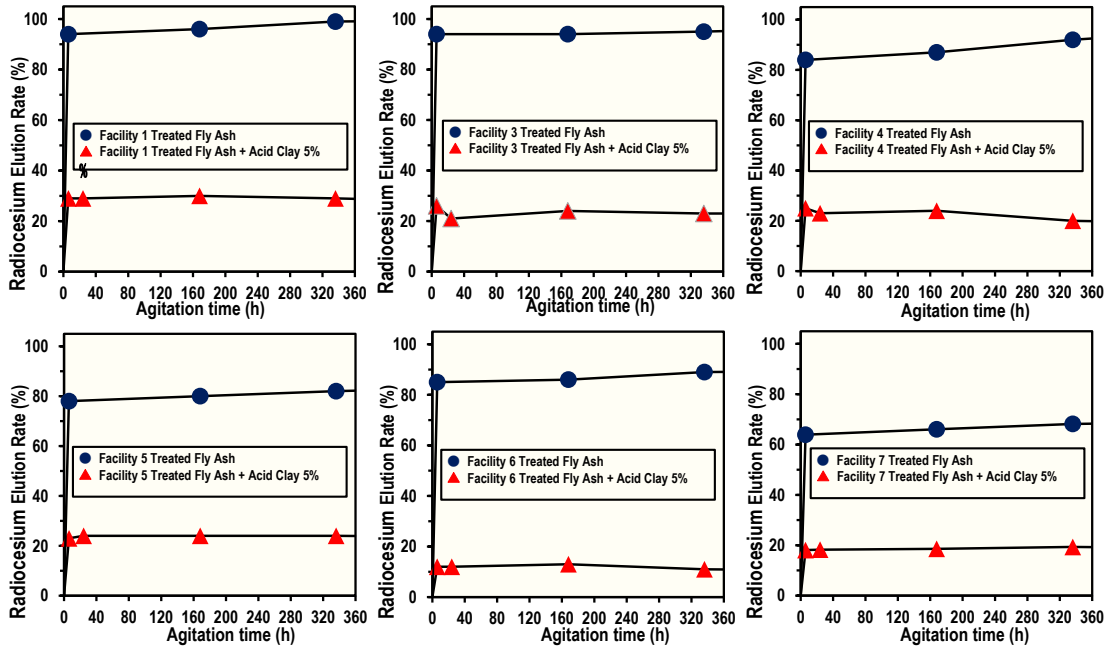


Figure 2. Results of radiocesium elution suppression tests (radiocesium elution rates)

C Radiocesium elution suppression tests (MP-AES / ion chromatography test)

Table 7 summarizes the concentrations of metals and others in the eluate. As a result of mixing an acid clay into treated fly ash by 5% in weight and agitating the mixture for six hours or 30 days, it was found that the long-term agitation did not result in significant differences in the concentrations of metals and others. As a result of comparing 30-day agitation without mixing an acid clay and 30-day agitation after mixing an acid clay, some cases were observed in which acid clay mixture resulted in low concentrations, but generally the obtained concentrations showed a similar tendency and suggested that the mixing of an acid clay does not block the effect of chelate.

Table 7. Results of radiocesium elution suppression test
(concentrations of metals and others in eluates) * mg/L **g/L

Facility	Sample	Metal									Anion			pH	EC (mS/m)
		Zn ⁺	Sr ⁺	Cu ⁺	Pb ⁺	Ba ⁺	Li ⁺	Ca ⁺⁺	Na ⁺⁺	K ⁺⁺	Cl ⁻	Br ⁻	SO ₄ ²⁻		
Facility 1	Treated fly ash + Acid clay 5%, Stirred for 6 hours	1.3	14.1	0.6	27.1	1.9	0.9	5.9	1.5	2.4	19	53	1240	12.3	4,580
	Treated fly ash + Acid clay 5%, Stirred for 30 days	0.7	13.5	0.4	11.1	1.9	0.6	5.2	1.3	1.9	17	52	990	12.2	4,260
	Treated fly ash, Agitated for 30 days	2.1	15	0.4	55.2	1.2	1	7	1.8	2.8	25	85	940	12.2	5,440
Facility 3	Treated fly ash + Acid clay 5%, Stirred for 6 hours	0.1	11.6	0.4	0.7	2.7	1.3	2.1	3.5	2.8	12	24	170	12.4	3,570
	Treated fly ash + Acid clay 5%, Stirred for 30 days	0.1	12.6	0.4	0.6	18.2	1.7	1.8	3.3	2.5	13	41	10	12.1	2,820
	Treated fly ash, Agitated for 30 days	0.1	12.8	0.4	0.8	13.3	2.6	2.3	4.1	3.2	15	50	10	12.3	4,350
Facility 4	Treated fly ash + Acid clay 5%, Stirred for 6 hours	0.1	10.4	0.4	0.8	1	1.1	2.5	2.1	2.2	11	30	440	12.4	3,110
	Treated fly ash + Acid clay 5%, Stirred for 30 days	0.2	11.4	0.3	0.6	2.7	1.8	2.2	2	2	11	43	80	11.9	2,920
	Treated fly ash, Agitated for 30 days	0.1	11.9	0.4	0.3	3.1	2.6	2.5	2.3	2.5	13	63	10	11.9	3,920
Facility 5	Treated fly ash + Acid clay 5%, Stirred for 6 hours	0.1	8.8	0.4	0.7	6.4	1	0.8	2.5	2.2	8	12	20	11.5	2,150
	Treated fly ash + Acid clay 5%, Stirred for 30 days	0.2	9.3	0.3	0.7	8.7	1.3	0.9	2.5	2	8	16	10	10.9	2,260
	Treated fly ash, Agitated for 30 days	0.1	10.2	0.5	0.6	6	1.9	1.2	3.3	2.8	11	32	40	10.6	3,110
Facility 6	Treated fly ash + Acid clay 5%, Stirred for 6 hours	0	11.8	0.4	0.4	2.7	1.3	2.6	2.7	2.4	11	57	380	12.3	3,320
	Treated fly ash + Acid clay 5%, Stirred for 30 days	0.1	13.3	0.3	0.5	10.7	1.6	2.2	2.6	2.2	12	73	40	11.7	3,130
	Treated fly ash, Agitated for 30 days	0.1	13.8	0.4	0.3	6.6	2.4	2.5	3	2.7	16	91	30	11.7	3,910
Facility 7	Treated fly ash + Acid clay 5%, Stirred for 6 hours	0.1	13.2	0.4	1.7	2.4	1.1	0.6	2.4	2.4	6	38	730	11.3	1,910
	Treated fly ash + Acid clay 5%, Stirred for 30 days	0.2	14.5	0.3	0.6	3.4	1.7	0.5	2.5	2.3	7	46	190	10.6	2,060
	Treated fly ash, Agitated for 30 days	0.1	16	0.4	0.4	9	2.5	0.8	3.2	3.3	10	63	1060	9.4	2,950
Facility 8	Treated fly ash + Acid clay 5%, Stirred for 6 hours	0	7.6	0.3	0.7	0.9	1.1	1.5	2.8	2.3	10	26	900	12.3	2,940
	Treated fly ash + Acid clay 5%, Stirred for 30 days	0.3	9.2	0.3	0.7	1.1	1.3	1.3	3	2.4	11	58	70	11.2	2,840
	Treated fly ash, Agitated for 30 days	0.1	10.5	0.4	0.6	0.6	2.2	1.3	3.2	2.8	14	68	70	11.2	3,650

(2) Tests on radiocesium elution suppression in incineration ash at municipal waste incineration facilities

A Tests during a normal operation

(a) Germanium semiconductor detector test, JIS K 0058-1 elution test and the Environment Agency's Notice No. 13 elution test

Figures 3 to 5 show the daily fluctuations of radiocesium concentrations (contained or elution concentrations) and elution rates in the bottom ash, fly ash and treated fly ash sampled in normal operation tests. These results indicate a tendency in which fly ash and treated fly ash rather than bottom ash showed higher radiocesium contents, elution quantities and elution rates.

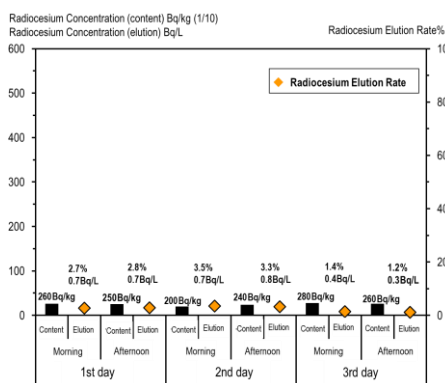


Figure 3. Daily fluctuations of radiocesium concentrations in bottom ash (normal operation)

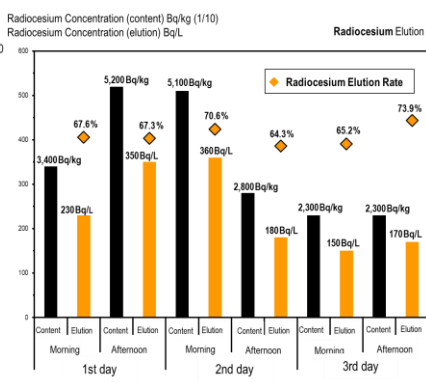


Figure 4. Daily fluctuations of radiocesium concentrations in fly ash (normal operation)

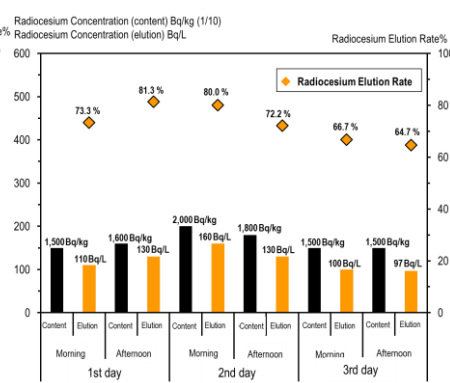


Figure 5. Daily fluctuations of radiocesium concentrations in chelated fly ash (normal operation)

Radiocesium contents were 200 to 280 Bq/kg (248 Bq/kg on average) for bottom ash, 2,300 to 5,200 Bq/kg (3,517 Bq/kg on average) for fly ash, and 1,500 to 2,000 Bq/kg (1,650 Bq/kg on average) for treated fly ash. The quantities of radiocesium elution were 0.3 to 0.8 Bq/L (0.6 Bq/L on average) for bottom ash, 150 to 360 Bq/L (240 Bq/L on average) for fly ash, and 97 to 160 Bq/L (121 Bq/L on average) for treated fly ash.

Radiocesium elution rates were 1.2 to 3.3% (2.5% on average) for bottom ash, 64.3 to 73.9% (68.2% on average) for fly ash, and 64.7 to 81.3% (73.0% on average) for treated fly ash, and therefore the results of the Environment Agency's Notice No. 13 elution test generally satisfied the basic requirements for heavy metals and others.

(b) Repetitive elution tests (JIS K 0058-1)

Table 7 (bottom ash) and Table 8 (treated fly ash) show the results of repetitive elution tests. This time, samples taken in the afternoon (14:00) of the first day were used. Radiocesium elution property indicated by each sample and also the results of the repetitive elution tests showed a tendency in which radiocesium elution rates were higher in the case of treated fly ash than bottom ash. The cumulative rate of radiocesium elution from bottom ash was 3.2% and that from treated fly ash was 81.9% in the four tests. The samples of the first test showed the highest amount and rate of radiocesium elution, which gradually decreased as the number

of tests increased.

The values of EC also tended to decrease as the number of elution tests increased. Results regarding heavy metals and others did not show any anomalous value and suggested a trend in which their values decreased as the number of elution tests increased similarly to the EC results.

Table 8. Results of repetitive elution tests using bottom ash (normal operation)

Item	Unit	Bottom Ash (1st day afternoon)			
		1st	2nd	3rd	4th
Radiocesium Concentration (elution) ¹	Bq/L	0.5	0.3	0	0
pH	-	11.7	11.3	10.8	10.9
EC	mS/m	420	109	55.0	42.9
Radiocesium Elution Rate ²	%	2.0	1.2	0	0
Hg	mg/L	<0.0005	<0.0005	<0.0005	<0.0005
Cd		<0.009	<0.009	<0.009	<0.009
Pb		<0.03	<0.03	<0.03	<0.03
As		<0.01	<0.01	<0.01	<0.01
Se		<0.01	<0.01	<0.01	<0.01
Cr		<0.02	<0.02	<0.02	<0.02
Cl-		1,010	136	46.0	14.7

Table 9. Results of repetitive elution tests using treated fly ash (normal operation)

Item	Unit	Chelated Fly Ash (1st day afternoon)			
		1st	2nd	3rd	4th
Radiocesium Concentration (elution) ¹	Bq/L	120	10	1	0
pH	-	12.4	12.5	12.6	12.6
EC	mS/m	3,380	1,150	911	871
Radiocesium Elution Rate ²	%	75.0	6.3	0.6	0
Hg	mg/L	0.0006	<0.0005	<0.0005	<0.0005
Cd		<0.009	<0.009	<0.009	<0.009
Pb		0.16	0.10	0.14	0.14
As		<0.01	<0.01	<0.01	<0.01
Se		<0.01	<0.01	<0.01	<0.01
Cr		0.07	<0.02	<0.02	<0.02
Cl-		10,400	1,200	256	88.6

* Each value is calculated with its radiocesium concentration (content) as of 250 Bq/kg. * Each value is calculated with its radiocesium concentration (content) as of 1,600 Bq/kg.

From the results of the test described in 2.A(a) and the repetitive elution tests, it was found that the radiocesium concentrations (of contained or eluted radiocesium) in treated fly ash and the rates of radiocesium elution from it were higher compared with bottom ash and that the suppression of radiocesium elution by means of chelate agent treatment is difficult as the elution rate was high even before the earthquake. Therefore, it is particularly important to study the methods of suppressing radiocesium elution from the treated fly ash in municipal waste incineration ash.

(c) Zeolite addition test in laboratory

Tables 10 (fly ash) and 11 (treated fly ash) show test results. In order to investigate the presence or absence of a zeolite addition effect on heavy metals and others in the test of adding zeolite to fly ash, zeolite was added by different ratios (5%, 10%, 15%, 20%) to the treated fly ash (chelate agent addition ratio: 2% across the board) before the test.

Table 10. Results of adding zeolite to fly ash in laboratory

Item	Unit	Fly Ash (1st day afternoon)	Fly Ash (1st day afternoon) + Chelate Agent 2%				
		Not added	5% added	10% added	15% added	20% added	
Radiocesium Concentration (content) ¹⁾	Bq/kg	5,200	3,100	3,000	2,900	2,700	
Moisture content	%	-	28.9	29.6	29.8	29.8	
JISK0058-1	Radiocesium Concentration (elution) ¹⁾	Bq/L	350	98	56	40	28
	pH	-	12.4	12.4	12.4	12.4	12.4
	EC	mS/m	5,490	3,860	3,720	3,630	3,560
Radiocesium Elution Rate	%	67.3	31.6	18.7	13.8	10.4	
Notice No. 13	Hg		<0.0005 ²⁾	<0.0005	<0.0005	<0.0005	<0.0005
	Cd		<0.009 ²⁾	<0.009	<0.009	<0.009	<0.009
	Pb		9.2 ²⁾	<0.03	<0.03	<0.03	<0.03
	As		<0.01 ²⁾	<0.01	<0.01	<0.01	<0.01
	Se		0.02 ²⁾	<0.01	<0.01	<0.01	<0.01
	Cr		0.14 ²⁾	0.13	0.11	0.09	0.07
	Cl-		20,000 ²⁾	12,000	9,980	11,000	10,700

* Value without chelate addition

Table 11. Results of adding zeolite to chelated ash in laboratory

Item	Unit	Chelated Fly Ash (2 nd day morning)					
		Not added	5% added	10% added	15% added	20% added	
Radiocesium Concentration (content) ¹⁾	Bq/kg	2,000	1,300	1,300	1,200	1,100	
Moisture content	%	-	29.0	29.4	29.5	29.6	
JISK0058-1	Radiocesium Concentration (elution) ¹⁾	Bq/L	160	29	15	10	7
	pH	-	12.2	12.4	12.4	12.4	12.4
	EC	mS/m	3,740	2,820	2,720	2,620	2,550
Radiocesium Elution Rate	%	80.0	22.3	11.5	8.3	6.4	
Notice No. 13	Hg		<0.0005	<0.0005	<0.0005	<0.0005	<0.0005
	Cd		<0.009	<0.009	<0.009	<0.009	<0.009
	Pb		0.06	0.13	0.08	0.06	0.04
	As		<0.01	<0.01	<0.01	<0.01	<0.01
	Se		<0.01	<0.01	<0.01	<0.01	<0.01
	Cr		0.16	0.02	<0.02	<0.02	<0.02
	Cl-		11,200	7,770	7,060	6,840	6,490

The comparison of the test results indicated that the addition of zeolite to fly ash and treated fly ash suppresses radiocesium elution. A tendency in which an increase in zeolite addition ratio increased a radiocesium elution suppression effect was also observed. The test results concerning heavy metal elution indicated that the addition of zeolite does not block the effect of chelate agent.

In chemical mixture addition and mixing addition tests at actual facilities, a goal of suppressing the total ratio of Cs 134 and 137 elution from the finally generated treated ash to 10 Bq/L was set, and the test results revealed that zeolite must be added by at least 15% with each method to achieve the goal. Therefore, while taking into account the results of daily radiocesium concentration fluctuations, each addition test at actual facilities was performed by mixing (kneading) zeolite and the chemical mixture so that zeolite is added by about 20%.

B Tests on zeolite addition to an exhaust gas treatment agent at actual facilities

(a) Exhaust gas composition analysis tests

Table 12 shows the results of exhaust gas composition analysis tests. A comparison with the results obtained during normal operation revealed that the injection of a chemical mixture (containing zeolite) did not result in any anomalous values of the basic items, with the standard values satisfied.

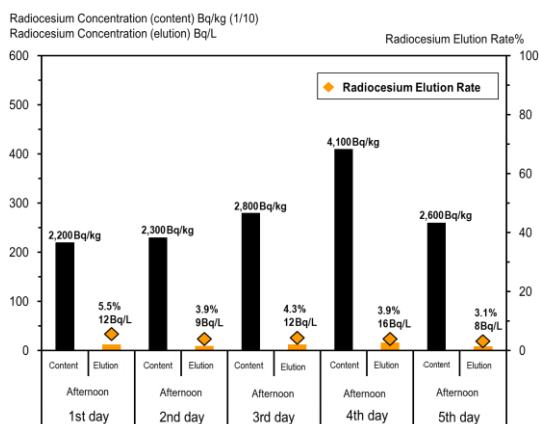
Table 12. Results of analyzing exhaust gas Composition

Sample	Unit	Normal	Blowing-in
Exhaust gas temperature	°C	141	155
Flow velocity	m/s	17.2	16
Wet exhaust gas volume	m ³ (N)/h	34,000	30,400
Dry exhaust gas volume	m ³ (N)/h	24,200	18,700
Moisture content	vol%	28.7	38.3
Carbon dioxide	vol%	9	9.2
Oxygen	vol%	11	10.8
Carbon monoxide	vol%	<0.2	<0.2
Nitrogen	vol%	80	80
Air ratio	-	2.07	2.03
Dust (dust concentration)	g/m ³ (N)	0.039	0.014
Dust (12% conversion ratio)	g/m ³ (N)	0.036	0.013
Sulfur oxides	ppm	9	7
Sulfur oxide emissions	m ³ (N)/h	0.21	0.13
Nitrogen oxide	ppm	57	110
Nitrogen oxide (12% conversion ratio)	ppm	51	100
Nitrogen oxide emissions	m ³ (N)/h	1.3	2
Hydrogen chloride	mg/m ³ (N)	16	39
Hydrogen chloride (12% conversion ratio)	mg/m ³ (N)	15	35
Hydrogen chloride	ppm	10	23
Hydrogen chloride (12% conversion ratio)	ppm	9	21
Cs-134	Bq/m ³ (N)	Less than the lower limit of detection	Less than the lower limit of detection
Cs-137	Bq/m ³ (N)	Less than the lower limit of detection	Less than the lower limit of detection
Cs-134+137	Bq/m ³ (N)	Not detected	Not detected

(b) Germanium semiconductor detector test, JIS K 0058-1 elution test and the Environment Agency's Notice No. 13 elution test

Table 13 shows the concentrations of radiocesium, heavy metals and others in sampled treated fly ash. Figure 6 shows the daily fluctuations of radiocesium concentrations (of contained or eluted radiocesium) and the summarized radiocesium elution rates based on the results of Table 13. First, radiocesium contents were 2,200 to 4,100 Bq/kg (2,800 Bq/kg on average), the quantities of radiocesium elution were 8 to 16 Bq/L (11 Bq/L on average) and radiocesium elution rates were 3.1 to 5.5% (4.1% on average).

The comparison of each average value of radiocesium in treated ash obtained from normal operation tests and each average value of radiocesium obtained from chemical mixture addition tests performed this time indicated that the injection of zeolite significantly reduced quantities of radiocesium elution (normal operation: 121 Bq/L → after chemical mixture addition: 11 Bq/L) and radiocesium elution rate (normal operation: 73.0% → after chemical mixture addition: 4.1%). The results of the Environment Agency's Notice No.



13 elution test indicated that, as with the results of zeolite addition test in laboratory, the blow injection of the mixture of hydrated lime and zeolite at an actual facility also did not block the effect of a chelate agent.

Figure 6. Daily fluctuations of chelated fly ash concentrations (after blow injection)

Table 13. Results regarding chelated fly ash (blow injection)

Item	Unit	Chelated Fly Ash					
		1st day	2nd day	3rd day	4th day	5th day	
Radiocesium Concentration (content) ¹⁾	Bq/kg	2,200	2,300	2,800	4,100	2,600	
JISK0058-1	Radiocesium Concentration (elution) ¹⁾	Bq/L	12	9	12	16	8
	pH	-	12.3	12.3	12.3	12.3	12.4
	EC	mS/m	3,440	3,060	2,710	2,800	2,250
Radiocesium Elution Rate	%	5.5	3.9	4.3	3.9	3.1	
Notice No. 13	Hg		<0.0005	<0.0005	<0.0005	<0.0005	<0.0005
	Cd		<0.009	<0.009	<0.009	<0.009	<0.009
	Pb		<0.03	0.09	<0.03	<0.03	<0.03
	As	mg/L	<0.01	<0.01	<0.01	<0.01	<0.01
	Se		<0.01	<0.01	<0.01	<0.01	<0.01
	Cr		0.16	0.05	0.03	0.05	0.07
	Cl-		10,400	9,520	7,890	8,140	6,310

(c) Repetitive elution tests (JIS K 0058-1)

Tables 14 (solvent: ultrapure water) and 15 (solvent: artificial seawater) show the results of repetitive elution tests. This time, treated fly ash sampled on the third day, whose radiocesium concentration was closest to the average value of treated fly ash sampled during chemical mixture addition test period, was used.

With regard to radiocesium elution properties, when four tests were performed using ultrapure water as a solvent, 14% of radiocesium eluted in total. When this was compared with the results of treated fly ash not added with zeolite shown in Table 9, zeolite was found to significantly suppress radiocesium elution (total elution rate of the four-time tests: 81.9% → four-time total elution rate after chemical mixture addition: 14%).

However, when artificial seawater was used as a solvent, the total radiocesium elution rate increased (total elution rate using ultrapure water 4 times: 14% → artificial seawater 4 times: 56.1%). It was found that regardless of the use of the either solvent, treated fly ash added with zeolite showed a

Table 14. Results of repetitive elution tests on chelated fly ash (solvent: ultrapure water)

Item	Unit	Chelated Fly Ash (3rd day afternoon), Ultra Pure Water				
		1st	2nd	3rd	4th	
JISK0058-1	Radiocesium Concentration (elution) ¹⁾	Bq/L	35	3	0.7	0.3
	pH	-	11.6	11.8	11.9	11.9
	EC	mS/m	2,270	437	214	155
	Radiocesium Elution Rate ²⁾	%	12.5	1.1	0.3	0.1
	Hg		<0.0005	<0.0005	<0.0005	<0.0005
	Cd		<0.001	<0.001	<0.001	<0.001
	Pb		<0.01	<0.01	<0.01	<0.01
	As	mg/L	<0.01	<0.01	<0.01	<0.01
	Se		<0.01	<0.01	<0.01	<0.01
	Cr		0.05	<0.02	<0.02	<0.02
Cl-		7,970	1,110	254	78	

Table 15. Results of repetitive elution tests on the elution of chelated fly ash (solvent: artificial seawater)

Item	Unit	Chelated Fly Ash (3rd day afternoon), Artificial seawater				
		1st	2nd	3rd	4th	
JISK0058-1	Radiocesium Concentration (elution) ¹⁾	Bq/L	80	33	25	19
	pH	-	10.8	9.8	9.2	9.1
	EC	mS/m	6,910	5,770	5,720	5,660
	Radiocesium Elution Rate ²⁾	%	28.6	11.8	8.9	6.8
	Hg		<0.0005	<0.0005	<0.0005	<0.0005
	Cd		<0.001	<0.001	<0.001	<0.001
	Pb		<0.01	<0.01	<0.01	<0.01
	As	mg/L	<0.01	<0.01	<0.01	<0.01
	Se		<0.01	<0.01	<0.01	<0.01
	Cr		0.09	0.12	0.07	0.04
Cl-		28,000	22,800	22,900	22,900	

certain radiocesium elution suppression effect compared with treated fly ash not added with it. The heavy metal elution when ultrapure water or artificial seawater was used also did not result in any anomalous values.

C Tests regarding zeolite addition to the mixture of fly ash and chelate agent (mixture using a kneader) at actual facilities

(a) Germanium semiconductor detector test, JIS K 0058-1 elution test and the Environment Agency's Notice No. 13 elution test

Table 16 shows the results of the concentrations of radiocesium, heavy metals and others in sampled treated fly ash. Figure 7 shows the daily fluctuations of radiocesium concentrations (contained and eluted radiocesium) and radiocesium elution rates based on the results of Table 16. First, radiocesium contents were 1,200 to 1,400 Bq/kg (1,280 Bq/kg on average), quantities of radiocesium elution were 6 to 11 Bq/L (8 Bq/L on average) and radiocesium elution rates were 4.6 to 7.9% (5.9% on average).

The comparison of radiocesium average values in treated fly ash sampled in chemical mixture addition tests and mixing addition tests indicated that the quantities of radiocesium elution were similar in both cases (11 Bq/L for chemical mixture addition, 8 Bq/L for mixing addition, and 121 Bq/L for normal operation) and radiocesium elution rates (4.1% for chemical mixture addition, 5.9% for mixing addition, and 73% for normal operation). Thus it was concluded that, regardless of zeolite addition method (the blow injection or mixing of zeolite), its addition itself has the effect of suppressing the elution of radiocesium. The results of the Environment Agency's Notice No. 13 elution tests indicate that similar to the results obtained from zeolite addition tests and chemical mixture addition tests in the laboratory, the simultaneous mixing of fly ash, a chelate agent and zeolite at actual facilities did not block the effect of the chelate agent.

Table 16. Results regarding chelated fly ash (mixed with zeolite)

Item	Unit	Chelated Fly Ash (afternoon)					
		1st	2nd	3rd	4th	5th	
Radiocesium Concentration (content)	Bq/kg	1,400	1,200	1,200	1,300	1,300	
JISK0058-1	Radiocesium Concentration (elution)	Bq/L	11	8	6	7	6
	pH	-	12.5	12.5	12.5	12.4	11.8
	EC	mS/m	3,370	2,980	2,840	2,350	2,170
Radiocesium Elution Rate		%	7.9	6.7	5.0	5.4	4.6
Environment Agency Notice No. 13	Hg		<0.0005	<0.0005	<0.0005	<0.0005	<0.0005
	Cd		<0.009	<0.009	<0.009	<0.009	<0.009
	Pb		<0.03	<0.03	<0.03	<0.03	<0.03
	As		<0.01	<0.01	<0.01	<0.01	<0.01
	Se		<0.01	<0.01	<0.01	<0.01	<0.01
	Cr		0.11	0.13	0.04	0.06	0.05
	Cl-		10,000	8,930	8,080	6,970	7,290

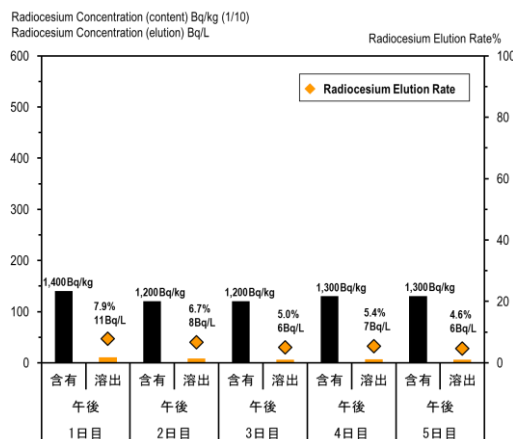


Figure 7. Daily fluctuation of chelated fly ash (mixed with zeolite)

(b) Repetitive elution tests (JIS K 0058-1)

Tables 17 (solvent: ultrapure water) and 18 (solvent: artificial seawater) show the results of repetitive elution tests. This time, treated fly ash sampled on the fourth day of the zeolite-mixing test period, whose radiocesium concentration was closest to the average value, was used.

Table 17. Results of repetitive elution tests on elution from chelated fly ash (ultrapure water)

Item	Unit	Chelated Fly Ash (4th day afternoon), Ultra Pure Water			
		1st	2nd	3rd	4th
Radiocesium Concentration (elution) ¹⁾	Bq/L	12	1	0.4	0
pH	-	12.0	12.1	12.0	12.0
EC	mS/m	2,240	664	316	235
Radiocesium Elution Rate ²⁾	%	9.2	0.8	0.3	0
Hg	mg/L	<0.0005	<0.0005	<0.0005	<0.0005
Cd		<0.001	<0.001	<0.001	<0.001
Pb		<0.01	<0.01	<0.01	<0.01
As		<0.01	<0.01	<0.01	<0.01
Se		<0.01	<0.01	<0.01	<0.01
Cr		0.05	<0.02	<0.02	<0.02
Cl-		6,660	1,140	340	108

* Each value is calculated with its radiocesium concentration (content) as of 1,300 Bq/kg.

Table 18. Results of repetitive elution tests on elution from chelated fly ash (artificial seawater)

Item	Unit	Chelated Fly Ash (4th day afternoon), Artificial Seawater			
		1st	2nd	3rd	4th
Radiocesium Concentration (elution) ¹⁾	Bq/L	26	12	10	8
pH	-	11.4	11.0	9.9	9.2
EC	mS/m	6,820	5,920	5,740	5,680
Radiocesium Elution Rate ²⁾	%	20.0	9.2	7.7	6.2
Hg	mg/L	<0.0005	<0.0005	<0.0005	<0.0005
Cd		<0.001	<0.001	<0.001	<0.001
Pb		<0.01	<0.01	<0.01	<0.01
As		<0.01	<0.01	<0.01	<0.01
Se		<0.01	<0.01	<0.01	<0.01
Cr		0.11	0.21	0.29	0.18
Cl-		27,400	23,900	22,300	22,400

* Each value is calculated with its radiocesium concentration (content) as of 1,300 Bq/kg.

First, regarding radiocesium elution properties, when four tests were carried out using ultrapure water as a solvent, radiocesium eluted by 10.3% in total. The results (81.9% radiocesium elution in total in four tests during normal operation → 14% radiocesium elution in total in four tests with the addition of chemical mixture, and 10.3% elution in total in four tests using a mixing method) were broadly similar to the results of treated fly ash sampled in the chemical mixture addition tests shown in Table 14.

When four tests were carried out using artificial seawater as a solvent, similar results were obtained (56.1% elution in total for artificial seawater added with chemical mixture and 43.1% elution in total for artificial seawater mixed with chemical mixture). Results regarding heavy metal elution also did not show any anomalous value regardless of whether ultrapure water or artificial seawater was used as a solvent.

Given the effect of zeolite in suppressing radiocesium elution shown in the zeolite mixing addition tests and the results of laboratory tests on zeolite addition to treated fly ash, before the repacking of ash whose treatment is difficult because of its high radiocesium concentration to a new container, the addition and mixing of zeolite into the treated fly ash seems to be one of effective means of enhancing safety.

While both the zeolite addition methods (the method using the chemical mixture and the zeolite mixing method) were found effective in suppressing radiocesium elution, when it comes to the burial of ash at a landfill disposal site, the excessive addition of zeolite to the ash may increase the total landfill volume, so the addition of zeolite by 20% of total volume at a maximum is deemed appropriate.

In applying a zeolite addition method, either by using chemical mixture or by the mixing addition of zeolite, the modification of the facility may be necessary.

In the case of the chemical mixture addition method, an existing hydrated lime silo can be used and all of the hydrated lime needs are to be replaced with the chemical mixture for radiocesium elution suppression. However, unlike the blow addition of hydrated lime alone during a periodical inspection, this method may cause pipe abrasion or may clog the bag filter, so careful measures in details may have to be taken.

In the case of adopting a mixing addition method, a silo equipped with a chelate agent kneading machine and a mechanism capable of adding zeolite may need to be newly built, and in such a case, periodical inspections may be needed to carefully check the abrasion of such a machine. Therefore, optimal addition method and quantity should be selected according to the characteristics of disposal facility to ensure applicability to it.

(3) Status of landfills and radiocesium elution

Table 19 shows radiocesium analysis results in FY 2015. Radiocesium was detected in leachate (seeping water) and discharged water from disposal sites A and B, where incineration ash was buried, and from disposal site D, where fly ash was buried without contact with rainwater. On the other hand, radiocesium in leachate and discharged water was below the lower detection limit (about 1 Bq/L) for disposal site C, where no incineration ash was buried, disposal site E, where incineration ash was buried by preventing its contact with rainwater, and disposal sites F and G, where only bottom ash was buried. None of these disposal sites exceeded the lower detection limit (about 1 Bq/L) in terms of radiocesium concentration in nearby underground water.

Table 19. Results of analyzing radiocesium in leachate and others in FY 2015
Units: Bq/L for leachate and discharged water, Bq/kg for sludge
Lower detection limit: 1 Bq/L or Bq/kg

	Disposal Site A			Disposal Site B			Disposal Site C			Disposal Site D			Disposal Site E			Disposal Site F			Disposal Site G			
	Leachate (Bq/L)	Discharged water (Bq/L)	Sludge (Bq/kg)	Leachate (Bq/L)	Discharged water (Bq/L)	Sludge (Bq/kg)	Leachate (Bq/L)	Discharged water (Bq/L)	Sludge (Bq/kg)	Leachate (Bq/L)	Discharged water (Bq/L)	Sludge (Bq/kg)	Leachate (Bq/L)	Discharged water (Bq/L)	Sludge (Bq/kg)	Leachate (Bq/L)	Discharged water (Bq/L)	Sludge (Bq/kg)	Leachate (Bq/L)	Discharged water (Bq/L)	Sludge (Bq/kg)	
Jan	2.6	1.9	1.9	10.9	11.2	8.4	N.D.	N.D.	N.D.	2.4	1.6	5.3	N.D.	N.D.	N.D.	N.D.	N.D.	N.D.	N.D.	N.D.	N.D.	N.D.
Feb	1.8	1.6	3.1	10	10.3	6.6	N.D.	N.D.	N.D.	1.7	N.D.	2.5	N.D.	N.D.	N.D.	N.D.	N.D.	N.D.	N.D.	N.D.	N.D.	1.0
Mar	2.2	1.7	1.8	9.7	10.7	6.0	N.D.	N.D.	N.D.	2.2	1.6	1.5	N.D.	N.D.	1.1	N.D.	N.D.	N.D.	N.D.	N.D.	N.D.	N.D.

Table 20 shows radiocesium analysis results in FY 2016. Radiocesium was detected in leachate (seeping water) and discharged water from the disposal site H only, where fly ash had been buried as it is. Radiocesium concentrations in underground water at all the landfill disposal sites shown in Table 20 were below the lower detection limit (0.1 Bq/L).

Table 20. Results of analyzing radiocesium in leachate and others in FY 2016
Lower detection limit: 1 Bq/kg or Bq/L

	Disposal Site C			Disposal Site E			Disposal Site F			Disposal Site G			Disposal Site H			Disposal Site I		
	Leachate (Bq/L)	Discharged water (Bq/L)	Sludge (Bq/kg)	Leachate (Bq/L)	Discharged water (Bq/L)	Sludge (Bq/kg)	Leachate (Bq/L)	Discharged water (Bq/L)	Sludge (Bq/kg)	Leachate (Bq/L)	Discharged water (Bq/L)	Sludge (Bq/kg)	Leachate (Bq/L)	Discharged water (Bq/L)	Sludge (Bq/kg)	Leachate (Bq/L)	Discharged water (Bq/L)	Sludge (Bq/kg)
Nov	<0.1	<0.1	—	<0.1	<0.1	0.42	<0.1	<0.1	0.24	<0.1	<0.1	0.38	7.1	6.7	4.9	<0.1	<0.1	0.87
Feb	<0.1	<0.1	—	<0.1	<0.1	0.17	<0.1	<0.1	0.26	<0.1	<0.1	0.11	3.9	4.5	6.0	<0.1	<0.1	0.19

Based on the results in FYs 2015 and 2016, it was likely that radiocesium was detected

in leachate and discharged water only at landfill disposal sites having buried radiocesium-containing fly ash without preventing its contact with rainwater. Regarding disposal site D, where radiocesium was detected in leachate although the site had buried fly ash while preventing its contact with rainwater, a detailed on-site hearing concerning the landfill situation revealed that a part of the fly ash had been buried without a rainwater contact prevention measure during a period immediately after the Fukushima accident, namely from the period of reconstructing the incineration facility until the Ministry of the Environment's notice ordering the halt of incineration ash burial. It is likely that radiocesium continuously eluted from the incineration fly ash in question and leached from the disposal site D through discharged water.

(4) Correlation between the annual elution of radiocesium and other elements

Tables 21 and 22 show measurement results in FYs 2017 and 2018. Figures 8 and 9 are the graphs of measured results in the same years, intended to clarify the presence or absence of a seasonality (seasonal factor) common among the disposal sites. These results did not indicate a seasonality common among them.

Figures 10 to 13 are graphs using the two years' results, intended to clarify the presence or absence of a seasonality in terms of radiocesium elution at each disposal site

Table 21. Results of analyzing radiocesium in leachate and others in FY 2017
Units: Bq/L for leachate and discharged water and Bq/kg for sludge
Lower detection limit: 1 Bq/kg or Bq/kg

	Disposal Site A			Disposal Site B			Disposal Site D			Disposal Site H		
	Leachate (Bq/L)	Discharged water (Bq/L)	Sludge (Bq/kg)	Leachate (Bq/L)	Discharged water (Bq/L)	Sludge (Bq/kg)	Leachate (Bq/L)	Discharged water (Bq/L)	Sludge (Bq/kg)	Leachate (Bq/L)	Discharged water (Bq/L)	Sludge (Bq/kg)
Apr	N.D.	4	3	8	10	18	1	1	4	8	5	3
May	1	N.D.	1	8	9	9	2	N.D.	6	1	1	2
Jun	3	2	2	10	10	6	N.D.	N.D.	3	N.D.	N.D.	4
Jul	3	3	3	13	13	6	2	1	8	N.D.	N.D.	4
Aug	4	4	5	11	10	7	3	3	12	N.D.	N.D.	4
Sep	4	4	2	10	9	5	2	1	8	N.D.	N.D.	2
Oct	4	4	4	10	11	5	N.D.	1	5	N.D.	N.D.	2
Nov	5	5	3	11	10	6	N.D.	2	6	N.D.	N.D.	2
Dec	4	5	3	9	10	9	2	1	3	1	1	1
Jan	4	4	4	8	9	4	1	N.D.	4	2	2	2
Feb	5	5	5	10	9	4	1	N.D.	10	3	3	3
Mar	5	5	3	12	10	5	2	N.D.	5	2	3	3

Table 22. Results of analyzing radiocesium in leachate and others in FY 2018
Units: Bq/L for leachate and discharged water
Lower detection limit: 1 Bq/kg

	Disposal Site A		Disposal Site B		Disposal Site D		Disposal Site H	
	Leachate (Bq/L)	Discharged water (Bq/L)						
Apr	3	3	10	10	N.D.	1	2	2
May	3	3	9	9	1	1	1	1
Jun	3	3	6	6	N.D.	2	1	1
Jul	2	2	4	4	0.4	2	1	1
Aug	1	2	5	4	N.D.	2	1	1
Sep	3	2	5	7	2	2	2	1
Oct	2	2	11	10	1	2	1	1
Nov	1	1	10	10	N.D.	1	1	1
Dec	1	1	6	6	N.D.	1	1	1
Jan	1	1	10	8	N.D.	N.D.	1	1

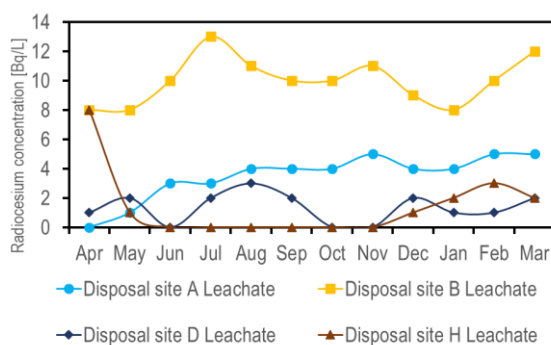


Figure 8. Measured results in FY 2017

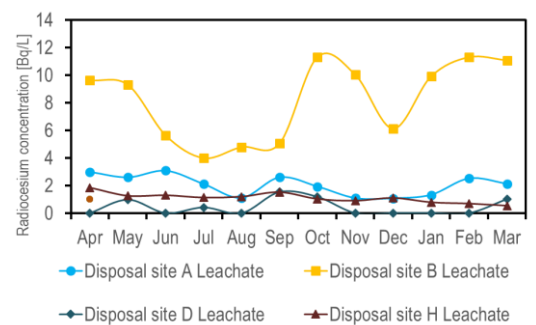


Figure 9. Measured results in FY 2018

A Disposal site A

The highest radiocesium concentration in leachate at disposal site A was about 5 Bq/L. In FY 2017, radiocesium concentrations in April were low but increased toward March next year. In FY 2018, radiocesium concentrations in April to June were high but decreased in winter. In comparison, these do not suggest a seasonality in radiocesium elution.

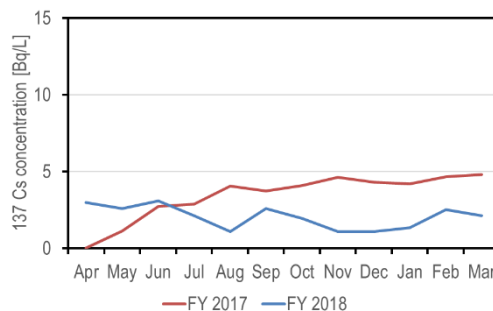


Figure 10. Radiocesium concentrations in leachate at disposal site A

B Disposal site B

The highest radiocesium concentration in leachate at disposal site B was about 13 Bq/L. In FY 2017, radiocesium concentrations were high in July, November, and March but low in May and December to February next year. In FY 2018, radiocesium concentrations from July to September, and December were low, but were high in April, May, October, November, and January to March the next year. This comparison suggested a trend of radiocesium concentration increasing in winter but does not warrant a conclusion that seasonality is inherent to the landfill disposal site exists.

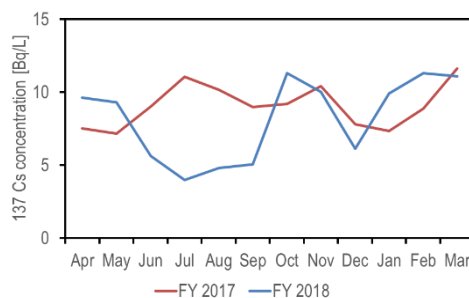


Figure 11. Radiocesium concentrations in leachate at disposal site B

C Disposal site D

The highest radiocesium concentration in leachate at disposal site D was about 3 Bq/L. The concentrations were generally low, often below the lower detection limit, thus a seasonality was not confirmed.

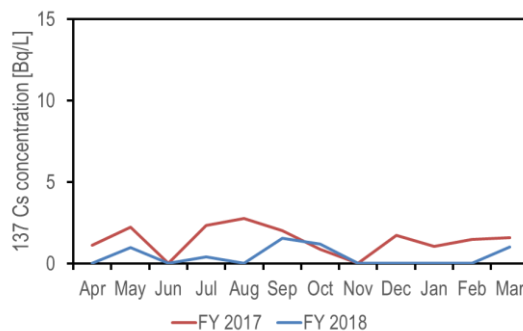


Figure 12. Radiocesium concentrations in leachate at disposal site D

D Disposal site H

The highest radiocesium concentration in leachate at disposal site H was about 8 Bq/L. In FY 2017, radiocesium concentrations from June to November were below the lower detection limit, and in FY 2018, they were about 1 Bq/L throughout the fiscal year. While a fluctuation was observed in radiocesium concentration in FY 2017, no commonality with data in FY 2018 was confirmed, thus indicating the absence of a seasonality in radiocesium elution.

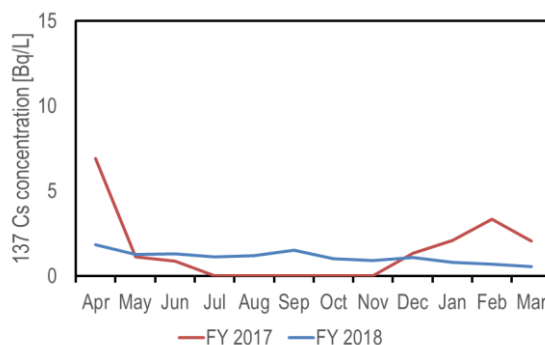


Figure 13. Radiocesium concentrations in leachate at disposal site H

Table 23 shows the results of analyzing elements in leachate at landfill disposal sites in FY 2017, namely radiocesium and chloride ion concentrations. A possibility was suggested that the higher the chloride ion concentration, the higher the radiocesium concentration becomes. A correlation diagram (Figure 14) was developed by plotting radiocesium concentrations on the vertical axis and chloride ion concentrations on the horizontal axis. The diagram indicated a positive correlation between them.

Table 23. Radiocesium and chloride ion concentrations

	Disposal Site A		Disposal Site B		Disposal Site D		Disposal Site H	
	Leachate (Bq/L)	Chloride ion (mg/L)						
Apr	0	83	8	13000	1	1400	8	4800
May	1	2000	8	12000	2	1800	1	5200
Jun	3	5100	10	12000	0	310	0	3900
Jul	3	5700	13	13000	2	2300	0	3600
Aug	4	7800	11	13000	3	1600	0	3000
Sep	4	7600	10	13000	2	1900	0	4000
Oct	4	7300	10	12000	0	1000	0	3900
Nov	5	7600	11	12000	0	1000	0	2800
Dec	4	7500	9	11000	2	1800	1	3700
Jan	4	7500	8	12000	1	980	2	7200
Feb	5	7800	10	12000	1	2100	3	8000
Mar	5	8700	12	12000	2	1800	2	6400

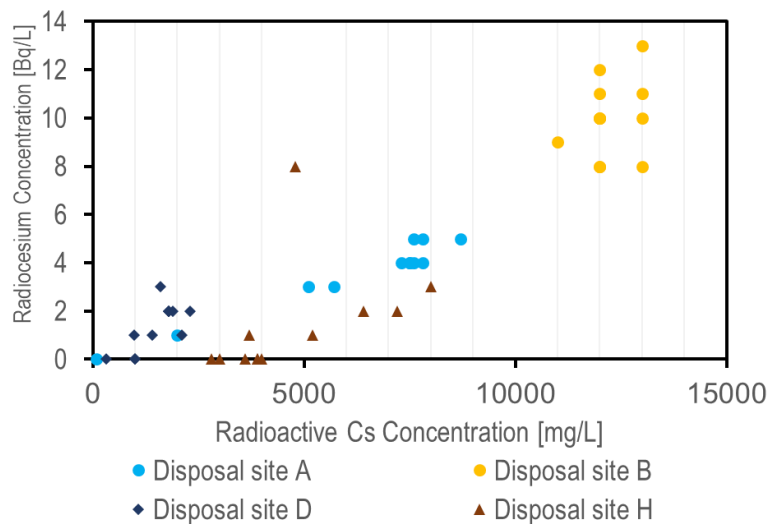


Figure 14. Correlation between radiocesium and chloride ion concentrations

5.5. Conclusions

The surveys conducted this time have confirmed that the burial of fly ash at landfill disposal sites without elution-preventing measures such as water shielding results in the elution of radiocesium. Regarding elution situations at the disposal sites, it is presumed that neither seasonality is common to them nor seasonality at each of them is present. Moreover, a positive correlation was observed between radiocesium concentration and chloride ion concentration suggested a possibility that chloride ions in incineration ash are affecting radiocesium elution.

As a result of testing radiocesium elution from incineration ash (bottom ash, treated bottom ash, fly ash and treated fly ash), which seems to be the cause of radiocesium detected from leachate (seeping water) at the landfill disposal sites, radiocesium concentrations in and radiocesium elution from the fly ash (including treated fly ash) were higher compared with bottom ash (including treated bottom ash) at each site. When an acid clay was added to and mixed with treated fly ash having a high radiocesium elution property, the radiocesium elution decreased and the acid clay did not block the heavy metal elution prevention effect of chelate.

Tests were performed at actual facilities in which fly ash was added with zeolite, whose radiocesium elution suppression effect had been recognized in the final report of the previous project. The results of the tests confirmed that both the methods of mixing zeolite into a blow-in chemical such as hydrated lime and the method of adding zeolite immediately before adding and mixing a chelate agent significantly suppress radiocesium elution and does not block the heavy metal elution prevention effect of the chelate agent. Based on these results combined with laboratory results, these methods are effective in suppressing radiocesium elution not only for fly ash to be generated at incineration facilities in the future but also for incineration ash temporarily stored at present. However, the application of these methods to actual disposal facilities requires the consideration of the characteristics of each incineration facility and landfill disposal site, including consideration of an increase in the amount of landfill disposal due to zeolite addition as well as facility structure and capacity.

Report summary

Except for FIP4, this report covers activities from FY2013, focusing on activities from FY2018 and FY2019. Since FIP4 was completed in FY2015, we report on the activities from FY2013 to FY2015 with some wordings revised and update added since the theme ended in FY2015. The reports on each theme are summarized as follows.

FIP1: Survey, and evaluation of the effect of radiocaesium dynamics in the aquatic systems

We are continuing to observe the concentration of suspended and dissolved radioactive cesium in river water in Fukushima Prefecture. As a result, for both forms of radiocesium, the tendency to decrease with the passage of time, which had been observed immediately after the accident, was maintained. Furthermore, it was confirmed that decontamination in river basins has a strong effect on the concentration of suspended cesium-137 in river water. For the simulation for future prediction of the concentration of radioactive cesium in river water, the calculation was refined for normal flow conditions, and a trial calculation was carried out under high flow flood conditions.

FIP2: Survey of radionuclide movement with wildlife

As a result of confirming the seasonal change of cesium-137 concentrations in the muscles of wild boar and Asian black bear, even in recent years, individuals with high concentrations that greatly exceeded the standard value of radioactive cesium concentration in general foods were captured. The long-term fluctuation of cesium-137 concentration in the muscles of wild boar and Asian black bear showed a decrease over time during the entire period, both the low concentration period and the high concentration period. The model now needs to be reconsidered to provide a better estimate of the long-term fluctuations of radiocesium in the animals, particularly during the high concentration period. In addition, wild boars in Fukushima Prefecture are genetically divided into two strain groups, suggesting that their movement may be restricted from east to west with the Abukuma River and around as the boundary.

FIP3: Sustainable countermeasures to radioactive materials in freshwater system

The sustainability of the decontamination effect was continuously verified at the riverside area where the decontamination demonstration test was conducted in 2014. Even under the condition of overgrown vegetation on the riverbed, the air dose rate continued to decrease. No significant accumulation of radiocesium was observed, confirming that the effect of the decontamination was maintained.

In addition, in order to verify the presence or absence of recontamination around the river due to the passage of Typhoon No. 19 in 2019, the air dose rate was measured and field reconnaissance was conducted at riverside areas and parks. An increase in the air dose rate was not generally confirmed, but rather the air dose rate decreased significantly near the river, and the effect of the natural attenuation associated with flooding was confirmed.

FIP4: Development of environmental mapping technology using GPS walking surveys

A GPS-linked dose rate measurement device, KURAMA from Kyoto University, was used as a basis and the configuration was made more suitable for walking surveys. Then, the GIS data processing system was prepared on the assumption that it would be linked with the analysis of the obtained data and the monitoring of aircraft surveys by UAV. In addition, it has become possible to measure the dose rate in a walking survey by collecting data necessary for measurement such as directional characteristics and calibration constants. We conducted walking surveys at several points and confirmed that it was possible to measure dose rates and create contour maps using a GIS data processing system. A manual was prepared so that even inexperienced people can use the system. Since fiscal 2016, it has been used for conducting walking surveys and has been rented out at the request of municipalities. In recent years, walking surveys have been utilized in the public projects for monitoring of the air dose rates (e.g., Satoyama Restriction Model Project).

FIP5: Study of proper treatment of waste containing radioactive material

Surveys and tests were conducted at landfill sites and waste incinerators to examine treatment, disposal and management methods for waste containing radiocesium generated in the prefecture. A survey of leachate at the landfill site confirmed that when the incinerated fly ash was buried in contact with rainwater, radiocesium was eluted from the incinerated fly ash and was detected in the leachate. In order to suppress the elution of radiocesium from this incinerated fly ash, various incineration ash elution tests and incineration ash sparingly soluble tests were conducted in laboratories and facilities. As a result, it was found that the addition of zeolite into the incineration ash has a remarkable effect of suppressing the elution of radiocesium. However, in the application to the implementation facility, it is added according to the target incineration facility or landfill site, and so it is considered necessary to further study the method and the amount of zeolite added.